

Studies on Lipoamide Dehydrogenase

CENTRALE LANDBOUWCATALOGUS



0000 0489 4321

BIBLIOTHEEK
LANDBOUWUNIVERSITEIT
WAGENINGEN

Promotor : Dr. C. Veeger
hoogleraar in de Biochemie

Co-promotor : Dr. A. de Kok
universitair hoofddocent

NN0801, 1497

Jacques A. E. Benen

Studies on Lipoamide Dehydrogenase

Proefschrift

ter verkrijging van de graad van doctor
in de landbouw- en milieuwetenschappen
op gezag van rector magnificus,
Dr. H. C. van der Plas,
in het openbaar te verdedigen
op vrijdag 8 mei 1992
des namiddags te 13.30 uur in de Aula
van de Landbouwuniversiteit te Wageningen.

Aan Anja
Aan mijn moeder
Ter nagedachtenis van mijn vader

Het verdient aanbeveling de term conservatief in relatie tot aminozuursubstituties met meer omzichtigheid te benaderen.

Dit proefschrift, hoofdstuk 2-4.

De eenvoudige manier om redoxpotentialen van flavoproteinen te bepalen zoals voorgesteld door Massey, werkt alleen voor eenvoudige flavoproteinen.

Massey, V. (1990) in *Flavins and Flavoproteins 1990* (Curti, B., Ronchi, S. and Zanetti, G. eds) pp 55-66, Walter de Gruyter and Co, Berlin - New York.

De uit de enzymologie bekende 'negatieve coöperativiteit' blijkt ook bij de Europese unificatie opgeld te doen.

Ricard, J. and Cornish-Bowden, A. (1987) *Eur. J. Biochem.* 166, 255-272.

De voorspellende waarde van de circulair dichroïsme methode voor eiwitstructuren is voornamelijk niet hoog.

Provencher, S. W. and Glockner, J. (1981) *Biochemistry* 20, 33-37.

Wishart, D. S., Sykes, B. D. and Richards, F. M. (1991) *FEBS Let.* 293, 72-80.

In tegenstelling tot de bewering van Scrutton *et al.* is de afwezigheid van reductie van het flavine in Cys47->Ser gemuteerd *E. coli* glutathion reductase door NADPH niet te verwachten.

Scrutton, N. S., Berry, A., Deonarian, M. P. and Perham, R. N. (1990) *Proc. R. Soc. London* 242, 217-224.

De bewering door Borges *et al.* dat in *Pseudomonas fluorescens* een tweede gen voor lipopeptide dehydrogenase zou zijn aangetoond door Benen *et al.* is fout.

Borges, A., Hawkins, C. F., Packman, L. C. and Perham, R. N. (1990) *Eur. J. Biochem.* 194, 95-102.

Benen, J. A. E., Van Berkel, W. J. H., Van Dongen, W. M. A. M., Müller, F. and De Kok, A. (1989) *J. Gen Microbiol.* 135, 1787-1797.

De opvatting dat alle flavine-afhankelijke oxidases een flavine-N5-sulfiet adduct vormen verdient aanpassing.

Müller, F. (1987) *Free Radical Biology Medicine* 3, 215-230.

De verwachte 5% daling van verkeersslachtoffers, ten gevolge van de maatregel overdag verplicht licht te voeren op alle gemotoriseerde vervoermiddelen, is niet gecorrigeerd voor de te verwachten toename van het aantal slachtoffers onder motorrijders.

De excessieve veiligheidsmaatregelen waarmee asbest is omgeven zal, gezien de maatregelen ten aanzien van AIDS preventie, ertoe leiden dat het afsluiten van een levensverzekering gepaard zal gaan met een asbest-antecedenten onderzoek.

Stellingen behorende bij het proefschrift

'Studies on lipoamide dehydrogenase'

Wageningen, 8 mei 1992.

Jacques A. E. Benen.

Voorwoord

Graag wil ik op deze plaats iedereen bedanken die bij de totstandkoming van dit proefschrift heeft bijgedragen.

Cees Veeger, mijn promotor, met wie pittige discussies werden gevoerd over ook 'zijn' enzym.

Aart de Kok die als co-promotor optrad. Aart bedankt voor je geduldig oor en voor de vrijheid die je me hebt gelaten in onderzoek en vorming.

Willem van Berkel bij wie menig wetenschappelijk proeballonnetje werd opgelaten dat vaak werd doorgeprikt en die veel heeft bijgedragen aan het hele proefschrift.

Adrie Westphal, die het gen coderend voor lipoamide dehydrogenase cloneerde, niet alleen een fijn collega en kamergenoot maar ook een gezellige kerel buiten werktijd.

Miriam Gilissen, Fenneke Linker, Erna Hissink, Nicole Dieteren en Sandra Japenga die in het kader van een afstudeervak aan verschillende aspecten van lipoamide dehydrogenase werkten.

Zdzislaw Zak who spent three months on tedious titrations of mutated enzymes and who recorded the CD spectra.

Charles Williams Jr. who invited me to visit his lab in Ann Arbor, Michigan, USA, in order to be able to do rapid scan analysis. David Arscott who made me familiar with the complex apparatus. Charles and David thanks a lot. Without this opportunity, fruitful cooperation and discussions Chapter 3 would have had less impact. I hope the cooperation will be continued in the future.

Walter van Dongen die de correctie van hoofdstuk 5 voor zijn rekening nam.

Andrea Mattevi, Bram Schierbeek en Wim Hol van de kristallogroefgroep van de universiteit van Groningen die de structuur beschikbaar stelden voordat deze gepubliceerd was en die aanzienlijk meer mutaties voorstelden dan één promovendus kan maken en bestuderen.

Alle medewerkers van de afdeling Biochemie die ervoor zorgden dat er altijd een prima werksfeertje was en waarbij je je gal kon spuwen als het weer eens mis ging.

Mijn moeder, familie en vrienden die altijd geïnteresseerd waren in de voortgang.

Anja, die nooit klaagde als ik weer te laat thuis was of in het weekend moest werken. Die me in tijden van tegenslag altijd uit de put hielp, kortom, die een geweldige steun voor me was. Anja bedankt !

Chapters 2 and 5 have been published and chapters 3 and 4 will be published separately.

- Chapter 2: Benen, J., Van Berkel, W., Zak, Z., Visser, T., Veeger, C. and de Kok, A. (1991) *Eur. J. Biochem.* 202, 863-872.
- Chapter 3: Benen, J., van Berkel, W., Dieteren, N., Arscott, D., Williams Jr., C., Veeger, C. and de Kok, A. (1992) *Eur. J. Biochem.*, (submitted)
- Chapter 4: Benen, J., Van Berkel, W., Veeger, C and de Kok, A. (1992) *Eur. J. Biochem.*, (submitted)
- Chapter 5: Benen, J. A. E., Van Berkel, W. J. H., Van Dongen, W. M. A. M., Müller, F. and de Kok, A. (1989) *J. Gen. Microbiol.* 135, 1787-1797.

The research described in this thesis was carried out at the Department of Biochemistry, Agricultural University, Wageningen, The Netherlands, under the direction of Prof. Dr. C. Veeger.

The investigations were financially supported by the Netherlands Organisation for Scientific Research (N. W. O.) under the auspices of the Foundation for Chemical Research (S.O.N.).

Contents

	Page
Abbreviations	9
List of enzymes	10
Chapter 1. Introduction	11
Chapter 2. Lipoamide dehydrogenase from <i>Azotobacter vinelandii</i> : site directed mutagenesis of the His450-Glu455 diad. Spectral properties of wild-type and mutated enzymes.	43
Chapter 3. Lipoamide dehydrogenase from <i>Azotobacter vinelandii</i> : site directed mutagenesis of the His450-Glu455 diad. Kinetics of wild-type and mutated enzymes.	53
Chapter 4. Lipoamide dehydrogenase from <i>Azotobacter vinelandii</i> : Role of the C-terminus in catalysis and dimer stabilization.	79
Chapter 5. Molecular cloning and sequence determination of the <i>lpd</i> -gene encoding lipoamide dehydrogenase from <i>Pseudomonas fluorescens</i> .	95
Chapter 6. Lipoamide dehydrogenase from <i>Pseudomonas fluorescens</i> . A characterization of the enzyme.	107
General discussion	115
Samenvatting	123
Curriculum vitae	131
List of publications	131

Abbreviations

AAD ⁺	3-aminopyridine adenine dinucleotide
AcPyAd ⁺	3-acetylpyridine adenine dinucleotide
AcPyAd ⁺ H	3-acetylpyridine adenine dinucleotide reduced
BCOADC	branched-chain oxo acid dehydrogenase complex
Cl ₂ Ind	2,6-dichlorophenolindophenol
C _m	midpoint concentration of Gdn/HCl required for unfolding
CT	530 nm charge transfer species.
ΔG	standard Gibbs energy
E _{ox}	oxidized (mutated) lipoamide dehydrogenase
EH ₂	2-electron reduced (mutated) lipoamide dehydrogenase with disulfide reduced (530 nm charge-transfer- and tautomeric species).
EH ⁻	EH ₂ one step deprotonated
E ²⁻	EH ₂ two steps deprotonated
EH ₄	general descriptive term for 4-electron reduced (mutated) lipoamide dehydrogenase
EDTA	ethylene diamine tetraacetate
E _m	midpoint redox potential
FAD(H ⁻)	flavin adenine dinucleotide (reduced)
FL	fluorescent species.
FIH ⁻	2 electron reduced species with electrons on the flavin.
Gdn/HCl	guanidinium hydrochloride
h	Hill coefficient
Hepps/EDTA	Hepps/EDTA buffer, pH 8.0
k	rate constant
kb	kilo basepairs
k _{cat}	turnover rate, μmole product per active site per second.
K _d	dissociation constant
K _i	inhibition constant
K _m	Michaelis Menten constant
LipS ₂	D,L - 6,8 - thioctic acid amide; lipoamide
Lip(SH) ₂	reduced lipoamide
<i>lpa</i> -gene	gene encoding lipoamide dehydrogenase
NAD(P) ⁺	nicotinamide dinucleotide (phosphate) oxidized
NAD(P)H	nicotinamide dinucleotide (phosphate) reduced
Meq (s).	Molar equivalent(s)

M_r	relative molecular mass
Nbs ₂	5,5'-dithiobis(2-nitrobenzoate)
nm	nanometer
PDC	pyruvate dehydrogenase complex
pK _a	-log(proton dissociation constant)
PPI/EDTA-buffer	50 mM sodium pyrophosphate, 0.5 mM EDTA, pH 8.0
PrfX	unknown protein encoded by an open reading frame downstream of the <i>lpd</i> gene in <i>Azotobacter vinelandii</i> and <i>Pseudomonas fluorescens</i>
OGDC	2-oxo glutarate dehydrogenase complex
ORF	open reading frame
SDS	sodiumdodecylsulfate
6×SSC	0.9 M NaCl, 0.09 M Na ₃ citrate·2 H ₂ O, pH 7.0
SSE	20 % (w/v) sucrose, 150 mM NaCl, 100 mM EDTA, pH 7.6
<i>SucA</i>	gene encoding 2-oxo glutarate dehydrogenase
<i>SucB</i>	gene encoding succinyl transferase
t_m	melting temperature
U	unit of activity: 1 μmole product per minute
v	apparent velocity, μmoles product per mg enzyme per minute
V	maximal velocity, μmoles product per mg enzyme per minute

List of enzymes

1. lipoamide dehydrogenase, NADH:lipoamide oxidoreductase (EC. 1.8.1.4)
2. DNA restriction endonucleases *Alu* I, *Bam*H1, *Eco*R1, *Hinc* II, *Hind*III, *Kpn*I, *Not*I, *Pst*I, *Sau*3A I, *Sma*I, *Sph*I, *Sst*I, (EC 3.1.24.4)
3. DNA polymerase I (Klenow fragment)(EC 2.7.7.7)
4. DNA ligase (EC 6.5.1.1)
5. T4-DNA polymerase (EC 2.7.7.7)
6. Glucose-6-phosphate dehydrogenase, D-Glucose-6-phosphate: NADP 1-oxidoreductase (EC 1.1.1.49)
7. Xanthine oxidase, xanthine: oxygen oxidoreductase (EC 1.1.3.22)

Chapter 1

Introduction

Occurrence and function of lipoamide dehydrogenase

Lipoamide dehydrogenase is the common name for NADH:lipoamide oxidoreductase (EC 1.8.1.4). The enzyme was first described by Straub [1] and has been known for years as Straub diaphorase as it readily transfers electrons from NADH to artificial electron acceptors like 2,6-dichlorophenolindophenol and methylene blue [2]. Massey [3] and Searls and Sanadi [4] showed that Straub diaphorase is identical with lipoamide dehydrogenase. Lipoamide dehydrogenase is widely spread through nature as it was isolated from many eukaryotic and prokaryotic species (A complete list is given by Williams [5, 6]). It is a constituent of several multi-enzyme complexes. These complexes are the pyruvate dehydrogenase complex [PDC] [7, 8], the α -ketoglutarate dehydrogenase complex [OGDC] [3, 4], the branched chain oxo acid dehydrogenase complex [BCOADC] [9] and the glycine cleavage system [10, 11]. Lipoamide dehydrogenase functions also in the galactose and maltose uptake system of *E. coli* [12, 13].

Multienzyme complexes. In the multi-enzyme complexes in which lipoamide dehydrogenase catalyses the reoxidation of covalently bound dihydrolipoic acid and reduction of NAD^+ , the lipoic acid is the carrier of the acyl function and is reduced after the acyl part has been transferred to either CoA (in the PDC, OGDC and BCOADC) or tetrahydrofolate (in the glycine cleavage system). The lipoic acid (6,8-dithioctic acid) is in all complexes coupled via amide linkage to a lysine of the acyl transferase component [14, 15] or of a separate carrier protein in the glycine oxidation system [16, 17]. This is shown in Fig. 1.

The flexible arm formed by lipoic acid and the lysine (the lipoyl group) is assumed to carry the substrate from one active site of the complex to the other. In all the complexes after the acyl part has been transferred to either CoA (in the PDC, OGDC and BCOADC) or tetrahydrofolate (in the glycine oxidation system) the lipoyl group is reduced and becomes reoxidized by lipoamide dehydrogenase. It has been shown that in the complexes only the 6R-lipoyl group is present [18].

For the 2-oxo acid dehydrogenase complexes the reaction sequence has been studied extensively [19] and is depicted in Fig. 2. Component E1 of the complexes is the 2-oxo acid dehydrogenase that catalyses the decarboxylation of the 2-oxo acids and the subsequent alkylation of the lipoyl group that is covalently attached to the

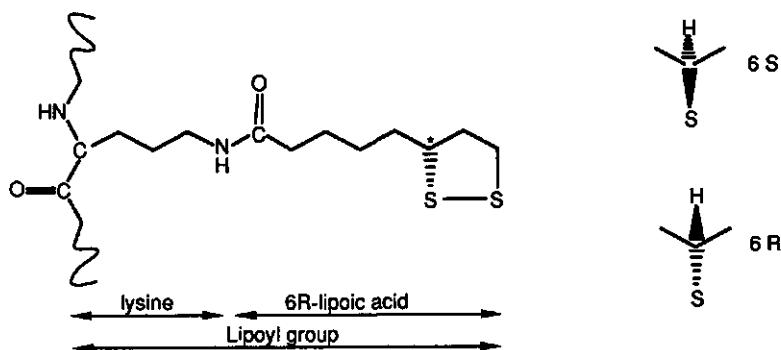


Fig. 1. Structure of lipoic acid linked to a lysine residue. The asterisk (*) denotes a chiral carbon atom of lipoic acid yielding the 6R or 6S configuration (L or D configuration respectively).

E2 component. The cofactor of component E1 is thiamine pyrophosphate (TPP). Component E2 is the acyl transferase that catalyses the transfer of the acyl group from the alkylated lipoyl group to coenzyme A. The reduced lipoyl group left after release of the acyl group is reoxidized by component E3, lipoamide dehydrogenase.

In order to be able to catalyse this oxidation, lipoamide dehydrogenase possesses a non-covalently linked FAD and a redox active active disulfide. The structure of the FAD is shown in Fig. 3.

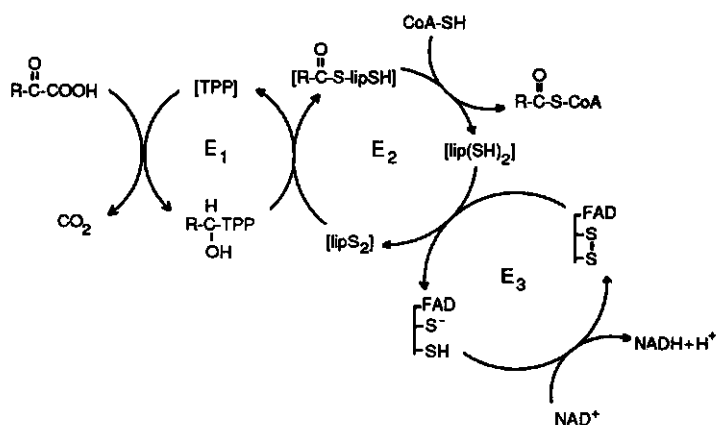


Fig. 2. Reaction sequence of the 2-oxo acid dehydrogenase complexes.

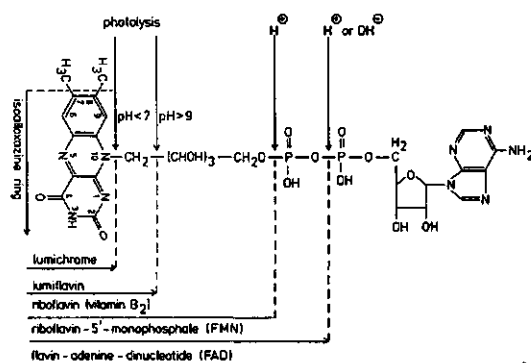


Fig. 3. Structure of FAD.

The reaction sequence for the glycine oxidation system is presented in Fig. 4. The oxidation of glycine results in the formation of methylene tetrahydrofolate, ammonia and CO₂. The reaction requires four enzymes: a pyridoxal phosphate containing enzyme (P- or P1-protein), an enzyme carrying the lipoyl group (H- or P2-protein), an enzyme catalysing the tetrahydrofolate step of the reaction (T- or P4-protein) and lipoamide dehydrogenase (L- or P3 protein). Abbreviated names are according to [11] and [10] respectively.

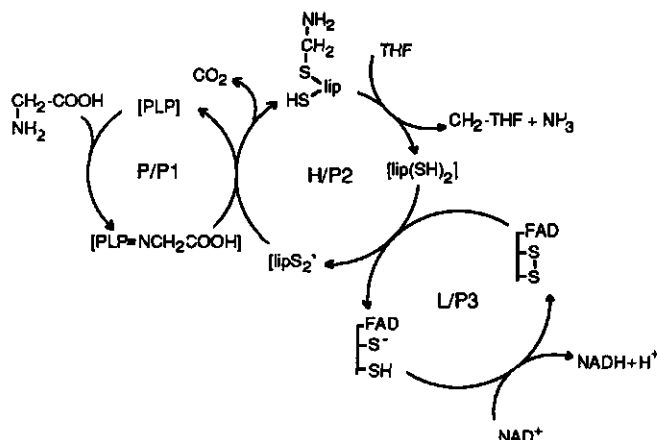


Fig. 4. Reaction sequence of the glycine oxidation system.

The role of lipoamide dehydrogenase in the galactose-, maltose uptake system is as yet not clear [13].

A family of enzymes

Lipoamide dehydrogenase as isolated from all sources investigated so far is a homodimeric enzyme with one FAD and one redox-active disulfide bridge per monomer. These features are not exclusive to lipoamide dehydrogenase but are characteristic for a group of enzymes. As a family, these enzymes are known as the pyridine nucleotide disulfide oxidoreductases. Other, well studied members of this family are glutathione reductase [EC 1.6.4.2], trypanothione reductase [EC 1.6.4.8], thioredoxin reductase [EC 1.6.4.5] and mercuric ion reductase [EC 1.16.1.1]. Less extensively studied are CoA-glutathione reductase [EC 1.6.4.6], cystine reductase [EC 1.6.4.1], asparaginate reductase [EC 1.6.4.7], bis- γ -glutamylcystine reductase and sulfhydryl oxidase. With the exceptions of mercuric ion reductase and sulfhydryl oxidase, all enzymes in this group catalyse electron transfer between NAD(P)(H) and a disulfide/dithiol. Lipoamide dehydrogenase and sulfhydryl oxidase are unique in this group since in the physiological direction the flow of electrons is from reduced substrate via FAD to NAD(P)⁺, while this flow is reversed in the other members. Nevertheless lipoamide dehydrogenase readily reduces lipoamide at the expense of NADH [3, 4].

For an excellent overview on this family of enzymes the reader is referred to a recent review by C.H. Williams Jr. [6].

Homology among pyridine nucleotide disulfide oxidoreductases

The genes encoding several of the pyridine nucleotide disulfide oxidoreductases have been cloned and sequenced, thus establishing the primary structures of these enzymes. From different sources sequences of the *lpd* gene, encoding lipoamide dehydrogenase, were reported. These comprise prokaryotic sequences, from *Escherichia coli* [20], *Pseudomonas putida* [21-23] and *Azotobacter vinelandii* [24], and three eukaryotic sequences, human [25], porcine [25] and yeast [26, 27]. In *Pseudomonas putida* three *lpd* genes were identified, two of the three *lpd* genes encode lipoamide dehydrogenases that function in the three different 2-oxo acid dehydrogenase complexes [9, 28]. The third *lpd* gene encodes a lipoamide dehydrogenase whose function in the wild-type organism is not clear yet [23]. Also the genes encoding mercuric ion reductase from different origin were sequenced [29, 30,

31], as were genes encoding glutathione reductase [32], trypanothione reductase [33] and thioredoxin reductase [34]. Not only DNA sequences yielded primary structures of the enzymes. Some parts of the amino acid sequences were obtained by peptide analysis long before the DNA-derived sequences became available as for example for lipoamide dehydrogenase [35, 36], glutathione reductase [37.] and thioredoxin reductase [38]. These partial sequences already showed that a considerable amount of amino acid identity exists between the different enzymes. This strong homology was reinforced by all the DNA derived primary structures. Table 1 lists the sequence identity.

	<i>E. coli</i> LD	<i>P. put.</i> LD	Pig LD	Hum. LD	<i>E. coli</i> GR	Hum. GR	Tn501 MR	Tn21 MR
<i>A. vin.</i> LD	40	42	47	48	25	27	29	29
<i>E. coli</i> LD		42	44	40	26	28	29	27
<i>P. put.</i> LD			39	39	24	21	24	24
Pig LD				95	29	28	27	27
Hum. LD					27	28	27	27
<i>E. coli</i> GR						54	27	27
Hum. GR							26	26
Tn501 MR								86

Table 1. Amino acid sequence identity matrix of several disulfide oxidoreductases. LD, lipoamide dehydrogenase; GR, glutathione reductase; MR, mercuric reductase; Hum., human; *P. put.*, *P. putida*; *A. vin.*, *A. vinelandii*.

Three dimensional x-ray structures. The homology between the enzymes is not only confined to the primary structures but also extends to the three dimensional structures as revealed by the structures of glutathione reductase [39-43], lipoamide dehydrogenase [44-46], thioredoxin reductase [47] and mercuric ion reductase [48]. Impressive is the similarity of the three dimensional x-ray structures of lipoamide dehydrogenase from *A. vinelandii* and human erythrocyte glutathione reductase. Although 'only' 27 % of sequence identity exists between those two enzymes, the overall structures are very similar [45].

For both enzymes the structure of the monomer can be divided into four domains: the FAD binding domain, the NAD⁺ binding domain, the central domain and the interface domain [39-46]. The interface domain contains the residues necessary for dimer formation. A schematic representation of the dimer is presented in Fig. 5. The FAD appears to be bound in an extended conformation in both enzymes [39, 45]. For

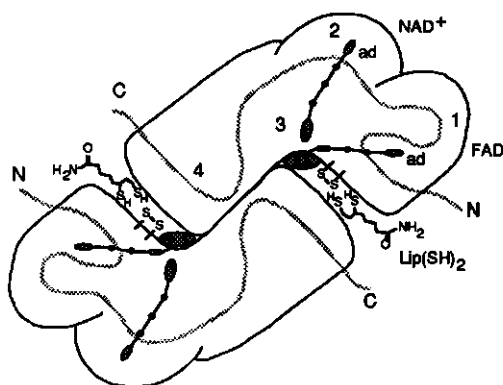


Fig. 5. Diagrammatic representation of the dimer structure of lipoamide dehydrogenase from *Azotobacter vinelandii*.

glutathione reductase crystal structures have been obtained with several ligands bound e.g. NADP⁺ and glutathione [42, 43]. Furthermore the structure of the 2-electron reduced enzyme was solved [42, 43]. Until now for *A. vinelandii* lipoamide dehydrogenase only the structure of the unliganded enzyme in its oxidized state was obtained, but from the extensive structural similarity with glutathione reductase and lipoamide dehydrogenase from *P. putida* [42, 43, 46] it is evident that binding of NAD⁺ occurs in an equivalent position to that of NADP⁺ in glutathione reductase.

Fig. 6 shows a drawing of the active site. This drawing is provided as an overview and is not claimed to be an accurate detail. The numbering of the amino acids is according to the *A. vinelandii* lipoamide dehydrogenase. A prime (') following a residue's number indicates that this residue is from the second subunit. Thus the drawing shows that each active site is built from elements of the FAD binding domain, the NAD binding and the central domain of one subunit as well as from the interface domain of the other subunit. The isoalloxazine part of the FAD divides the active site into two parts, at the *si*-side the dihydrolipoamide [lip(SH)₂] binding site and at the *re*-side the NAD⁺ binding site. The *re*- and *si*-faces of flavin are assigned following the rules of Hanson [49] with N-5 as the central atom. Accordingly the front and rear sides of the flavin in Fig. 3 are the *si*- and *re*-faces, respectively. The histidine at the *si*-side, His450', is the so-called 'active site base' and is oriented with N-3 toward the disulfide bridge, somewhat closer in the lipoamide dehydrogenase and glutathione reductase structures to the N-terminal Cys48/58 than to Cys53/63 [41, 42, 45], and plays a very important role in catalysis as will become clear in the following sections. Cys48 and Cys53 form the redox-active disulfide bridge. The sulfur of Cys48 faces out in the lip(SH)₂ binding site and suggests that this sulfur reacts with the substrate.

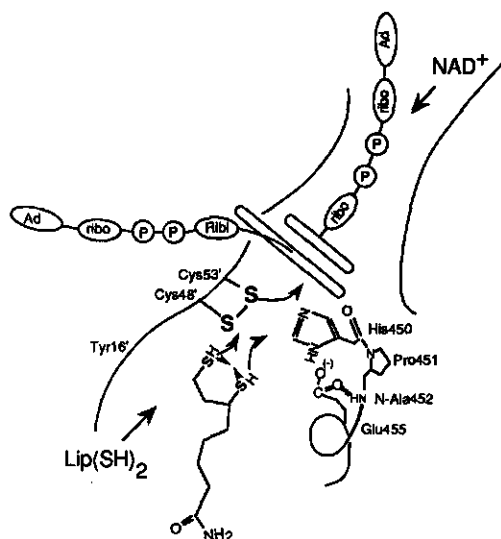


Fig. 6. Schematic representation of the active site of lipamide dehydrogenase from *Azotobacter vinelandii*.

For glutathione reductase, structural evidence for the formation of this bond between glutathione and Cys58 (the equivalent of Cys48 of the lipamide dehydrogenase structure) was obtained [42, 43]. Therefore Cys48 is referred to as the 'interchange thiol'. Upon reduction of the disulfide, the two protons associated with this process are presumed to be shared between the two thiols and the active site base. This results, as evidenced by spectral studies, in the formation of a red intermediate (this will be discussed in the next sections). The red colour has been ascribed to a charge-transfer complex in which the FAD is the acceptor and a thiolate is the donor [50]. The structural data now clearly show that the only possible candidate for a role as charge donor is the thiolate of Cys53. The negative charge of the thiolate is proposed to be stabilized by the positive charge on the protonated histidine [51] and by a dipole originating from an α -helix by residues 325 to 340 [42, 43, 45].

The glutamate at position 455' forms a short strong hydrogen bond with N-1 of His450'. An identical feature was found in the glutathione reductase structure and this prompted Pai and Schulz [43] to suggest that this glutamate is responsible for raising the pK_a of the active site base. The observation of a high pK_a of the active site base originated from spectral and kinetic studies on pig heart and *E. coli* lipamide dehydrogenase and glutathione reductase [51-57].

The structural data concerning the NAD^+ binding to lipamide dehydrogenase from *P. putida* shows that the binding to the oxidized enzyme is in a conformation that cannot

lead to effective electron transfer when bound in a similar way to the reduced enzyme [46]. In glutathione reductase NADPH binds in an extended conformation but before effective binding occurs, the incoming NADPH must displace a tyrosine (Tyr197) that shields the FAD from the solvent [43]. The pyridinium ring adopts a stacked conformation with the isoalloxazine with N-4 of the pyridinium close to N-5 of the isoalloxazine to allow good overlap of the π -orbitals (suggested already in 1960 [58]), and there is a close approach of N-4 to the Lys66/Glu201 ion pair [42, 43] that forms a salt bridge beneath the FAD in the vicinity of N-5. This ion pair is thought to be catalytically involved [43, 59]. In *A. vinelandii* lipoamide dehydrogenase the lys66/Glu201 ion-pair counterpart is formed by the ion-pair Lys57/Glu194 [45], however the Tyr197 counterpart is a valine.

Spectral properties

The spectral properties of lipoamide dehydrogenase are closely linked to kinetic properties. In order to understand the spectral features, key elements of the kinetics, that will be discussed in depth in following sections, will be presented here. Although there are two active sites per dimer, here it is assumed for simplicity that the active sites act independently and equivalently. Therefore the phenomena described will refer to one active site unless explicitly stated otherwise.

The presence of two redox-active groups in the active site, the FAD and the disulfide, indicates that the enzyme can take up four reducing equivalents. It was shown that the reducing equivalents are transferred in pairs [60]. Thus, three reduction levels can be discerned: the non-reduced enzyme, or as it will be referred to 'the enzyme in its oxidized state' [Eox], the 2-electron reduced enzyme [EH₂], and the 4-electron reduced enzyme [EH₄]. With respect to effective catalysis, only Eox and EH₂ are relevant [60, 61], during turnover the enzyme shuttles between Eox and EH₂.

For all lipoamide dehydrogenases studied so far catalysis in the forward direction takes place according to a ping-pong mechanism [56, 58, 62-64] although this has been questioned [65, 66]. The reactions can be represented as follows:



According to these reactions EH₂ is a 'free' unliganded enzyme species and studies of this species might give more insight into the mechanism of the enzyme. EH₂ cannot

only be obtained by reduction of Eox by lip(SH)_2 but also by dithionite, borohydride or dithiothreitol, avoiding any complications of the presence of lipS_2 .

Oxidized enzyme. In Fig. 7 representative spectra of Eox, EH_2 and EH_4 of pig heart lipoamide dehydrogenase are shown [52, 58]. When compared to free FAD, the spectrum of Eox shows that the major flavin band at 455 nm is 5 nm red-shifted. The two major absorption bands have much more vibrational fine structure as demonstrated

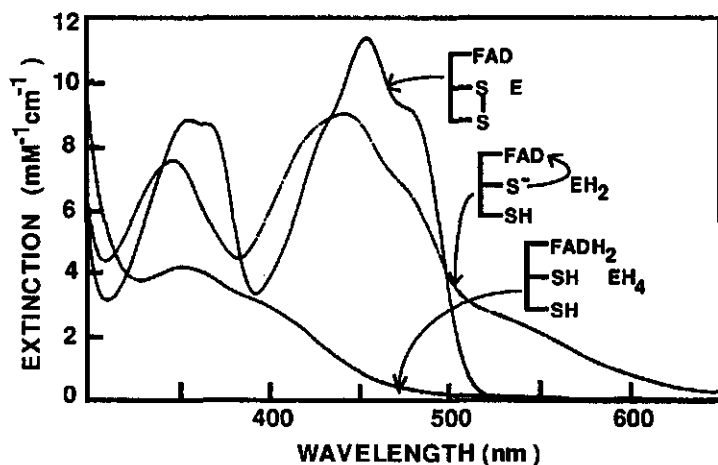


Fig. 7. Spectra of pig heart lipoamide dehydrogenase. The reductant was dithionite, pH 7.6. From ref. [6].

by the shoulders at 370, 440 and 480 nm. These features are indicative for a flavin in an apolar environment [67]. The extinction coefficient at 455 nm is $11.3 \text{ mM}^{-1} \text{ cm}^{-1}$ [68]. Eox is also fluorescent. For glutathione reductase a similar absorbance spectrum was reported (λ_{max} at 460 nm) however this enzyme is almost not fluorescent due to the presence of a stacked tyrosine. From site directed mutagenesis studies on *E. coli* lipoamide dehydrogenase, the Eox spectrum of the wild-type enzyme almost identical to pig heart enzyme and also highly fluorescent, it appeared that similar spectral properties (shift of absorbance maximum to 462 nm and strong quenching of fluorescence) as reported for glutathione reductase were obtained after changing Ile184, the counterpart of Tyr197 of glutathione reductase, into Tyr [69].

2-electron reduced enzyme. In the late fifties and early sixties extensive studies on pig heart lipoamide dehydrogenase were performed. The addition of one molar equivalent with respect to FAD of lip(SH)_2 or dithionite resulted in a typical spectrum, designated EH_2 in Fig. 7. Studies with arsenite showed that the typical spectrum was

due to the presence of a reduced disulfide and mechanisms involving flavin-sulfur-bi-radicals were proposed [58, 60]. It was Kosower [50] who suggested that the typical spectrum arose from a charge-transfer interaction between a thiolate and FAD in which the thiolate is the donor and the oxidized FAD the acceptor. Therefore EH_2 with the spectrum showing the typical absorbance at 530 nm is now called the 530 nm charge-transfer species. The ability to isolate monomeric apoenzyme under nonreducing conditions showed that the disulfide is not between the subunits but within one subunit [63, 70]. Peptide sequence analysis of pig heart enzyme showed that the two cysteines forming the disulfide are only separated by five amino acids [36].

The EH_2 spectrum of pig heart enzyme thus shows that the reducing equivalents mainly reside on the disulfide and it was shown that a large excess of $\text{lip}(\text{SH})_2$ did not reduce the enzyme beyond the EH_2 level [60], demonstrating that the EH_2 species is stable under anaerobic conditions. Further reduction than EH_2 was however easily accomplished by reduction with more than one molar equivalent of dithionite which resulted in formation in EH_4 [4, 52, 58]. For *E. coli* lipoamide dehydrogenase it was reported that a small excess of $\text{lip}(\text{SH})_2$ resulted in over-reduction to EH_4 and the addition of one molar equivalent of $\text{lip}(\text{SH})_2$ resulted in an EH_2 spectrum with a less intense 530 nm charge-transfer band [63]. These phenomena will be discussed later.

Thiol to FAD electron transfer. The characteristic EH_2 spectra were also obtained for glutathione reductase and mercuric ion reductase after reduction with one molar equivalent of dithionite [5, 71, 72]. When both EH_2 of pig heart lipoamide dehydrogenase and glutathione reductase were reacted with the thiolate specific reagent iodoacetamide it appeared that only one mole of iodoacetamide reacted per mole of FAD, while two moles of thiol(ate)s are present per FAD [54, 73-75]. Furthermore the spectrum of pig heart enzyme changed to a spectrum typical for FAD (enzyme) in its non-reduced state, however, 7 nm blue shifted, while the spectrum of glutathione reductase retained its typical EH_2 spectrum. For the monoalkylated glutathione reductase as well as the monoalkylated lipoamide dehydrogenase it was shown that differential reactivity of the two nascent thiols exists and that in both cases the cysteine closer to the N-terminus was labeled [73]. The resulting spectrum of monoalkylated glutathione reductase shows that the charge-transfer thiol is not alkylated [54]. For lipoamide dehydrogenase this was shown by titration of the monoalkylated enzyme with NAD^+ [74, 75] which resulted in a partial bleaching of the spectrum (see Fig. 8) with a concomitant rise of the absorbance at 380 nm. Only 1.2 moles of NAD^+ reacted with the 2 moles of active site per mole of dimer. Extrapolation of the spectra to full formation on both monomers resulted in the dotted spectrum of Fig. 8. This spectrum bears close resemblance to a C4a-thio-substituted-dihydroflavin

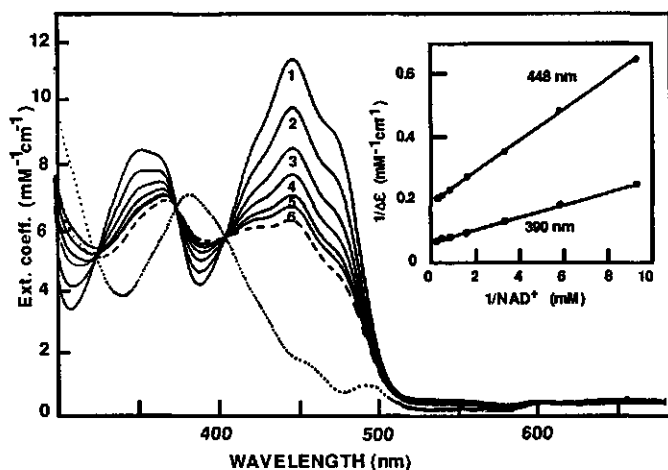
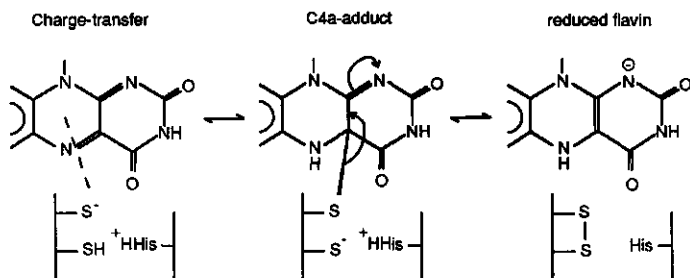


Fig. 8. Spectral changes induced by titration of monoalkylated pig heart enzyme (1) as mixed with increasing concentrations of NAD^+ (2-6 respectively). Equal concentrations of NAD^+ were added to the reference cuvette. The dashed line is the spectrum extrapolated to infinite NAD^+ by using the $1/\Delta\epsilon_{448}$ intercept from a double reciprocal plot (inset). The dotted line is an estimate of the spectrum of the modified flavin species after correction from the contribution of residual unmodified flavin. From ref. [75].



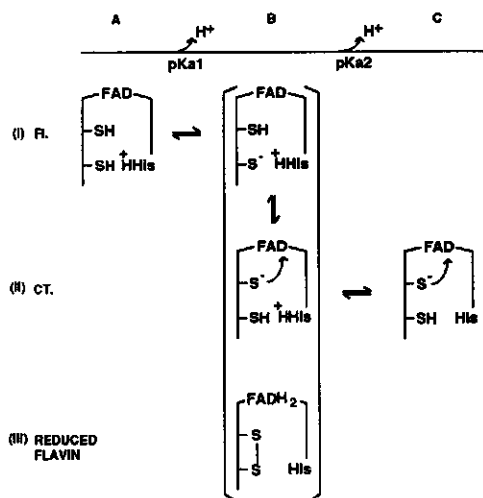
Scheme 1. Formation and breakdown of the thiolate to C4a-FAD adduct. From ref. [75].

derivative and it was therefore concluded that NAD^+ induces adduct formation between the remaining non alkylated sulfur of the carboxy-terminal cysteine and the FAD at the C4a position [74, 75]. This adduct formation has been observed in 1-deaza-FAD substituted thioredoxin reductase [76] and in wild-type and mutated mercuric ion reductase [77, 78]. Since its discovery the C4a adduct, which is formed within 3 ms and is fully reversible, is proposed as the catalytic intermediate upon transfer of the electrons from the reduced disulfide via the flavin to NAD^+ or vice versa. The adduct formation is presented in Scheme 1. The specificity of the alkylation of the N-terminal cysteine indicates that this thiol is most exposed and likely interacts with the substrates,

hence its name 'interchange thiol'. The thiol closer to the FAD, the C-terminal cystine, was named 'charge-transfer thiol'.

A base in the active site. For simplicity the above results are presented in a way as though protons are not involved in the process of reduction of lipoamide dehydrogenase. They are however involved, but it doesn't change the conclusions drawn. Williams [5] first suggested the involvement of a base in the active site in order to accept a proton of the substrate lip(SH)₂ allowing facilitated nucleophilic attack of the disulfide by the thiolate of the substrate. Evidence for this base was obtained from studies on the pH dependence of the redox potentials and from pre-steady state kinetics (see sections on redox potentials and pre-steady state kinetics for details). Further evidence for this base was gained from studies on *E. coli* lipoamide dehydrogenase using a bifunctional arsenoxide [79, 80] which demonstrated that this base is a histidine. The latter finding was confirmed by the three dimensional X-ray structure of glutathione reductase [39-43] and lipoamide dehydrogenase [44-46], and by site directed mutagenesis experiments on both these enzymes where the histidine was replaced by other residues [81-83].

pH dependent spectral properties of EH₂. The presence of the histidine and two cysteines in the active site thus demonstrates that at least three titratable groups can contribute to the spectral properties of EH₂. A very careful analysis of the pH dependent properties of *E. coli* lipoamide dehydrogenase by Wilkinson and Williams [53, 84] yielded much insight into the distribution of tautomeric/electronic species at the EH₂ level which are depicted in Scheme 2. The central column shows the three forms that predominate at neutral pH. The central form is the charge-transfer species which is non-fluorescent and favored by high pH. The upper form is the fluorescent prototropic tautomer of the charge-transfer species favored by low pH. The lower species in the central column has the electrons on the flavin and is somewhat favored by low pH. The assignment of the high pK_a to the histidine was based on kinetic studies [51]. For *E. coli* enzyme the pK_a values as attributed to the charge-transfer thiol and histidine are 5.7 and 8.2 respectively [53], 5.9 and 7.5 respectively in 0.2 M guanidinium hydrochloride [84]. Extrapolation to fully formed EH₂ at each pH yielded values for fluorescence and 530 nm charge-transfer absorbance which in turn were extrapolated to zero fluorescence and zero charge-transfer absorbance in order to obtain the maximal charge-transfer absorbance and the maximal fluorescence respectively. It appeared that the maximal charge-transfer reached an extinction coefficient of 3.3 mM⁻¹ cm⁻¹ and the maximal fluorescence was 68% of the Eox. From stopped flow experiments a similar high value for the extinction coefficient of the charge-transfer absorbance



Scheme 2. Model for the pH dependence of the spectroscopic properties of *E. coli* lipoamide dehydrogenase at the EH_2 level. The protonation states are represented by the columns labeled A, B and C. The three spectrally distinct species are represented by rows and are labeled I, II and III. The arrows of forms IIB and IIC signify the charge-transfer interactions between the thiolates and the FAD and are drawn from the donor to the acceptor. From ref. [53].

was obtained immediately after mixing of the enzyme with $\text{lip}(\text{SH})_2$ however it decreased gradually in time [53] as a result of tautomerisation and formation of the reduced FAD EH_2 species (FIH^- species) and over-reduction to EH_4 . The maximal value of $3.3 \text{ mM}^{-1} \text{ cm}^{-1}$ for the extinction coefficient was also obtained for EH_2 of pig heart enzyme [55] showing that the lower charge-transfer absorbance of *E. coli* enzyme is due to the presence of the other two species [53] and suggesting that in pig heart enzyme the charge-transfer species prevails.

A complicating factor in the studies of the *E. coli* enzyme was a phenomenon known as disproportionation [53, 84] that accounted for a loss of charge-transfer absorbance of 20 %. This means that 2EH_2 react to Eox and EH_4 . Disproportionation appeared to be enhanced in the presence of lipS_2 or reaction products after dithionite reduction [53]. The reverse process, formation of EH_2 from Eox and EH_4 was also observed and is known as comproportionation [53]. In pig heart enzyme disproportionation was observed though this contributed to a much lesser extent [55]. The difference in extent of disproportionation was attributed to differences in redox potentials between the enzymes.

The pH dependence of the spectral properties of EH_2 of pig heart lipoamide dehydrogenase and glutathione reductase essentially follows Scheme 2, with the

exception that the charge-transfer absorbance is much higher which is explained in terms of the equilibrium among the different electronic species being in favor of the charge-transfer species [55]. The pK_a values obtained for pig heart enzyme and glutathione reductase are respectively; 4.4 and 4.8 for the charge-transfer thiol and 8.7 and 9.2 for the histidine [55].

In an attempt to simplify the titration behaviour of EH_2 site directed mutagenesis experiments were performed recently to replace either of the thiols or the histidine by non-titratable residues [57, 81-83 , 85]. Replacement of the interchange cysteine resulted in enzymes showing 530 nm charge-transfer absorbance in their oxidized state. The general conclusion is that replacing the interchange thiol affects both pK_a 's of the wild-type enzyme; the pK_a of the charge-transfer thiol is lowered while the pK_a of the histidine is raised. The shift of the pK_a 's was explained by mutual influences of the charge-transfer thiolate and the imidazolium in analogy to papain [51]. Upon replacement of the histidine in *E. coli* lipoamide dehydrogenase by glutamine the pK_a of the charge-transfer thiol increases to 7.4 [83].

Spectral changes in the presence of pyridine nucleotides. The spectral properties of lipoamide dehydrogenase in the presence of (reduced) pyridine nucleotides are quite different from those presented above. Fig. 9 depicts pig heart enzyme reduced by 3 molar equivalents of NADH and the effect of addition of NAD^+ to this reduced species (from ref. [86]). Typical for reduction by NADH of all lipoamide dehydrogenases studied in this respect is the formation of a long wavelength absorbance, extending beyond 750 nm, which shows considerably different intensities at 750 nm depending on the source of the enzyme. This long wavelength absorbance is attributed to a charge-transfer complex between reduced flavin and NAD^+ [58, 60, 87]. In case of pig heart enzyme the intensity at 750 nm is low while the absorbance at 530 nm is high (see Fig. 9). This has led to the proposal that upon reduction with NADH in pig heart enzyme the electrons mainly reside on the disulfide. Further reduction beyond the level shown cannot be accomplished with NADH [86]. Addition of NAD^+ to the NADH reduced enzyme resulted in a shift of the long wavelength absorbance with a maximum around 570-580 nm [86]. The spectral change induced upon addition of NAD^+ appeared to be very rapid (complete within 3 ms) and from this it was concluded that this species might be a catalytic intermediate [86]. Matthews and coworkers [88] titrated EH_2 , generated by reduction with dithionite, with NAD^+ and found a similar spectrum as shown in Fig. 9. Their conclusion was that the spectrum represented an enzyme species with the electrons on the disulfide and with NAD^+ bound. Titration of pig heart lipoamide dehydrogenase in the presence of NADase with NADH

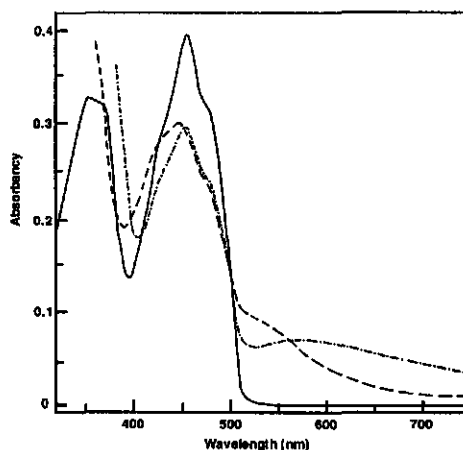


Fig. 9. Visible absorbance spectra of pig heart lipoamide as obtained after reduction with 3 molar equivalents of NADH (---) followed by addition of 100 molar equivalents of NAD^+ (- · - · -) at pH 7.6. (—) Eox (35 μM). From ref. [86].

preincubated with NADase led to further reduction than shown in Fig. 9. Addition of NAD^+ restored the spectrum, though, due to the presence of NADase, the spectrum gradually changed to the one of a more reduced FAD with concomitant loss of the absorbance at 530 nm and a rise at 750 nm [60]. From this, and from kinetic studies (see section on kinetics) it was concluded that NAD^+ prevents the pig heart enzyme from being over-reduced to the EH_4 state.

The spectral changes upon reduction by NADH reported for *E. coli* lipoamide dehydrogenase are somewhat different than those reported for pig heart enzyme [63]. One molar equivalent of NADH resulted in a further reduction of the FAD than reported for pig heart enzyme and a much lower 530 nm absorbance while the long wavelength absorbance (>600 nm) was higher [63]. Also the enzyme was easily further reduced toward the EH_4 level by excess of NADH indicating that there is a difference in redox potential between pig heart and *E. coli* enzyme [61]. Also for *E. coli* enzyme NAD^+ appears to prevent the enzyme from being over-reduced to EH_4 though not fully and at much higher NAD^+ concentrations [61].

For both *E. coli* and pig heart enzyme it was shown that arsenite blocks the disulfide of pre-reduced enzyme [60, 63]. Addition of NADH to these enzymes results in reduction of the FAD with special characteristics: the shoulders of the FAD are retained and a long wavelength absorbance develops with a maximum around 700-730 nm [60, 63]. Treatment of the enzymes showing this spectrum with NADase resulted in a loss of this long wavelength absorbance. Therefore it was concluded that this absorbance

arises from a charge-transfer complex between the reduced FAD and NAD⁺. This charge-transfer complex could be different from the one previously mentioned in this section due to the slightly shifted maximum.

Spectral properties of the enzymes were also studied using other pyridine nucleotides then the physiological substrates NAD⁺ and NADH. For both enzymes it was shown that NADPH was a reductant. The spectra were however similar to those obtained by reduction with dithionite or lip(SH)₂, i.e. no long wavelength absorbance typical for a charge-transfer interaction between reduced flavin and NADP⁺ was detected [63, 87] showing that no correct binding of NADP⁺(+)(H) occurred. Other NAD⁺ analogs, like 3-acetylpyridine adenine dinucleotide [AcPyAde⁺], 3-aminopyridine adenine dinucleotide [AAD⁺] and nicotinamide hypoxanthine dinucleotide [NHD⁺] and their reduced forms did however result in spectral characteristics upon reacting with either reduced or oxidized enzyme as was shown by Matthews and coworkers [88].

A marked change of both the *E. coli* and the pig heart EH₂ spectrum occurred after the addition of AAD⁺: a shift of the 530 nm absorbance to longer wavelength took place accompanied by a rise of the absorbance [84, 88]. As to the nature of the species exhibiting this spectrum no clues were obtained about the electron distribution between the disulfide and the FAD [88].

Reduction of pig heart enzyme with AcPyAdeH in the stopped flow instrument revealed a dead time spectrum with low long wavelength absorbance from 510 nm extending beyond 750 nm with no clear maximum [88]. Furthermore it was shown that in the dead time no AcPyAdeH was oxidized. Additionally, no isotope effect was found for the formation of the dead time spectrum, while an isotope effect of 2.6 was found for the hydride transfer leading to formation of EH₂. These observations led to the conclusion that the dead time spectrum represented the Michaelis complex of Eox and AcPyAdeH and that the low long wavelength absorbance was due to the charge-transfer complex between FAD and AcPyAdeH [88]. Due to the very high rate of reduction by NADH of any lipoamide dehydrogenase studied in this respect, no spectral evidence for an Eox-NADH complex was ever observed.

During the reoxidation of pig heart EH₂ by AcPyAde⁺ and NHD⁺ in the stopped flow instrument dead time spectra were obtained with a maximum around 580 nm [88], similar to the spectrum shown in Fig. 9 after addition of NAD⁺ to the reduced enzyme. Also reduction by NHDH yielded such a spectrum [88]. It was concluded that these spectra represent a species with the disulfide reduced (dithiol), the FAD oxidized and a pyridine nucleotide bound [88]. From the change in these spectra when compared to EH₂ it was inferred that the binding of a pyridine nucleotide influences the equilibrium distribution of electrons between the FAD and the reduced disulfide such as to increase

the amount of reduced FAD [88]. This implication will be addressed in the section on redox potentials.

Recently, mutated *E. coli* lipoamide dehydrogenases were described in which Lys53 was replaced with arginine or Ile184 with tyrosine [59, 69]. The lysine is the counterpart of Lys66 of glutathione reductase where the lysine forms an ionpair with Glu201. This ionpair is very close to N-5 of the FAD [45] and is thought to be involved in modulating the redox potential of the FAD [43, 59]. Ile184 is the counterpart of Tyr197, the residue to be displaced when NADPH binds to glutathione reductase [43] (see section on three dimensional structures). Upon reduction of the Lys53→Arg and Ile184→Tyr mutated enzymes by one molar equivalent of NADH the spectra revealed a much stronger reduction of the FAD and especially for enzyme Lys53→Arg an increased FADH⁻-NAD⁺ charge-transfer when compared to the wild-type enzyme [59]. The differences in FADH⁻-NAD⁺ charge-transfer among the wild-type and the mutated enzymes is most likely attributable to differences in affinity for NAD⁺ [59]. Furthermore in the Ile184→Tyr mutated enzyme the spectrum of Eox closely resembles the spectrum of glutathione reductase, a shift of the absorbance maximum to 462 nm. Also the fluorescence quantum yield of this enzyme decreased significantly and was similar to that as found for glutathione reductase [59, 69].

Summary of spectral species. In Fig. 10 (p 28) all species of lipoamide dehydrogenase that were spectrally identified are presented together with the absorbance maxima of the charge-transfer band and visible appearance.

Redox potentials

In the active site of lipoamide dehydrogenase two redox active groups are present, the disulfide and the FAD. The formation of a stable EH₂ form in pig heart enzyme with the reducing equivalents on the dithiol as evidenced by the 530 nm charge-transfer absorbance indicates that the redox potentials of the disulfide and the FAD are well separated. In the *E. coli* enzyme relatively easy over-reduction to the EH₄ state occurs, suggesting that the redox potentials of those two groups are less well separated [53]. For both enzymes the redox potential of each couple was determined [52, 53]. For pig heart enzyme the reported potentials of the couple E₂ for the disulfide/dithiol (Eox/EH₂) and of the couple E₁ for FAD/FADH⁻ (EH₂/EH₄) are -0.280 V and -0.348 V respectively at pH 7.0 [52]. The pH dependence $\Delta E/\Delta pH$ was shown to be -0.06 V in the pH range 5.5 to 7.6 for both couples. From this pH dependence, showing that two protons as well as two electrons are involved while simultaneously thiolate to FAD

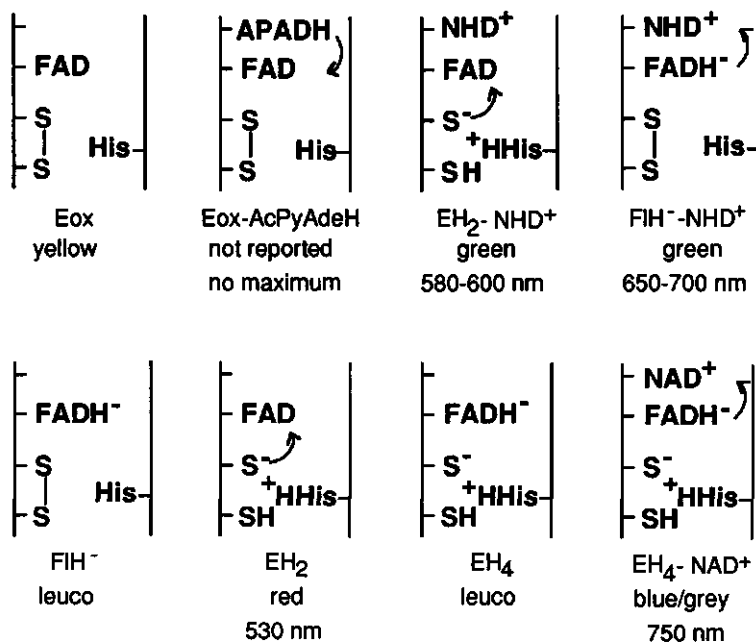


Fig. 10. Summary of spectrally identified catalytic intermediate species of liponamide dehydrogenase.

charge-transfer was observed, it was tentatively concluded that a base participates in the active site [52]. For the *E. coli* enzyme the potentials at pH 7.0 are -0.264 V for couple E_2 and -0.317 V for couple E_1 [ref. [167] in [6]] with the same pH dependence as found for the pig heart enzyme [53]. Both potentials are more positive in the *E. coli* enzyme than in the pig heart enzyme and the difference between them is less, making the *E. coli* enzyme more easily reducible to the EH_4 level. The redox potentials at pH 7.0 of the couples $\text{lipS}_2/\text{lip}(\text{SH})_2$ and NAD^+/NADH are -0.281 V and -0.320 V respectively. Since the pH dependence of the couple NAD^+/NADH is -0.03 V / pH unit, the reduction of EH_2 to EH_4 by NADH is more easily accomplished at low pH [52].

During catalysis the electron flow is from dithiol via FAD to NAD^+ . Purely based on the redox potentials of the respective couples, especially in the pig heart enzyme, the electrons have to overcome a thermodynamic hill, the FAD moiety. It is therefore likely that the redox potential of the FAD in the NAD^+ bound enzyme is higher than in the free enzyme and thus NAD^+ serves as an effector to facilitate electron transfer from the dithiol to the FAD. This effector role of NAD^+ was indicated in two different ways. The first one was by spectral analysis of titration of pig heart EH_2 with NAD^+ and NHD^+ . This

resulted in a clear shift of the charge-transfer absorbance maximum to 580 nm and was explained in terms of a decreased excited state oxidation-reduction potential of the charge donor (thiolate) and acceptor (FAD) implying a decreased energy necessary for ground state electron transfer [52]. The second indication was obtained by calculation of the redox potentials of the couples E_1 and E_2 for pig heart enzyme based on steady state kinetic- and dissociation constants which revealed that both couples were 30 mV more positive in the NAD^+ bound enzyme [89].

Kinetics of the forward and reverse reactions

Steady state kinetics. All lipoamide dehydrogenases studied thus far in this respect, except for lipoamide dehydrogenase from *A. vinelandii* and pig heart [66, 65], function according to a ping pong bi bi mechanism in the physiological direction [56, 60-64]. The kinetic parameters of the enzymes are presented in Table 2. For pig heart and rat liver enzyme it was shown that the reverse reaction proceeds via the same mechanism [62, 64], which was questioned too [65], and remains the same in pig heart enzyme when studied with lipoamide dehydrogenase complexed in the OGDC [90]. For both the pig heart [65] and the *A. vinelandii* enzyme [66] a ternary complex mechanism was proposed. This was based on the fact that the LB-plots were convergent and on product inhibition studies [65]. This was supported for pig heart enzyme by the communication of two NAD^+ binding sites, one high affinity site ($K_d = 50-60 \mu M$) and one low affinity site ($K_d=200-250 \mu M$) per monomer on the oxidized enzyme [91]. However, Wilkinson and Williams [61] argued that the apparent ordered mechanism could be explained by assuming dead end complexes to occur, a phenomenon that is common to ping pong enzymes and was demonstrated for the rat liver and *E. coli* enzyme [61, 64].

The physiological reaction of *E. coli* lipoamide dehydrogenase proved difficult to study due to severe product inhibition [63]. Use of an electron acceptor with higher midpoint potential than NAD^+ , *in casu* $AcPyAde^+$, revealed that the mechanism of this enzyme is also ping pong bi bi [63]. Later studies, using the stopped flow spectrophotometer, allowed the use of NAD^+ as a substrate [56]. These studies reinforced the finding that the enzyme functions according to a ping pong bi bi mechanism. Furthermore these studies showed that the plot of NAD^+ versus velocity did not obey the simple Michaelis Menten equation, but required an equation taking cooperativity into account. The Hill coefficient of 1.1-1.4 indicated modest positive cooperativity at the EH_2 level. From steady state kinetics no further indications of cooperativity for the other lipoamide dehydrogenases were reported except for rat liver enzyme which showed slight negative cooperativity at the first substrate level at $25^\circ C$

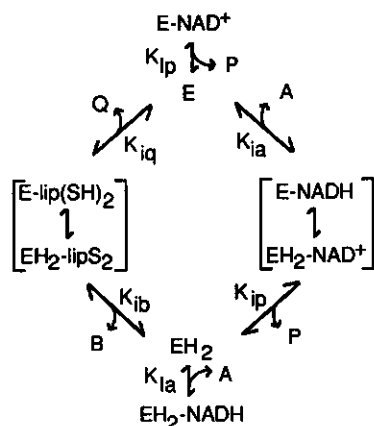
Parameter	pig heart	rat liver	<i>E. coli</i>
Forward reaction			
K_m lip(SH) ₂ (μ M)	300	490	-
K_m NAD ⁺ (μ M)	200	520	230
turnover number#	550	690	420
pK _a V	6.3	7.0	6.7
Reverse reaction			
K_m NADH (μ M)	-	62	-
K_m lipS ₂ (μ M)	-	84	-
turnover number#	530	248	-
pK _a V	7.9	-	-
assay conditions	25°C, pH 7.6	37°C, pH 8.0	25°C, pH 7.5
Reference	88	64	56

Table 2. Kinetic parameters for lipoamide dehydrogenases.
moles substrate \times mole FAD⁻¹ \times sec⁻¹.

[64]. For pig heart enzyme cooperativity was reported in monoalkylated enzyme titrated with NAD⁺ [75] (see above) and from titration experiments of Eox with NAD⁺ [91].

Studies of pig heart enzyme in the reverse reaction revealed a significant pH dependent lag in NADH oxidation by lipS₂. The rate of the reaction accelerated as NAD⁺ was produced, but was negligible if NADase was present in the assay mixture. NAD⁺ administration to the starting mixture abolished the lag-phase [60]. Closer examination of this phenomenon showed that the acceleration, optimum at pH 6.3, was not due to enhanced affinity of EH₂ for lipS₂ in the presence of NAD⁺ but was merely due to the reoxidation of inactive EH₄ to EH₂ by NAD⁺ and so enhancing the steady state concentration of EH₂ [92]. Additionally it was shown that NAD⁺ also acts as a product inhibitor though at higher concentrations (apparent $K_{\text{activation}} = 5 \mu\text{M}$, $K_{\text{inhibition}} = 280 \mu\text{M}$) [92].

For *E. coli* enzyme the same autocatalytic time course as found for pig heart enzyme was observed in the reverse reaction [61]. Detailed analysis of this reaction showed that the same conclusions drawn from the pig heart enzyme also apply to the *E. coli* enzyme [61]. NAD⁺ serves both as an activator, though with a pH dependent apparent binding constant of NAD⁺ with the optimum at pH 8.0 ($K_a = 0.4 \text{ mM}$), and as an inhibitor ($K_i = 1.0 \text{ mM}$). It was shown that inhibition was of the dead-end type with Eox-NAD⁺ as the dead-end complex. Furthermore, a dead-end inhibition by NADH was shown at the EH₂ level resulting eventually in formation of EH₄. The activation by NAD⁺ was again attributed to reoxidation of EH₄ to EH₂ [61]. In Scheme 3 a model is presented of the catalytic cycle and the dead end complexes.



Scheme 3. Model depicting the catalytic cycle and dead-end complexes in catalysis by liponamide dehydrogenase. A, B, P and Q are NADH, lipS₂, NAD⁺ and lip(SH)₂ respectively. From ref. [61].

Pre-steady state kinetics. The pre-steady state kinetics have most extensively been studied with the pig heart enzyme. Massey, Gibson and Veeger [62] were the first to determine the rates of reduction of the enzyme by lip(SH)₂ and reoxidation of EH₂ by NAD⁺. The reported rate constants at 25 °C, pH 7.6, 555 s⁻¹ for lip(SH)₂ reduction and > 800 s⁻¹ for reoxidation in relation with the steady state turnover number (575 s⁻¹) clearly demonstrated that the reductive reaction is rate limiting in overall catalysis and that species at the EH₂ level are relevant intermediates.

A very detailed analysis of the pre-steady state kinetics of pig heart enzyme comprising reductive and oxidative reactions was reported by Matthews and co-workers and has yielded much insight in the mechanism of the enzyme [51, 88]. The reduction of the enzyme by lip(SH)₂ appeared to proceed at a rate of 830 s⁻¹ between pH 5.5 and 8.0, thus is independent of pH in this range. The rate of the reoxidation reaction of EH₂ by lipS₂ however was maximal at pH 6.2 (880 s⁻¹) and appeared to be governed by a pK_a of 7.9 on the EH₂-lipS₂ complex [51]. These results, in conjunction with the pH dependence of the redox potential of E₂, provided conclusive evidence that a base is involved in catalysis which has a low pK_a (5.5) in Eox and a high pK_a (7.9) in EH₂ [51].

The presence of the base as proposed by Williams [5], now known to be a histidine, substantiates the proposed mechanism of proton abstraction from the substrate by the His forming a thiolate anion and facilitating nucleophilic attack of the disulfide. According to this mechanism, presented in Scheme 4, upon reaction of the activated

in the reverse reaction, the reductive reaction appeared to be rate limiting, the rate of reduction being decreased by two orders when compared to NADH. In the reaction $\text{lip(SH)}_2 / \text{AcPyAde}^+$ at pH 8.0, the reoxidation by AcPyAde^+ was shown to be rate limiting. Here also the rate of the analog decreased two to three orders of magnitude, at pH 7.6 and 6.3 respectively. Identical studies with the analogs NHD(H)^+ showed that the rate of reduction by NHDH had decreased one order and the rate of reoxidation of EH_2 had decreased two orders [88].

The slower rates of the analogs in all reactions enabled the spectral identification of several possible intermediates in the reaction mechanism of pig heart lipoamide dehydrogenase [88]. These species were presented in the section on spectral properties of lipoamide dehydrogenase. Attempts to identify the FAD-C4a adduct species were unsuccessful.

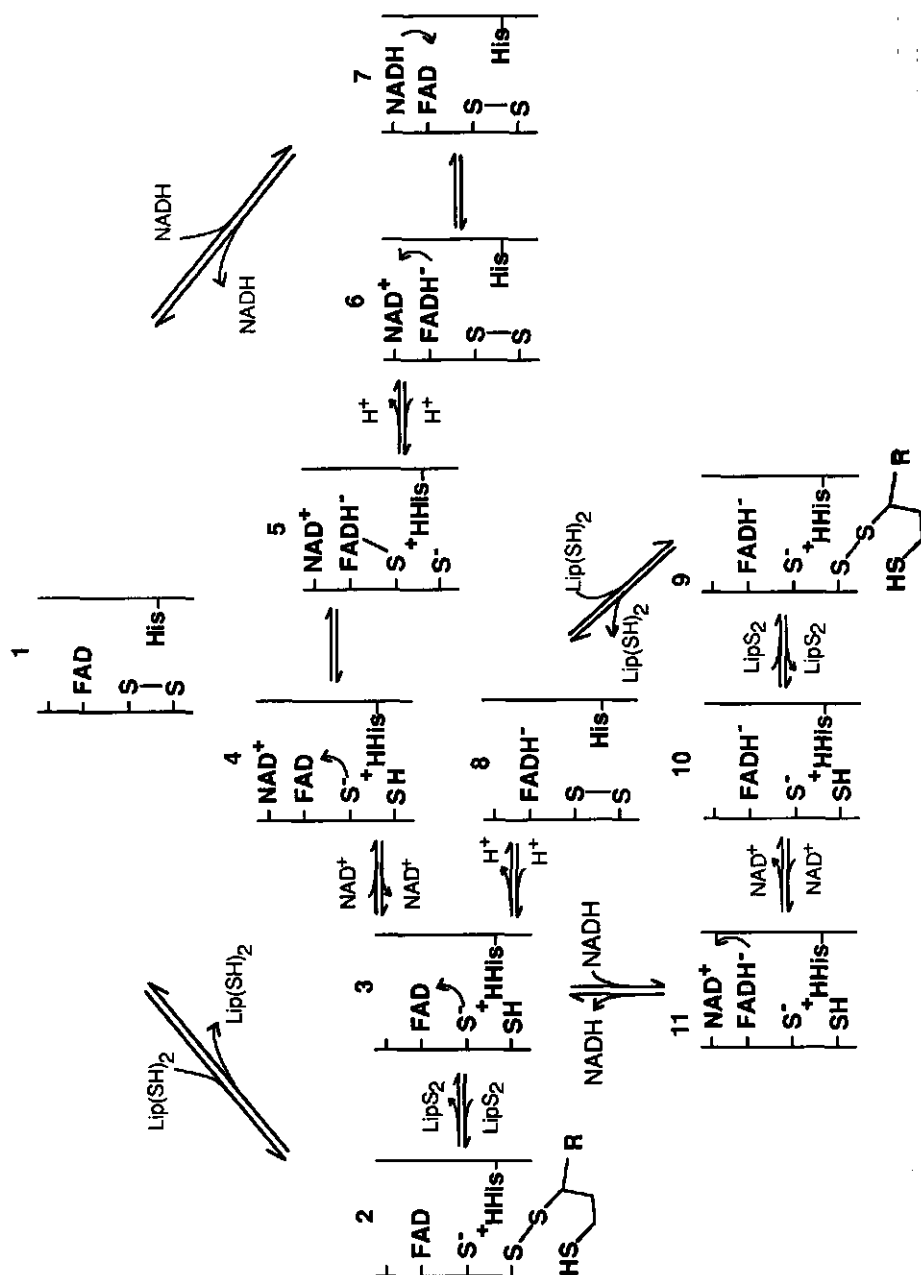
For *E. coli* enzyme it was reported that both the reductive reactions to EH_2 by lip(SH)_2 as well as NADH are very fast at pH 7.6 [63, 69], and are in fact complete within the dead-time of the stopped flow instrument. The further reduction to EH_4 proceeds at slower rates, 100 s^{-1} for NADH reduction and via a biphasic process for lip(SH)_2 reduction at rates of 0.6 s^{-1} and 0.35 s^{-1} [69].

All species involved in catalysis, identified and proposed, together with species resulting from over-reduction to EH_4 are shown in Scheme 5 (p 34).

Site specifically altered enzymes. As already mentioned in the section on spectral properties, site directed mutagenesis experiments on *E. coli* lipoamide dehydrogenase were reported very recently. The residues that were subjected to mutagenesis are Cys44, Cys49, Lys53, Ile184 and His444 [85, 59, 69, 82, 83].

Both cysteines were replaced by serine [85]. In view of the very important role of these residues in catalysis it is not surprising that these mutated enzymes lack any activity in the physiological reaction [85]. Nevertheless these mutated enzymes still possess some activity with the artificial electron acceptor ferricyanide when NADH is the donor. The turnover number is 10 % and 50 % when compared to wild-type enzyme for enzyme Cys44->Ser and Cys49->Ser respectively [85].

Lys53 forms a saltbridge with Glu188 (see section on three dimensional structures) and it was thought that the positive charge in the pyridine nucleotide binding site was involved in modulating the redox potential of the FAD. Therefore Lys53 was replaced by Arg for minimal disturbance [59]. For this mutated enzyme strong inhibition by the electron donor was reported in both the $\text{lip(SH)}_2/\text{NAD}^+$ and $\text{NADH}/\text{lipS}_2$ reaction, the activity being less than 0.2 % of wild-type enzyme in both directions [59]. It was not reported whether this inhibition is caused by over-reduction to EH_4 .



Scheme 5. Summary of identified and proposed intermediates in the reaction mechanism of lipoamide dehydrogenase. The physiological reaction is counter clockwise from species 1 to 7. Species 8 to 11 show the over-reduction to the EH₄ level. The arrows signify the charge-transfer interactions and are drawn from the donor to the acceptor.

The rationale of the mutation Ile184->Tyr is described in the section 'Spectral changes in the presence of pyridine nucleotides' as are the effects of this mutation on the spectral properties of the enzyme. Turnover of this enzyme in the lip(SH)₂/NAD⁺ reaction is decreased ten-fold with a similar pH dependence as found for the wild-type enzyme [59, 69]. The NADH/lipS₂ reaction is decreased two-fold [59, 69]. For this enzyme too, inhibition by the electron donor was observed. Similarly as found for the wild-type enzyme NAD⁺ acts as an activator in the reverse reaction of the mutated enzyme though the activating effect was maximal at 20 μM NAD⁺ instead of 1 mM NAD⁺ as reported for the wild-type enzyme [61, 69]. Stopped flow data indicate that in the reduction of the mutated enzyme by NADH, the first step, reduction of the FAD, is only slightly decreased but the subsequent hydride transfer to the disulfide is markedly inhibited [69].

The mutation His444->Gln was prepared to better understand the role of the active site base [82, 83]. Only rapid reaction kinetics of the reduction by lip(SH)₂ were reported for this mutated enzyme. It was shown that the apparent rate of reduction by 5 molar equivalents of lip(SH)₂ was decreased to 0.4 s⁻¹ at pH 10.08 while the wild-type enzyme was reduced at a rate of 450-750 s⁻¹ by 2 molar equivalents of lip(SH)₂ at pH 9.85 [89], thus clearly demonstrating the important function of this histidine. The rate of reduction by lip(SH)₂ increased as the pH was increased and this was explained in terms of a better reactivity of the substrate in the mutated enzyme since the first pK_a of the substrate was 9.3 [51], however even the rates at high pH were very slow. It was argued that the severe drop in reduction rate cannot reflect only the function of this histidine as a base, but might also reflect deteriorated binding of the lip(SH)₂ anion in the apolar binding site and changes in the redox potential of the flavin, suggesting a further role for the active site base [83].

Conformational stability

Initial isolation procedures for the pig heart enzyme contained a heating step to 62°C [4] demonstrating that the enzyme in the Eox state is very heat stable. This was reinforced at 70°C [93]. The high stability of pig heart enzyme Eox was also demonstrated by urea denaturation, in 6.5 M urea the enzyme did not denature [68]. However, reduction of the enzyme by NADH or lip(SH)₂ was accompanied by a strongly decreased resistance towards urea denaturation which led to the conclusion that the active site disulfide was an intersubunit disulfide bridge holding the subunits together [68]. In addition it was suggested that the instability could be a result of the reduction of the FAD. Later studies aimed at the preparation of apoenzyme showed that it was possible to obtain monomeric apoenzyme under nonreducing conditions,

demonstrating that the active site disulfide bridge is an intrasubunit disulfide bridge [70], a finding that was confirmed later by peptide analysis of the fragment containing the active site disulfide [36].

Tryptic digestion studies with *A. vinelandii* enzyme have shown that Eox is not digested in contrast to the N-ethylmaleimide labeled enzyme (the active site disulfide is labeled) indicating a conformational change upon reduction of the disulfide had occurred [94]. Recently the stability of the different redox states of *A. vinelandii* enzyme was addressed in detail by van Berkel and co-workers [95]. A T_m of 80°C is reported for Eox which decreases to 39°C and 42°C when reduced with dithionite or NADH respectively. Upon reduction with lip(SH)₂ T_m is 53°C. Comparable results were obtained by studying the urea denaturation in 7 M urea at 25°C. Upon reduction with NADH or dithionite the rate of denaturation compared to Eox increased 200 or 400 fold respectively. Administration of NAD⁺ had a protective effect on the denaturation indicating that the formation of EH₄ is an important factor in respect to denaturation as already suggested, though rejected, by Massey and co-workers [68]. Reduction of the enzyme with lip(SH)₂ in 7 M urea increased the rate of denaturation only 2-3 fold. Spectral studies showed that in urea the charge-transfer species was favored, thus demonstrating that the EH₂ state is not conformationally unstable. The relatively low thermostability of EH₂ was explained by assuming that at t_m of EH₂ the enzyme becomes EH₄ due to over-reduction by the excess of lip(SH)₂ present. Upon proteolytic digestion of Eox, EH₂ prepared by lip(SH)₂ reduction and EH₄ prepared by NADH and dithionite reduction and apoenzyme, only the NADH and dithionite reduced enzyme and apoenzyme appeared to be significantly digested demonstrating that a conformational change of the enzyme occurs upon reduction from EH₂ to EH₄ which promotes dimer dissociation.

Outline of this thesis

At the onset of the investigations described in this thesis progress was being made on the elucidation of the crystal structure of the *Azotobacter vinelandii* lipoamide dehydrogenase. Also the gene encoding this enzyme was cloned in our laboratory. By this, a firm basis was laid to start site directed mutagenesis studies aimed at deepening the insight in the reaction mechanism of lipoamide dehydrogenase. At the start of this work no site directed mutated mutated lipoamide dehydrogenases were reported though for the *E. coli* enzyme some mutated enzymes were announced.

The first goal was to assess the function(s) of the active site base, histidine. Therefore the histidine was replaced by other residues and a glutamate, held responsible for affecting the pK_a of the histidine was mutagenised. It was expected that

the mutations would alter the reaction rates of the different reaction intermediates and that these intermediates could be identified and studied.

Chapter 2 describes the steady state spectral properties and in Chapter 3 the steady state and rapid reaction kinetics and some rapid reaction spectral properties of the wild-type and mutated enzymes are presented.

Since modeling studies suggested that Tyr16 was involved in substrate binding, this residue was replaced with other residues in order to stabilize the binding of the substrate, lipS₂, and hence to be able to grow crystals of the enzyme with the substrate bound. The results obtained with these mutated enzymes are presented in Chapter 4.

Preliminary experiments with *A. vinelandii*, *E. coli* and *P. fluorescens* lipoamide dehydrogenase showed strong reactivity of the latter enzyme with antibodies raised against *A. vinelandii* enzyme while no cross reactivity was observed with the *E. coli* enzyme. This indicates that high sequence homology is present between the *A. vinelandii* and the *P. fluorescens* enzymes and that the *P. fluorescens* enzyme constitutes a natural 'mutated' effective lipoamide dehydrogenase. Cloning and sequence analysis of this gene, described in Chapter 5 opens the way to site directed mutagenesis. In Chapter 6 a characterization of the *P. fluorescens* wild-type enzyme is presented.

References

1. Straub, F. B. (1939) *Biochem. J.* 33, 787-792.
2. Savage, N. (1957) *Biochem. J.* 67, 146-155.
3. Massey, V. (1960) *Biochim. Biophys. Acta* 37, 314-322.
4. Searls, R. L. and Sanadi, D. R. (1960) *J. Biol. Chem.* 235, 2485-2491.
5. Williams, C. H. Jr. (1976) in *The Enzymes* (Boyer, P. D. ed) Vol 13, 89-173, Academic Press, New York.
6. Williams, C. H. Jr. (1991) in *Chemistry and Biochemistry of Flavoenzymes* (Müller, F. ed) vol 3, in press, CRC Press Inc., Boca Raton.
7. Koike, M., Reed, L. J. and Carroll, W. R. (1963) *J. Biol. Chem.* 238, 30-34.
8. Lusty, C. J. and Singer, T. P. (1964) *J. Biol. Chem.* 239, 3733-3742.
9. Sokatch, J. R., McCully, V., Gebroski, J. and Sokatch, D. (1981) *J. Bacteriol.* 148, 639-646.
10. Klein, S. M. and Sagers, R. D. (1967) *J. Biol. Chem.* 242, 297-300.
11. Kochi, H. and Kikuchi, G. (1976) *Arch. Biochem. Biophys.* 173, 71-81.
12. Richarme, G. and Heine, H. (1986) *Eur. J. Biochem.* 156, 399-405.
13. Richarme, G. (1989) *J. Bacteriol.* 171, 6580-6585.
14. Nawa, H., Brady, W. T., Koike, M. and Reed, L. J. (1960) *J. Am. Chem. Soc.* 82, 896-903.
15. Ambrose, M. C. and Perham, R. N. (1976) *Biochem. J.* 155, 429-432.
16. Fujiwara, K., Okamura-Ikeda, K. and Motokawa, Y. (1986) *J. Biol. Chem.* 261, 8836-8841.
17. Freudenberg, W. and Andreesen, J. R. (1989) *J. Bacteriol.* 171, 2209-2215.
18. Yang, Y. and Frey, P. A. (1989) *Arch. Biochem. Biophys.* 268, 465-474.
19. Reed, L. J. (1974) *Acc. Chem. Res.* 7, 40-46.
20. Stephens, P. E., Lewis, H. M., Darlison, M. G. and Guest, J. R. (1983) *Eur. J. Biochem.* 135, 519-527.
21. Burns, G., Brown, T., Hatter, K. and Sokatch, J. R. (1989) *Eur. J. Biochem.* 179, 61-69.
22. Palmer, J. A., Hatter, K. and Sokatch, J. R. (1991) *J. Bacteriol.* 173, 3109-3116.
23. Palmer, J. A., Madhusudhan, K. T., Hatter, K. and Guest, J. R. (1991) *Eur. J. Biochem.* 202, 231-240.
24. Westphal, A. H. and De Kok, A. (1988) *Eur. J. Biochem.* 172, 299-305.
25. Otulakowski, G. and Robinson, B. H. (1987) *J. Biol. Chem.* 262, 17313-17318.
26. Ross, J., Reid, G. A. and Dawes, J. W. (1988) *J. Gen. Microbiol.* 134, 1131-1139.
27. Browning, K. S., Uhlinger, D. J. and Reed, L. J. (1988) *Proc. Natl. Acad. Sci. USA* 85, 1831-1834.

28. Sokatch, J. R. and Burns, G. (1984) *Arch. Biochem. Biophys.* **228**, 660-666.
29. Brown, N. L., Ford, S. J., Pridmore, R. D. and Fritsinger, D. C. (1983) *Biochemistry* **22**, 4089-4095.
30. Misra, T. K., Brown, N. L., Haberstroh, L., Schmidt, A., Goddette, D. and Silver, S. (1985) *Gene* **34**, 253-262.
31. Wang, Y., Moore, M., Levinson, H. S., Silver, S., Walsh, C. and Mahler, I. (1989) *J. Bacteriol.* **171**, 883-892.
32. Greer, S. and Perham, R. N. (1986) *Biochemistry* **25**, 2736-2742.
33. Shames, S. L., Kimmel, B. E., Peoples, O. P., Agabian, N. and Walsh, C. T. (1989) *Biochemistry* **27**, 5014-5019.
34. Russel, M. and Model, P. (1988) *J. Biol. Chem.* **263**, 9015-9019.
35. Burleigh, B. D. and Williams, C. H. Jr. (1972) *J. Biol. Chem.* **247**, 2077-2082.
36. Williams, C. H. Jr. and Arscott, L. D. (1972) *Z. Naturforsch.* **27**, 1078-1081.
37. Krohne-Ehrich, G., Schirmer, R. H. and Untucht-Grau, R. (1977) *Eur. J. Biochem.* **80**, 65-71.
38. Ronchi, S. and Williams, C. H. Jr. (1972) *J. Biol. Chem.* **247**, 2083-2086.
39. Schulz, G. E., Schirmer, R. H., Sachsenheimer, W. and Pai, E. F. (1978) *Nature* **273**, 120-124.
40. Thieme, R., Pai, E. F., Schirmer, R. H. and Schulz, G. E. (1981) *J. Mol. Biol.* **152**, 763-782.
41. Karplus, P. A. and Schulz, G. E. (1987) *J. Mol. Biol.* **195**, 701-729.
42. Karplus, P. A. and Schulz, G. E. (1989) *J. Mol. Biol.* **210**, 163-180.
43. Pai, E. F. and Schulz, G. E. (1983) *J. Biol. Chem.* **258**, 1752-1757.
44. Schierbeek, A. J., Swarte, M. B. A., Dijkstra, B. W., Vriend, G., Read, R. J., Hol, W. G. J., Drenth, J. and Betzel, C. (1989) *J. Mol. Biol.* **206**, 365-379.
45. Mattevi, A., Schierbeek, A. J. and Hol, W. G. J. (1991) *J. Mol. Biol.* **220**, 975-994.
46. Mattevi, A., Obmolova, G., Sokatch, J. R., Betzel, C. and Hol, W. J. G. (1991) submitted.
47. Kuriyan, J., Krishna, T. S. R., Wong, L., Guenther, B., Pahler, A., Williams, C. H. Jr. and Model, P. (1991) *Nature* **352**, 172-174.
48. Schiering, N., Kabsch, W., Moore, M. J., Distefano, M. D., Walsh, C. T. and Pai, E. F. (1991) *Nature* **352**, 168-172.
49. Hanson, K. R. (1966) *J. Amer. Chem. Soc.* **96**, 4345-4346.
50. Kopsower, E. M. (1966) in *Flavins and Flavoproteins* (Slater, E. C. ed), 1-14, Elsevier, Amsterdam.
51. Matthews, R. G., Ballou, D. P., Thorpe, C. and Williams, C. H. Jr. (1977) *J. Biol. Chem.* **252**, 3199-3207.
52. Matthews, R. G. and Williams, C. H. Jr. (1976) *J. Biol. Chem.* **251**, 3956-3964.

53. Wilkinson, K. D. and Williams C. H. Jr. (1979) *J. Biol. Chem.* 254, 852-862.
54. Arscott, L. D., Thorpe, C. and Williams, C. H. Jr. (1981) *Biochemistry* 20, 1513-1520.
55. Sahlman, L. and Williams, C. H. Jr. (1989) *J. Biol. Chem.* 264, 8033-8038.
56. Sahlman, L. and Williams, C. H. Jr. (1989) *J. Biol. Chem.* 264, 8039-8045.
57. Deonarain, M. P., Scrutton, N. S., Berry, A. and Perham, R. N. (1990) *Proc. R. Soc. Lond. B.* 241, 179-186.
58. Veeger, C. (1960) PhD Thesis, Free University, Amsterdam, The Netherlands.
59. Maeda-Yorita, K., Massey, V. Williams, C. H. Jr. Allison, N., Russel, G. C. and Guest, J. R. (1991) in *Flavins and Flavoproteins 1990* (Curti, B., Ronchi, S. and Zanetti, G. eds.) pp 573-576, Walter de Gruyter and Co. Berlin-New York.
60. Massey, V. and Veeger, C. (1961) *Biochim. Biophys. Acta* 48, 33-47.
61. Wilkinson, K. D. and Williams C. H. Jr. (1981) *J. Biol. Chem.* 256, 2307-2314.
62. Massey, V. Gibson, Q. H. and Veeger, C. (1960) *Biochem. J.* 77, 341-351.
63. Williams, C. H. Jr. (1965) *J. Biol. Chem.* 240, 4793-4800.
64. Reed, J. K. (1973) *J. Biol. Chem.* 248, 4834-4839.
65. Visser, J., Voetberg, H. and Veeger, C. (1969) in *Pyridine Nucleotide Dependent Dehydrogenases* (Sung, H. ed), 359-373, Springer Verlag, Berlin.
66. Broek van den, H.W.J. (1971) PhD Thesis, University of Wageningen, The Netherlands.
67. Harbury, H. A., LaNoue, K. F., Loach, P. A. and Amick, R. M. (1959) *Proc. Natl. Acad. Sci. USA* 45, 1708-1717.
68. Massey, V., Hofmann, T. and Palmer, G. (1962) *J. Biol. Chem.* 237, 3820-3828.
69. Meada-Yorita, K., Russel, G. C., Guest, J. R., Massey, V. and Williams, C. H. Jr. (1991) *Biochemistry* 30, in the press.
70. Kalse, J. F. and Veeger, C. (1968) *Biochim. Biophys. Acta* 159, 244-256.
71. Fox, B. S. and Walsh, C. T. (1982) *J. Biol. Chem.* 257, 2498-2503.
72. Fox, B. S. and Walsh, C. T. (1982) *Biochemistry* 22, 4082-4088.
73. Thorpe, C. and Williams, C. H. Jr. (1976) *J. Biol. Chem.* 251, 3553-3557.
74. Thorpe, C. and Williams, C. H. Jr. (1976) *J. Biol. Chem.* 251, 7726-7728.
75. Thorpe, C. and Williams, C. H. Jr. (1981) *Biochemistry* 20, 1507-1513.
76. O'Donnel, M. E. and Williams, C. H. Jr. (1984) *J. Biol. Chem.* 259, 2243-2251.
77. Sahlman, L., Lambeir, A. and Lindskog, S. (1986) *Eur. J. Biochem.* 156, 479-488.
78. Miller, S. M., Massey, V., Ballou, D. P., Williams, C. H. Jr., Distefano, M. D., Moore, M. J. and Walsh, C. T. (1990) *Biochemistry* 29, 2831-2841.
79. Adamson, S. R. and Stevenson, K. J. (1981) *Biochemistry* 20, 3418-3424.
80. Adamson, S. R., Robinson, J. A. and Stevenson, K. J. (1984) *Biochemistry* 23, 1269-1274.

81. Berry, A., Scrutton, N. S. and Perham, R. N. (1989) *Biochemistry* 28, 1264-1269.
82. Williams, C.H. Jr., Allison, N., Russel, G.C., Prongay, A.J., Arscott, D.L., Datta, S., Sahlman, L. and Guest, J.R. (1989) *Ann. N.Y. Acad. Sci.* 573, 55-65.
83. Williams, C. H. Jr., Arscott, L. D., Gamm, D., Hopkins, N., Allison, N. and Guest, J. R. (1990) in *Flavins and Flavoproteins 1990* (Curti, B., Zanetti, G. and Ronchi, S. eds.), pp. 577-580, Walter de Gruyter, Berlin-New York.
84. Wilkinson, K. D. and Williams C. H. Jr. (1979) *J. Biol. Chem.* 254, 863-871.
85. Hopkins, N. and Williams C. H. Jr., Russel, G. C. and Guest, J. R. (1990) in *Flavins and Flavoproteins 1990* (Curti, B., Zanetti, G. and Ronchi, S. eds.), pp. 581-584, Walter de Gruyter, Berlin-New York.
86. Veeger, C and Massey, V. (1963) *Biochim. Biophys. Acta* 67, 679-681.
87. Massey, V. and Palmer, G. (1962) *J. Biol. Chem.* 237, 2347-2358.
88. Matthews, R. G., Ballou, D. P. and Williams, C. H. Jr. (1979) *J. Biol. Chem.* 254, 4974-4981.
89. Maeda-Yorita, K. and Aki, K. (1984) *J. Biochem.* 96, 683-690.
90. Koike, M and Koike, K. (1976) in *Flavins and Flavoproteins* (Singer, T. P. ed), 473-484, Elsevier Amsterdam.
91. Muiswinkel-Voetberg, H. and Veeger, C. (1973) *Eur. J. Biochem* 33, 285-291.
92. Matthews, R. G., Wilkinson, K. D., Ballou, D. P. and Williams, C. H. Jr. (1976) in *Flavins and Flavoproteins* (Singer, T. P. ed), 464-472, Elsevier Amsterdam.
93. Muiswinkel-Voetberg, H., Visser, J. and Veeger, C. (1973) *Eur. J. Biochem* 33, 265-270.
94. Kok de, A. and Visser, A. J. W. G. (1984) in *Flavins and Flavoproteins* (Bray, R. C., Engel, P. C. and Mayhew, S. G., eds), 149-152, W, de Gruyter, Berlin.
95. Berkel van, W. J. H., Regelink, A. G., Beintema, J. J. and De Kok, A. (1991) *Eur. J. Biochem* 202, 1049-1055.

Errata to Chapter 2.

- 1) Pro455->Ala should read Pro451->Ala.
- 2) The multiplication factor 10^{-6} (p 47) for the quenching constants (K_Q) should be omitted.

Chapter 2

Lipoamide Dehydrogenase from *Azotobacter vinelandii*: site-directed mutagenesis of the His450–Glu455 diad

Spectral properties of wild type and mutated enzymes

Jacques BENEN, Willem van BERKEL, Zdzislaw ZAK, Ton VISSER, Cees VEÉGER and Arie de KOK
Department of Biochemistry, Agricultural University, Wageningen, The Netherlands

(Received April 22/July 30, 1991) — EJB 91 0522

Three amino acid residues in the active site of lipoamide dehydrogenase from *Azotobacter vinelandii* were replaced by other residues. His450, the active-site base, was changed into Ser, Tyr and Phe. Pro451, in *cis* conformation, was changed into Ala. Glu455 was replaced with Asp and Gln.

Absorption, fluorescence and CD spectroscopy of the mutated enzymes in their oxidized state (E_{ox}) showed only minor changes with respect to the wild-type enzyme, whereas considerable changes were observed in the spectra of the two-electron-reduced (EH_2) species of the enzymes upon reduction by the substrate dihydrolipoamide. Differences in extent of reduction of the flavin by NADH indicate that the redox potential of the flavin is altered by the mutations. Enzyme Pro455→Ala showed the greatest deviation from wild type. The enzyme is very easily over-reduced to the four-electron reduced state (EH_4) by dihydrolipoamide. This is probably due to a change in the backbone conformation caused by the *cis-trans* conversion.

From studies on the pH dependence of the thiolate charge-transfer absorption and the relative fluorescence of EH_2 of the enzymes, it is concluded that mutation of His450 results in a relatively simple and easily interpreted distribution of electronic species at the EH_2 level. For all three His450-mutated enzymes an apparent pK_{a1} near 5.5 is calculated that is assigned to the interchange thiol. A second apparent pK_{a2} is calculated of 6.9, 7.5 and 7.1 for the His450→Phe, -Ser and -Tyr enzymes, respectively, and signifies the deprotonation of the tautomeric equilibrium between the interchange and charge-transfer thiols. The difference in apparent pK_{a2} values between the His450-mutated enzymes is explained by changes in micropolarity.

At the EH_2 level the wild-type enzyme consists of multiple electronic forms as reported for the *Escherichia coli* enzyme [Wilkinson, K. D. and Williams C. H. Jr (1979) *J. Biol. Chem.* 254, 852–862]. Based on the results obtained with the His450-mutated enzymes, it is concluded that the lowest pK_a is associated with the interchange thiol. A model for the equilibrium species of the wild-type enzyme at the EH_2 level is presented which takes three pK_a values into account.

The results of the pH dependence of the electronic species at the EH_2 level of Glu455-mutated enzymes essentially follow the model proposed for the wild-type enzyme. However mutation of Glu455 shifts the tautomeric equilibrium of EH_2 in favor of the charge-transfer species. This effect is explained by impaired ion-pair formation between the protonated His and the interchange thiolate and a lowering of the pK_a of His450.

Lipoamide dehydrogenase is the flavoprotein component of the pyruvate, oxoglutarate and branched-chain oxoacid dehydrogenase complexes [1, 2]. In the physiological direction

Correspondence to Dr. A. de Kok, Department of Biochemistry, Agricultural University, Dreyenlaan 3, NL-6703 HA Wageningen, The Netherlands

Abbreviations. E_{ox} , oxidized (mutated) lipoamide dehydrogenase; EH_2 , two-electron reduced lipoamide dehydrogenase; EH_4 , four-electron reduced lipoamide dehydrogenase; LipS₂, D,L-6,8-thioctic acid amide, lipoamide; Lip(SH)₂, reduced lipoamide; Nbs₂, 5,5'-dithiobis(2-nitrobenzoate); AcPyAde⁺, 3-acetylpyridine-adenine dinucleotide; PP_i/EDTA, sodium pyrophosphate/EDTA buffer, pH 8.0; FADH[•], reduced flavin; FIH[•], EH_2 species with flavin reduced; FL, fluorescent species; CT, charge transfer species.

Enzymes. Lipoamide dehydrogenase, NADH:lipoamide oxidoreductase (EC 1.8.1.4); DNA restriction endonuclease *Not*I, *Kpn*I, *Sst*I, *Sma*I (EC 3.1.24.4); DNA polymerase I (Klenow fragment) (EC 2.7.7.7)

it catalyses the oxidation by NAD⁺ of a reduced lipoyl group which is covalently attached to the core compound of these complexes. This lipoyl group can be replaced with free lipoamide. Lipoamide dehydrogenase belongs to the family of dimeric flavoenzymes that contain a disulfide participating in catalysis [1]. Other members of this family are glutathione reductase [1], mercuric ion reductase [3], trypanothione reductase [4] and thioredoxin reductase [5].

Extensive studies on lipoamide dehydrogenase have been performed on the enzymes as isolated from pig heart, rat liver and *Escherichia coli* [6–14]. Potentially, the enzyme can take up four electrons/monomer, but during catalysis the enzyme shuttles between the oxidized state (E_{ox}) and the two-electron-reduced state (EH_2) [15]. The four-electron reduced state (EH_4) is inactive and originates from the dead-end complex $EH_2 \cdot NADH$ [12]. All three lipoamide dehydrogenases were shown to act according to a ping-pong mechanism in the

physiological reaction [6, 8, 14]. A reaction mechanism involving a base in the active site that becomes protonated during catalysis was proposed [16]. Initially a histidine was put forward as the base. Later this idea gained strong support from studies with a bifunctional arsenoxide [17].

In the three-dimensional structure of E_{ox} from *Azotobacter vinelandii*, refined to 0.22 nm, a His residue is present in the active site with the carboxylate function of a Glu in close contact [18]. In E_{ox} the histidine is closer to the N-terminal Cys48, the interchange thiol in the reductive reaction, than to Cys53, the charge-transfer thiol. An identical feature was found in the related enzyme glutathione reductase in both the oxidized and reduced state [19–21]. It was also found that the active site is composed of both subunits.

Both kinetic and spectral studies revealed that the active-site His of lipoamide dehydrogenase and glutathione reductase in EH_2 showed a high pK_a of about 8.5 whereas the charge-transfer thiol showed an unusually low pK_a , about 4.5 [9, 13]. It has been argued that the pK_a shifts were due to mutual influences [9, 13]. In order to assess the role of the active-site histidine (His450) and the nearby glutamate (Glu455), site-directed mutagenesis experiments were performed. His450 was replaced with Ser, Tyr or Phe and Glu455 was replaced with Asp or Gln. Apart from these residues, we were also interested in the role of the backbone in this part of the active site. In the crystal structure of E_{ox} , Pro451 is in *cis*-conformation thereby positioning the backbone carbonyl of His450 towards the proton at N3 of the flavin (Mattevi, personal communication). This might have an influence on the redox properties of the flavin. Therefore Pro451 was replaced with Ala.

In this paper we report on the pH-dependent spectral properties of the wild-type and mutated enzymes of *Azotobacter vinelandii* lipoamide dehydrogenase.

MATERIALS AND METHODS

General

Restriction endonucleases were from Boehringer or Bethesda Research Laboratories (BRL). *E. coli* DNA polymerase I (Klenow fragment) was from BRL as was T4-DNA ligase. NAD⁺ (grade I), NADH (grade I) and all dNTPs and ddNTPs were from Boehringer. Lipoamide, 5,5'-dithiobis(2-nitrobenzoate) (Nbs₂), the NAD⁺ analog 3-acetyl-pyridine-adenine dinucleotide (AcPyAde⁺) and biological buffers were obtained from Sigma Inc. Dihydrolipoamide was synthesized according to Reed et al. [22] and the concentration was determined with Nbs₂. Oligonucleotides for mutagenesis were synthesized with a BioSearch Inc. oligonucleotide synthesizer. [α -³²P] dATP (3000 Ci mmol⁻¹; 11.1 TBq mmol⁻¹) was purchased from New England Nuclear (NEN). Chromatography resins were from Pharmacia. All chemicals used were of analytical grade.

E. coli TG2, a *rec A* version of TG1 [$\Delta(lac-pro)$, *thi*, *sup E*, *[Res⁻ Mod⁻ (k)] F'* (*traD36*, *proA⁺ B⁺*, *lacF⁺ ZAM15*)] was used throughout as a host for cloning and expression of cloned enzymes [23]. *E. coli* RZ1032 [*SupE*, *dut⁻*, *ung⁻*] [24] was used for generation of uracil-containing single-stranded DNA. Plasmid pAW104 containing the *A. vinelandii* wild-type lipoamide dehydrogenase gene has been described earlier [25] and was kindly provided by Mr A. H. Westphal.

Vectors M13mp18 and -19 were constructed by cloning the polylinker from the plasmid vector Bluescript KS (Stratagene Inc.) into vectors M13mp18 and -19. For this

the polylinker from Bluescript KS was cut out by digestion with *Sst*I and *Kpn*I and ligated into *Sst*I/*Kpn*I-digested M13mp18/19. As the insertion in the M13 vectors is in frame with the *lacZ* gene, the blue/white feature of the M13 vectors is retained while the number of unique restriction sites suitable for cloning is expanded.

Wild-type and mutated lipoamide dehydrogenase genes were expressed in transformed *E. coli* TG2 grown in 5-l batches of tryptone/yeast medium containing 75 μ g/ml ampicillin at 37°C with vigorous aeration.

Construction of mutants

The residues that were to be replaced, His450 with Tyr, Phe or Ser, Pro451 with Ala and Glu455 with Gln or Asp, are all located in the C-terminal part of the enzyme. Therefore a 420-bp *Not*I – *Kpn*I fragment containing the coding region for amino acid residues 391–477 (C-terminus) and the putative transcription terminator was subcloned into M13mp19 and used for mutagenesis according to the method described [24]. Single-stranded uracil-containing DNA was isolated when the ratio of infectivity of the phage for *E. coli* RZ1032 to *E. coli* TG2 was higher than 10⁶:1.

Single-stranded uracil-containing DNA was used for 'all-the-way-round' oligonucleotide directed *in vitro* mutagenesis. To 1 μ g single-stranded DNA (ssDNA), 10 pmol of phosphorylated oligonucleotide was annealed. The polymerase mixture contained 1 g annealed ssDNA, 250 μ M of each of the dNTPs, 5 mM dithiothreitol, 10.0 mM Tris/Cl, 10.0 mM MgCl₂, pH 8.0, and 1.5 U Klenow DNA polymerase I in a final volume of 20 μ l and was incubated for 2 h at 16°C. After addition of 1 μ l 10 mM ATP and 8 U T₄-DNA ligase, the incubation at 16°C was continued for 20 h. The reaction mixture was used to transform *E. coli* TG2. Phages obtained from the transformation were grown and ssDNA was isolated and screened for the mutation according to the Sanger dideoxy-chain-termination method using deaza-dGTP [26]. Clones carrying the mutation were sequenced entirely to screen for undesired mutations. Subsequently double-stranded DNA (dsDNA) was isolated and from this the mutated *Not*I – *Kpn*I fragment was isolated as a slightly longer *Not*I – *Sma*I fragment. In order to ligate the mutated fragment back into the gene, plasmid pAW104 was digested with *Not*I and *Sma*I, deleting the entire downstream region of the *Not*I site at position 2167. The mutated *Not*I – *Sma*I fragment was then ligated into the partial gene yielding an intact gene carrying a point mutation. Proper 'in-frame' ligation of the fragment was checked by subcloning the entire insert of the new construct into M13mp19 and sequencing the ligation point at the *Not*I site using the oligonucleotide used for mutagenesis as a sequencing-primer.

Sequencing of the mutated *Not*I – *Kpn*I cassette clearly demonstrated that the desired mutations were made.

Analytical methods

Large-scale isolation of the enzymes (up to 5-l cultures) was performed essentially as described [25] with one slight modification. The Sepharose 6B enzyme eluate was concentrated using an ultrafiltration set (Amicon) equipped with a YM30 membrane. The concentrate was then exhaustively dialyzed against 50 mM potassium phosphate, 0.5 mM EDTA, pH 7.0, and stored as 1.0-ml aliquots (5–7 mg/ml) under liquid nitrogen until use. The expression of the mutated lipoamide dehydrogenases was as high as for over-expressed

wild-type enzyme yielding 250 mg (mutated) lipamide dehydrogenase/5-l culture of transformed *E. coli* TG2.

FPLC analytical gel filtration was done as described [27].

For spectral studies, enzyme solutions were freshly thawed from liquid nitrogen and subsequently passed over BioGel P-6DG to change to the appropriate buffer.

When recording spectra under anaerobic conditions, enzyme solutions were transferred to anaerobic cuvettes that were closed with Subaseals. The cuvettes were subsequently evacuated seven times and gassed with argon. The argon was passed over a catalyst (BASF, R 3-11) to remove oxygen followed by passage through an illuminated solution containing reduced methyl viologen, EDTA and proflavin (3,6-diaminoacridine) to remove the last traces of oxygen. Solutions that were used to titrate/reduce the anaerobic enzymes were deoxygenated in an identical way.

Enzyme concentrations were determined spectrophotometrically using a molar absorption coefficient $\epsilon_{458} = 11\,300\text{ M}^{-1}\text{ cm}^{-1}$ for all mutated and wild-type lipamide dehydrogenases (λ_{max} of mutant Pro455→Ala is at 453 nm).

Visible absorption spectra were recorded at 25°C, on an Aminco DW-2a or computer-controlled Aminco DW-2000 spectrophotometer. The scan speed was 5 nm s^{-1} . Typically 45 μM enzyme solutions were used.

Fluorescence emission spectra were recorded on an automated Aminco SPF-500 fluorimeter (Olis Inc., Jefferson, GA) at 25°C.

Circular dichroic (CD) spectra were obtained with a Jobin Ivon mark V dichrograph connected to an IBM-PC. Quartz cells with 1.0 cm path length were used in the wavelength region 300–600 nm. In the ultraviolet range (190–300 nm), cells with 0.1 cm path length were used. The cell compartment was thermostatted at 25°C and purged with nitrogen. The scan speed was 1 nm s^{-1} . The spectra reported are averages of three independent experiments on different samples of the same preparation. All spectra were corrected for the appropriate blank solutions, recorded in the absence of enzyme. The values are expressed in terms of molar ellipticity $[\theta]$ and were calculated using the equation:

$$[\theta] = \frac{3300}{l \times c} \times \Delta\epsilon$$

where $\Delta\epsilon$ is the circular dichroism observed, l is the path length of the cell in cm and c is the molar concentration of the enzyme analyzed. Below 240 nm the ellipticity is expressed as mean residual ellipticity $[\theta]_{\text{mr}}$ (*A. vinelandii* lipamide dehydrogenase is composed of 476 amino acid residues [25]). In order to obtain spectra of two-electron-reduced enzymes, enzyme solutions were made anaerobic as described above and titrated with a 5 mM dihydrolipoamide stock solution. The reduction of the enzymes was monitored by recording the absorption spectra over 320–600 nm. When the characteristic spectrum of EH_2 was reached, CD spectra were recorded in the range 300–600 nm. The enzyme concentration varied from 1 μM (190–240 nm) to 50 μM (300–600 nm) in 50 mM potassium phosphate, 0.5 mM EDTA, pH 7.0.

For pH-dependent titrations the following buffers were used: 100 mM potassium acetate (pH 4.5–pH 5.3), 100 mM Mes (pH 5.5–6.5), 100 mM Hepes (pH 6.7–7.8) and 100 mM Hepes (pH 8.0–8.7). The ionic strength was adjusted to 150 mM with 1.0 M KCl. Enzyme solutions (45 μM concentration) were made anaerobic and subjected to titration using a gas-tight Hamilton syringe equipped with a dispenser enabling the addition of defined aliquots of titrant. After each addition

spectra were recorded until changes were complete. Additions of dihydrolipoamide were stopped after reaching maximal charge transfer. Data, corrected for dilution, were analyzed with a Levenberg-Marquardt algorithm provided by the program 'Igor' from WaveMetrics Inc. run on an Apple Macintosh. Routines were written to analyze the data for one, two or three pKa values where the routines also varied the absorption coefficient to give best fit to the data. In a separate set of experiments the pH-dependent fluorescence of both E_{ox} and EH_2 (10 μM concentration) was studied. The excitation wavelength was 458 nm (4-nm bandpass) and the emission wavelength 525 nm (4-nm bandpass). All titration experiments were performed at 25°C.

Activity determinations

NAD^+ and NADH concentrations were determined in 50 mM sodium pyrophosphate, 0.5 mM EDTA, pH 8.0 (PPi/EDTA), using $\epsilon_{260} = 18\,000\text{ M}^{-1}\text{ cm}^{-1}$ and $\epsilon_{340} = 6\,220\text{ M}^{-1}\text{ cm}^{-1}$ respectively. AcPyAde⁺ concentrations were determined by converting AcPyAde⁺ into AcPyAdeH ($\epsilon_{363} = 9\,100\text{ M}^{-1}\text{ cm}^{-1}$) using lipamide dehydrogenase from *Pseudomonas fluorescens* [28]: to 950 μl PPi/EDTA, 20 μl dihydrolipoamide (final concentration 1.0 mM) and 20 μl of several dilutions of the AcPyAde⁺ stock solution were added. The reaction was started with 10 μl of an 0.5 mg/ml enzyme solution and followed at 363 nm until changes were complete. Lipamide dehydrogenase from *Ps. fluorescens* was used because this enzyme appeared to be insensitive to inhibition by AcPyAdeH.

The forward reaction dihydrolipoamide/ NAD^+ was determined routinely in PPi/EDTA at 25°C. In a standard assay 1.0 mM NAD^+ and 1.0 mM dihydrolipoamide were used and the formation of NADH was monitored at 340 nm. In some cases AcPyAde⁺ instead of NAD^+ was used as electron acceptor and the formation of AcPyAdeH was followed at 363 nm.

RESULTS

General properties of mutated lipamide dehydrogenases

The monomer/dimer ratio of the mutated enzymes in solution was estimated using FPLC. Upon elution of the mutated enzymes on Superose-12, all profiles show one symmetrical peak with the same retention volume as found for dimeric wild-type lipamide dehydrogenase [29]. In this experiment it was also seen that no FAD was liberated indicating that the FAD binding of the mutated enzymes is not detectably altered when compared to wild-type lipamide dehydrogenase.

Considerable differences in activity exist among the several (mutated) enzymes. The enzymes His450→Tyr, His450→Phe and Pro455→Ala are almost completely inactive while enzyme His450→Ser shows 0.5% activity of the wild-type enzyme. The Glu455-mutated enzymes initially show kinetic traces comparable to wild-type lipamide dehydrogenase but, due to severe inhibition by the product NADH, kinetics can not be studied. When using the NAD^+ analog AcPyAde⁺ as an electron acceptor, the inhibition is almost negligible. The activity is 1.6% and 1.3% of wild-type lipamide dehydrogenase using AcPyAde⁺ for Glu455→Asp and Glu455→Gln mutated enzymes, respectively.

Spectral properties

For wild-type and mutated enzymes the A_{280}/A_{458} ratio is 4.8–4.9. This demonstrates that the enzymes are saturated

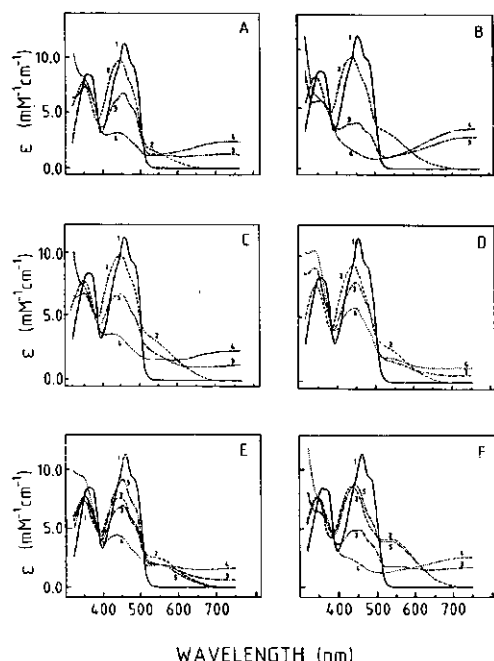


Fig. 1. Visible absorption spectra of *A. vinelandii* wild-type lipamide dehydrogenase and mutated enzymes. Spectra were recorded at 25°C in PPi/EDTA (1) before (—) (E_{ox}) and after the addition of (2) 5.0 mol/mol dihydrolipoamide (---) (EH_2) and before and after the addition of (3) 1.0 mol/mol NADH (---) and (4) 2.0 mol/mol NADH (····). Spectra shown were recorded when changes were complete. (A) Wild-type enzyme; (B) enzyme Glu455→Asp; (C) enzyme Glu455→Gln; (D) enzyme His450→Ser; (E) enzyme His450→Tyr; (F) enzyme His450→Phe. For the mutated enzymes His450→Tyr and His450→Phe a spectrum is presented (5) that depicts the final spectrum that was isobestic upon reduction with dihydrolipoamide (---).

with FAD and that the molar absorption coefficients for all enzymes are almost identical.

Fig. 1 shows the visible absorption spectra of wild-type and mutated enzymes. In the oxidized state flavin spectral properties of the enzymes are almost indistinguishable. The enzymes His450→Tyr and His450→Phe show a more pronounced shoulder at 480 nm indicating a relatively more apolar environment of the flavin-isoalloxazine ring. This feature is prominent in difference spectra (not shown). The spectrum of enzyme Pro455→Ala (not shown) however shows less pronounced vibrational fine structure. The absorption maximum at 453 nm and closer resemblance of the spectrum to that of free FAD are indicative of a more polar microenvironment of the isoalloxazine ring.

At pH 8.0, the spectrum of wild-type E_{ox} (Fig. 1A) closely resembles the spectra of pig heart and *E. coli* lipamide dehydrogenase [1]. Upon addition of a slight molar excess of dihydrolipoamide, EH_2 is formed within the mixing time. The spectrum is characterized by a shift of the major flavin peak to shorter wavelength and a typical absorption at 530 nm that is ascribed to a charge-transfer complex between the oxidized

flavin and a thiolate that originates from reduction of the disulfide bond [30]. This complex will be referred to as the 530-nm charge-transfer complex. The absorption at 530 nm is less intense than that of the EH_2 form of the pig heart enzyme but more intense than that of the *E. coli* enzyme [7, 14, 16].

At equilibrium, upon titration of the wild-type enzyme with one equivalent of NADH, the electrons are shared between the sulfur atoms, as evidenced by the 530-nm absorbance, and the flavin molecule, as evidenced by the 750-nm absorbance, indicating $FADH^{\cdot-}/NAD^+$ charge-transfer complex formation [15]. Note that half the 750-nm absorbance is formed upon addition of the first equivalent of NADH. Further reduction to EH_2 results from the addition of a further equivalent of NADH (Fig. 1A).

With enzymes Glu455→Asp and Glu455→Gln the reduction to EH_2 by dihydrolipoamide is also complete within mixing time. The spectra of EH_2 (Fig. 1B and 1C) show 530-nm absorbance remarkably higher than the wild-type enzyme.

Upon titration of enzyme Glu455→Asp with NADH, the absorption at 750 nm is considerably higher than that observed for wild-type enzyme. The 530-nm absorbance observed with the wild-type enzyme, after the initial addition of NADH, is not observed to the same extent in enzyme Glu455→Asp. With enzyme Glu455→Gln the absorbance at 750 nm is comparable to wild type but the 530-nm absorbance is very prominent (Fig. 1C). It is also noteworthy that the extent of reduction of the FAD varies between wild type and enzymes Glu455→Asp and Glu455→Gln after the addition of one or two equivalents of NADH (Fig. 1B and 1C). This difference suggests that the FAD in enzyme Glu455→Asp is more easily reduced in the presence of NAD^+ than is the FAD in wild-type or Glu455→Gln enzyme.

Like the wild-type lipamide dehydrogenase and the Glu455-mutated enzymes, the His450→Ser enzyme is rapidly reduced by dihydrolipoamide and forms a stable EH_2 (Fig. 1D). The spectrum is very similar to the Glu455-mutated enzymes, showing an intense absorption band at 530 nm, much higher than that of wild-type at this pH. Initial reduction of the His450→Ser enzyme by NADH at pH 8.0 is characterized by a high 530-nm absorbance with only small changes in FAD absorbance and high absorbance at 340 nm due to free NADH. Eventually, after addition of excess NADH, the FAD becomes fully reduced and the spectrum shows a high absorbance at 750 nm indicative of the formation of an $FADH^{\cdot-}/NAD^+$ charge-transfer complex (results not shown). The small extent of reduction of FAD of the enzyme His450→Ser suggests that the FAD is not as easily reduced in the presence of NAD^+ as in the wild-type enzyme.

The His450→Tyr and His450→Phe enzymes are very slowly reduced by dihydrolipoamide. The course of titration to EH_2 is different with respect to the wild-type enzyme and mutated enzymes described above (Fig. 1E and 1F). While the spectra of the previously described enzymes are isobestic during reduction with dihydrolipoamide until maximal 530-nm charge transfer is reached, spectra of these enzymes are only initially isobestic. Before maximal charge-transfer absorbance is reached the isobestic points shift, indicating formation of other reduced species. This effect is most pronounced with enzyme His450→Tyr: changes in spectra are isobestic until a certain amount of charge-transfer absorbance is reached (see Fig. 1E) which is retained for a few minutes. After this time interval, the charge-transfer absorbance increases further with simultaneous shift of isobestic points. With the enzyme His450→Phe this biphasic charge-

Table 1. Relative FAD fluorescence quantum yield of *A. vinelandii* wild-type lipamide dehydrogenase and mutated enzymes

The excitation wavelength was 450 nm and the emission wavelength 525 nm. All experiments were performed at 25°C in 50 mM potassium phosphate, 0.5 mM EDTA, pH 7.0. Enzyme concentrations were 2 μ M based on FAD absorption

Enzyme	FAD quantum yield (relative to wild type)
Wild-type	1.00
Glu455→Asp	0.63
Glu455→Gln	1.14
His450→Phe	0.73
His450→Ser	0.80
His450→Tyr	0.80
Pro455→Ala	0.64

transfer increase is not observed. Another typical aspect of the spectrum of EH₂ of these two His450-mutated enzymes is the large shift of the 458-nm peak of the flavin to 430–435 nm and a shift of the maximum from 530 nm to 540 nm, resulting in a clear resolution of the charge-transfer absorbance.

Unlike the slow reduction of His450→Phe and His450→Tyr enzymes by dihydrolipoamide, the reduction by NADH reaches equilibrium approximately as fast as in wild-type lipamide dehydrogenase. The extent of reduction in both mutated enzymes clearly differs however. In His450→Phe enzyme, FAD is almost fully reduced after the addition of 2 equivalents NADH. In enzyme His450→Tyr, FAD is reduced to a lesser extent, slightly more than enzyme His450→Ser. Thus apparently the ease of reduction of FAD of the mutated enzymes by NADH in the presence of NAD⁺ is different and might be related to shifts of either or both the redox potentials of the disulfide and the FAD.

Enzyme Pro455→Ala behaves quite differently during reduction. Upon reduction with dihydrolipoamide no 'stable' EH₂ species is formed. The enzyme is completely reduced after addition of two equivalents of dihydrolipoamide. Titration with dihydrolipoamide shows that initially the disulfide is reduced yielding a transient 530-nm charge-transfer absorption. After a few seconds charge transfer decreases with concomitant formation of reduced flavin (results not shown). This result indicates that in enzyme Pro455→Ala the electrons are easily transferred from the sulfurs to the flavin and suggests that the redox potentials of the disulfide and the flavin are very close. From modelling studies on the crystal structure of lipamide dehydrogenase, it is deduced that the mutation Pro455→Ala probably leads to a changed position of the backbone resulting in a breakage of the flavin N3-carbonyl oxygen interaction. Simultaneously the imidazole of His450 shifts out of the plane Cys48–Cys53–His450–Glu455 (Mattevi personal communication).

Fluorescence properties

The shape of the fluorescence emission and excitation spectra of the mutated enzymes are very similar to the shape of the spectra of wild-type lipamide dehydrogenase (results not shown); only differences in relative quantum yield are observed (see Table 1). The shifts of the emission and excitation maxima of enzyme Pro455→Ala are in accordance with the shifts of the two major flavin peaks of the visible absorption spectrum. From this we conclude that the effect

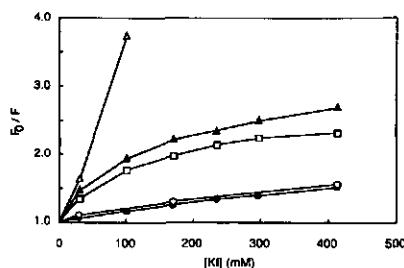


Fig. 2. Stern-Volmer plot of the FAD fluorescence quenching by iodide of *A. vinelandii* wild-type lipamide dehydrogenase and mutated enzymes. The data are corrected for salt effects. The excitation wavelength was 450 nm and the emission wavelength 525 nm. The enzyme concentrations in 50 mM potassium phosphate, 0.5 mM EDTA, pH 7.0 were adjusted to 2.0 μ M (FAD absorption). The three His450 enzymes and enzyme Pro455→Ala gave nearly identical results and are presented as one curve (●). Wild type enzyme (●); enzyme Glu455→Gln (▲); enzyme Glu455→Asp (□); FAD (Δ)

of the mutations is very local and does not disturb the overall structure of the enzymes in their oxidized state. This conclusion is supported by the far-ultraviolet CD spectra (see below).

Flavin accessibility of the mutated and wild-type enzymes was probed by iodide fluorescence quenching. Fig. 2 shows the Stern-Volmer plots obtained after correction for salt effects. Obviously, mutation of Glu455 influences the accessibility of the flavin for iodide. Slight quenching is observed in the wild-type and mutated enzymes that still possess Glu455, yielding quenching constants (K_Q) of approximately $1 \times 10^{-6} \text{ M}^{-1}$. Similar results were reported for the pig heart enzyme [31]. Strong quenching at low KI concentrations was seen in the Glu455 mutated enzymes ($K_Q = 15 \times 10^{-6} \text{ M}^{-1}$ for Glu455→Gln and $K_Q = 11 \times 10^{-6} \text{ M}^{-1}$ for Glu455→Asp). This indicates that the carboxylate function of Glu455 is the repelling force, preventing iodide from entering the active site. The nonlinear behavior of the plots at higher KI concentrations for the Glu455-mutated enzymes suggests minimally two possible conformations of the flavin binding region, one accessible and one less accessible. The presence of monomers was excluded by the fact that the F_0/F ratio as a function of enzyme concentration did not change at KI concentrations where strongest quenching was observed (not shown). At present it is not clear whether this different quenchability is an intrinsic property of the Glu455 mutated enzymes or that it is induced by the iodide present in the active site which might cause cooperativity of the active sites.

Possible charge effects of the quencher were probed using CsCl as a quencher. Free FAD was not as strongly quenched as found for KI; $K_Q(\text{CsCl}) = 0.5 \times 10^{-6} \text{ M}^{-1}$ and $K_Q(\text{KI}) = 28 \times 10^{-6} \text{ M}^{-1}$. Instead of quenching, a slight stimulation of fluorescence was observed with CsCl, of the same magnitude as found for NaCl and KCl.

Circular dichroic spectra

In the ultraviolet region (190–300 nm), only minor changes were recorded in the CD spectra of E_{ox}. In the far-ultraviolet, the CD spectra are essentially identical, indicating that no significant changes in the overall secondary structure between mutated and wild-type enzymes have occurred. In

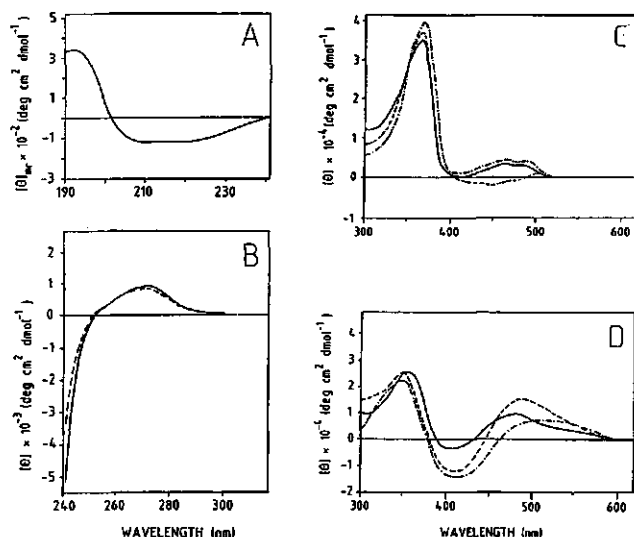


Fig. 3. Circular-dichroic spectra of *A. vinelandii* wild-type lipoamide dehydrogenase and some mutated enzymes. CD spectra of wild-type enzyme and enzymes deviating most from wild-type. Conditions and analysis are as described in Materials and Methods. (A–C) CD spectra of E_{ox} : wild-type enzyme (—); enzyme His450→Phe (---); enzyme Glu455→Asp (---). (A) Far-ultraviolet spectra (190–250 nm) of the enzymes are essentially identical, therefore only wild-type enzyme is shown. (B) Aromatic region of the spectrum (240–300 nm); wild-type enzyme and enzyme His450→Phe are identical, only wild-type and Glu455→Asp enzyme are shown. (C) Visible region (300–600 nm). (D) Visible region (300–600 nm) of EH_2 of wild-type enzyme and two mutated enzymes deviating most from wild-type enzyme (—), enzymes His450→Phe (---) and Glu455→Gln (---).

the near-ultraviolet only the amplitude of the positive Cotton effect ($\lambda_{max} = 274$ nm) varies slightly in all enzymes. No direct relation between the aromatic amino acid residue engineered, e.g. in the His450-mutated enzymes, and the Cotton effect could be established. Fig. 3A–C depicts the CD spectra of the E_{ox} of wild-type and two mutated enzymes, Glu455→Asp and His450→Phe, which show largest deviations from the spectrum of the wild-type enzyme. The CD spectra are very similar to the published spectra of the pig heart enzyme [32, 33]. In the visible region (300–600 nm), the CD spectra of all mutated enzymes and wild-type enzyme show a positive Cotton peak at 370 nm, and two unresolved CD bands at 465 nm and 490 nm, both either positive or negative, depending on the enzyme used. The positive bands at 370 nm, with nearly identical ellipticity, correspond to the second absorption band of FAD. The two bands at 465 nm and 490 nm arise from vibronic transitions of the first absorption band. The major differences in the CD spectra of E_{ox} are observed at the lowest energy absorption band of protein-bound FAD. The dichroism in this range varies from $-3.4 \times 10^3 \text{ deg M}^{-1} \text{ cm}^{-1}$ for enzyme Pro455→Ala to $4.8 \times 10^3 \text{ deg M}^{-1} \text{ cm}^{-1}$ for wild-type. The differences in molar ellipticity indicate slight changes in the microenvironment of the flavin.

The CD spectra of EH_2 (Fig. 3D shows spectra that deviated most from wild-type, Glu455→Gln and His450→Ser), indicate that differences occur between the enzymes at the lowest energy charge-transfer transition of the FAD. A negative dichroism of different amplitude was observed in the range around 400 nm and positive dichroism was observed above 440 nm. The positive dichroism extends far beyond the upper limit of dichroic activity of the flavin as found in E_{ox}

showing that the thiolate-FAD charge-transfer complex has rotational strength. The thiolate-FAD donor-acceptor interaction may lead to a shift of the (perturbed) first electronic transition of the FAD as suggested by the strong negative dichroism around 410 nm. The dichroism of the second absorption band, almost identical in all enzymes, decreases with respect to E_{ox} proportional to the absorption spectrum with a concomitant shift of the maximum to 350 nm.

pH dependence of absorption and fluorescence properties of E_{ox} and EH_2

In order to gain more insight into the influence of the mutations on the catalytically important protonation states of EH_2 , the pH dependence of the spectral properties of the enzymes was studied. For E_{ox} of wild-type and mutated enzymes, the molar absorption coefficient appears to be independent of pH. However the charge-transfer absorbance at the EH_2 level is highly dependent on pH and can be regarded as a monitor of protonation states at this level of reduction. Dihyrolipoamide was used as reducing agent since with dithionite no stoichiometric reduction could be achieved.

Fig. 4 shows the 530-nm absorbance of wild-type and mutated lipoamide dehydrogenases as a function of pH. During the course of the titrations the isosbestic points around 440 nm shifted before maximal charge transfer was reached, indicating the formation of other species. The shift is interpreted as the formation of an EH_2 species in which the electrons are transferred to the flavin [FlH^-] and/or disproportionation of EH_2 into EH_4 and E_{ox} analogous to the *E. coli* enzyme [11]. The disproportionation might be enhanced due to the fact

Table 2. Apparent pK_a values and absorption coefficients of the charge-transfer absorption of two-electron-reduced *A. vinelandii* wild-type lipoamide dehydrogenase and mutated enzymes

Experimental conditions and analysis are described under Materials and Methods. Data are presented in Fig. 4

Enzyme	pK_{a1}	ϵ_1	pK_{a2}	ϵ_2	pK_{a3}	ϵ_3
		$M^{-1} cm^{-1}$		$M^{-1} cm^{-1}$		$M^{-1} cm^{-1}$
Wild-type	4.8 ± 0.3	330 ± 150	6.7 ± 0.3	1060 ± 170	8.7 ± 0.5	1700 ± 800
Glu455→Asp	5.9 ± 0.1	2840 ± 60				
Glu455→Gln	5.6 ± 0.1	3010 ± 20	6.9 ± 0.4	600 ± 80		
His450→Ser	5.5 ± 0.1	730 ± 80	7.5 ± 0.1	2730 ± 80		
His450→Tyr	5.5 ± 0.3	1270 ± 80	7.1 ± 0.1	2580 ± 260		
His450→Phe	5.3 ± 0.2	1780 ± 250	6.9 ± 0.1	2150 ± 230		

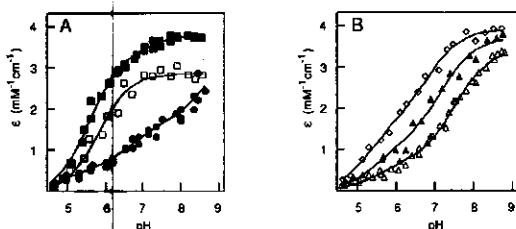


Fig. 4. pH dependence of the thiolate charge-transfer absorbance of *A. vinelandii* wild-type lipoamide dehydrogenase and mutated enzymes. Conditions and analysis are as described in Materials and Methods. The curves drawn through the data are calculated from the apparent pK_a values and absorption coefficients at 530 nm obtained from the best fit (Table 2). (A) Wild-type enzyme (●); enzyme Glu455→Asp (□); enzyme Glu455→Gln (■). (B) Enzyme His450→Ser (△); enzyme His450→Tyr (▲); enzyme His450→Phe (◇)

that dihydrolipoamide was used as reducing agent [11]. From the degree of reduction of the flavin it is estimated that these species contributed to maximally 10–15 % of the final spectrum. The formation of these species is highest in the wild-type enzyme and almost negligible in enzyme His450→Ser. No corrections are made for the disproportionation. Therefore the calculated pK_a values are approximations and the corresponding absorption coefficients, especially for the wild-type enzyme, are under-estimated. In Table 2, apparent pK_a values and absorption coefficients of the charge-transfer complex of the different enzymes are listed.

For the wild-type enzyme the data are best fitted with three pK_a values (Fig. 4A). Assuming the maximal charge-transfer absorption coefficient of the wild-type is $2800\text{--}3200\text{ M}^{-1}\text{ cm}^{-1}$ as reported for *E. coli* and pig heart enzymes [11, 14], the low, gradual absorption increase over the entire pH interval indicates that in *A. vinelandii* wild-type enzyme, as in *E. coli* wild-type enzyme, EH_2 is an equilibrium of several species [11] of which only one or two exhibit charge-transfer absorption. This conclusion is supported by the pH dependence of the fluorescence at the EH_2 level (see below).

Considerable changes when compared to wild-type enzyme occur in the pH profiles of both Glu455-mutated enzymes. The data of enzyme Glu455→Asp are well fitted assuming one apparent pK_a value (Fig. 4A). For enzyme Glu455→Gln the best fit is obtained with two apparent pK_a values. These data indicate that the loss of the orienting effect of Glu455 on His450 dramatically changes the influence of His450 on the pH dependence of the charge-transfer absorption.

The data of the His450-mutated enzymes are best fitted with two apparent pK_a values (Fig. 4B). The pK_{a2} value shifts to lower pH, proportional to the polarity of the side-chain engineered. In addition to this, the absorption coefficient of the charge-transfer absorption is increased when compared to the maximal values reported for pig heart and *E. coli* enzyme [11, 14].

In order to gain more insight into the groups that are associated with the apparent pK_a values summarized in Table 2, the pH dependence of the fluorescence properties of the enzymes were studied. Since the presence of a thiolate in the vicinity of the FAD acts as a fluorescence quencher, the fluorescence at the EH_2 level may be regarded to as a monitor for the deprotonation of the charge-transfer thiol.

For the E_{ox} studied (wild-type, Glu455→Gln, Glu455→Asp, His450→Phe and His450→Ser) the fluorescence is dependent on pH, unlike the *E. coli* enzyme [11]. The relative fluorescence quantum yield of the mutated enzymes with respect to the wild-type enzyme as presented in Table 1 is grossly retained over the pH interval studied.

Fig. 5A, B and C show the pH dependence of the fluorescence of E_{ox} and EH_2 . The pK_a values obtained from fitting are presented in Table 3. The pK_a values of the fluorescence of E_{ox} of the different enzymes demonstrate that at least one, and in enzyme His450→Ser two, protonation steps influence the fluorescence of E_{ox} .

Studies of the relative fluorescence of *E. coli* EH_2 have revealed that the extrapolated maximal fluorescence at zero charge-transfer absorbance reaches 70% of the fluorescence of E_{ox} [11] and thus the fluorescence quantum yield of fully protonated EH_2 is lower than that of E_{ox} . Assuming similarity between the *E. coli* and *A. vinelandii* enzymes in this respect, pK_a values are calculated from varying the fluorescence quantum yield of fully protonated EH_2 between 70–100% of E_{ox} . For enzyme His450→Ser the maximal difference between the fluorescence quantum yield of EH_2 and E_{ox} is given by the value at lowest pH since only small changes occur at low pH. The validity of the assumption is demonstrated by the large decrease in relative fluorescence of EH_2 in the wild-type and Glu455→Gln enzyme at low pH which cannot be correlated to a proportional increase of charge-transfer absorption. Again, no corrections are made for any contributions from E_{ox} resulting from disproportionation of EH_2 and thus the relative fluorescence for the wild-type enzyme especially is over-estimated.

The calculated apparent pK_a values for EH_2 shown in Fig. 5 are presented in Table 3. The largest changes in relative fluorescence seem to be associated with the lowest pK_a around 5.3 in wild-type and Glu455→Gln enzymes. However, since the fluorescence quantum yield of these enzymes at the fully

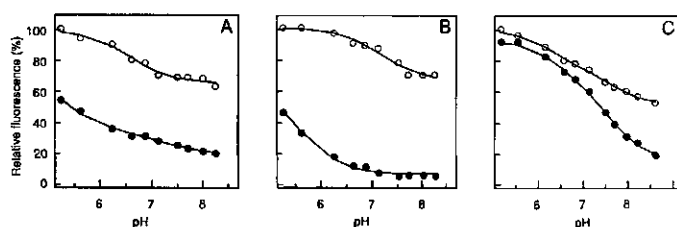


Fig. 5. pH dependence of the relative fluorescence of *A. vinelandii* wild-type lipamide dehydrogenase and enzymes Glu455→Gln and His450→Ser. Conditions and analysis are as described in Materials and Methods. The curves drawn through the data are calculated from the apparent pK_a values obtained from the best fit. (○) E_{ox} ; (●) EH_2 . (A) Wild-type enzyme; (B) enzyme Glu455→Gln; (C) enzyme His450→Ser

Table 3. Apparent pK_a values of the fluorescence quantum yield of oxidized and two-electron reduced *A. vinelandii* wild-type lipamide dehydrogenase and some mutated enzymes. Experimental conditions and analysis are described under Materials and Methods. Data, except for enzyme His450→Phe, are presented in Fig. 5

Enzyme	Reduction level	pK_{a1}	pK_{a2}
Wild-type	E_{ox}	6.5 ± 0.2	
Wild-type	EH_2	5.3 ± 0.2	7.3 ± 0.1
Glu455→Gln	E_{ox}	7.2 ± 0.1	
Glu455→Gln	EH_2	5.3 ± 0.2	
His450→Ser	E_{ox}	6.3 ± 0.3	7.7 ± 0.1
His450→Ser	EH_2	6.1 ± 0.4	7.6 ± 0.1
His450→Phe	EH_2	6.0 ± 0.2	7.0 ± 0.1

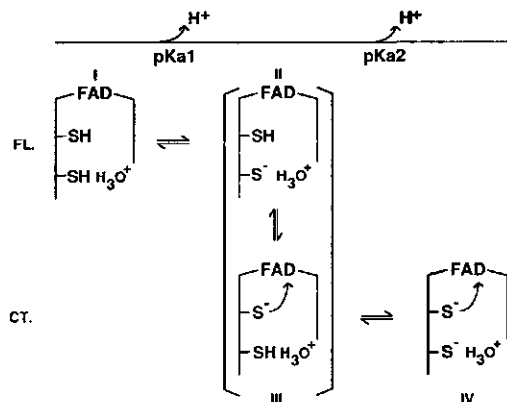
protonated EH_2 level is not precisely known, the data only have moderate value. Quite different in this respect are the relative fluorescence data for enzymes His450→Ser and His450→Phe which very closely follow the charge-transfer absorption.

DISCUSSION

For a better understanding of the catalytic mechanism of lipamide dehydrogenase from *A. vinelandii*, the active-site residue, His450, its hydrogen-bonding partner Glu455, and Pro451 were replaced with different amino acids. The low turnover rate of all mutated enzymes studied clearly shows that all three amino acid residues are essential for effective catalysis. The implications of the mutations on the kinetic properties of the enzymes will be presented separately. Here we have focussed on the spectral properties of the mutated enzymes.

With the exception of enzyme Pro455→Ala, the absorption, fluorescence and CD spectra of *A. vinelandii* wild-type and mutated E_{ox} are highly similar showing that the mutations have not introduced drastic structural changes.

The spectral similarities between the wild-type enzyme and the mutated enzymes disappear upon reduction. For *E. coli* and pig heart lipamide dehydrogenase differences with respect to stabilization of EH_2 have been reported [11, 14]. For *E. coli* enzyme an equilibrium of at least three species was proposed [11]. Only one of these species exhibits charge transfer. For pig heart enzyme the charge-transfer species prevails [14, 15]. The EH_2 state of pig heart enzyme is very stable, i.e. the enzyme cannot be over-reduced to EH_4 by the substrate dihydrolipoamide [6, 15]. In contrast, the *E. coli* enzyme is

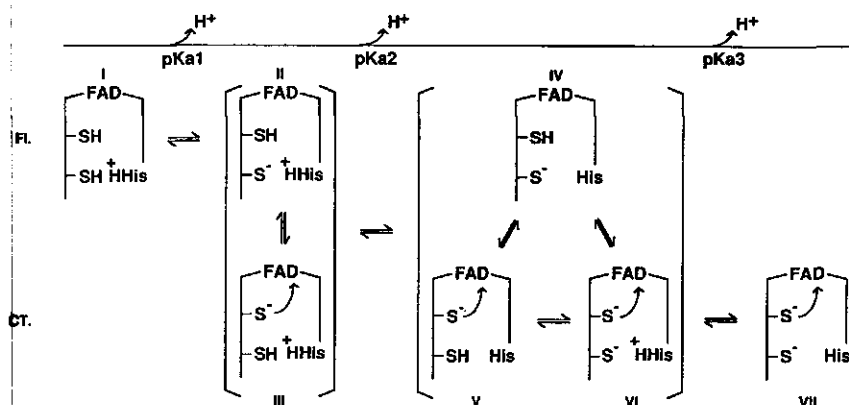


Scheme 1. Proposed model for the pH dependence of the predominant species of His450-mutated *A. vinelandii* lipamide dehydrogenases at the EH_2 level. Species I is the fully protonated species, EH_2 . Species II and III are equilibrium species of EH_2 after the first deprotonation. Species IV is the E^{2-} species after deprotonation of both 'thiols' at high pH. The arrow signifies the charge-transfer interaction between the thiolate and the FAD. FL, fluorescent species. CT., charge-transfer species

very easily over-reduced to EH_4 [7]. The *A. vinelandii* wild-type enzyme is less prone to over-reduction than the *E. coli* enzyme, but is more easily over-reduced than the pig heart enzyme.

From the crystal structures of *A. vinelandii* E_{ox} and oxidized and two-electron-reduced human glutathione reductase it is known that the glutamate and the histidine form a short but strong hydrogen bond [19–21]. It has been suggested that this interaction results in a rise of the pK_a of the histidine [19, 21]. The distance between the (protonated) histidine and the interchange thiol is also short and allows ion-pair interaction. The data from the pH-dependent studies on the enzymes will be interpreted in the light of these structural features. It should be noted here that only the interchange thiol, Cys48, the charge-transfer thiol, Cys53, and His450 are considered to contribute to the observed pH-dependent effects.

The results presented in this paper on the pH dependence of the charge-transfer absorption and the fluorescence of EH_2 of the *A. vinelandii* wild-type enzyme show that, as in the *E. coli* enzyme [11], at neutral pH, EH_2 consists of multiple



Scheme 2. Proposed model for the pH dependence of the predominant species of *A. vinelandii* lipoamide dehydrogenase at the EH_2 level. Species I is the fully protonated species, EH_3^+ . Species II and III are equilibrium species of EH_2 after the first deprotonation. Species IV, V and VI are the EH^- species after the second deprotonation. Species VII is E^{2-} , presumably predominant at high pH. The arrow signifies the charge-transfer interaction between the thiolate and the FAD. Not included are the species E_{ox} and EH_4 and the EH_2 species FIH^- . FL., fluorescent species, CT., charge-transfer species

electronic forms. The distribution of these forms is complex and quantitation is hampered by disproportionation. Before discussing the wild-type enzyme in more detail, the His450-mutated enzymes will be addressed since these show less complex behavior.

With all His450-mutated enzymes the data of the pH-dependent charge-transfer absorption were well fitted assuming two apparent pK_a values indicating the involvement of at least two titratable groups. The data on the relative fluorescence of enzyme His450→Ser show that the large decrease in fluorescence, expected from formation of a thiolate near the flavin, occurs with a pK_a of 7.7, matching perfectly with the pK_a obtained for the large increase of charge-transfer absorbance. Similar results were obtained for enzyme His450→Phe where the pK_a values for the largest increase in charge-transfer absorbance and decrease in relative fluorescence coincided. Scheme 1 depicts the major tautomeric species for the His450 mutated enzymes. The fact that charge-transfer absorption and high fluorescence is observed at low pH (apparent pK_a of 5.5 in all His450-mutated enzymes) demonstrates that tautomerization equilibrium between species II and III in Scheme 1 is almost completely shifted in favor of species II. Therefore the deprotonation that leads to the tautomerization, with an apparent pK_a of 5.5, is assigned to the interchange thiol.

At high pH both thiols become deprotonated (species IV in Scheme 1). The presence of two negative charges in the active site seems conflicting. However, bearing in mind the fact that the interchange thiol is readily accessible to water, the assumption is made that the negatively charged interchange thiolate is stabilized by interaction with a hydronium ion. Apart from this, the charge-transfer thiolate is stabilized via interaction with the flavin. The positive end of a helix dipole might contribute to the stabilization of both thiolates (Mattevi, personal communication).

The decrease of pK_{a2} in enzymes His450→Tyr and His450→Phe supports the assumption that charge compensation occurs. As known from modelling studies with the crystal structure, the interchange thiolate is still accessible for

water, the interaction with an hydronium ion as proposed for enzyme His450→Ser remains possible and will be enhanced in a more apolar environment. This results in less influence of the interchange thiolate on the charge-transfer thiol and lowers the pK_a of the latter. Moreover, upon deprotonation of the charge-transfer thiol the negative charge is more compensated by a stronger interaction with the flavin as evidenced by the unusual high charge-transfer absorption (ϵ about $3900 \text{ M}^{-1} \text{ cm}^{-1}$) and a shift of the absorption maximum from 530 nm to 540 nm.

Based on the proposed Scheme 1 for the His450-mutated enzymes, Scheme 2 depicts the protonation states of the wild-type enzyme (adapted from [11]). Not included are the EH_4 species and E_{ox} resulting from disproportionation and the species FIH^- .

At low pH, above pK_{a1} , the charge-transfer absorption is low and the relative fluorescence high. Thus the major species at this protonation level is species II in Scheme 2. Based on the results from the His450-mutated enzymes, it is concluded that in the wild-type enzyme also deprotonation of the interchange thiol leads to tautomerization that results in charge-transfer absorption.

At a pH above pK_{a2} , the tautomerization equilibrium shifts in favor of the charge-transfer thiolate species V and VI. Species IV is also present as indicated by the relative fluorescence. The third apparent pK_a is assigned to the histidine in analogy to *E. coli* and pig heart enzyme [9, 11, 14] and glutathione reductase [14].

Scheme 2, presented for the wild-type enzyme, also applies to the Glu455-mutated enzymes. With these enzymes, full deprotonation is compressed to a ΔpH of 1–2 resulting in co-titration of all three residues in EH_2 with only a small contribution in charge-transfer absorption associated with an apparent pK_a of 6.9 for enzyme Glu455→Gln. Replacement of Glu455 with Asp or Gln results in weakening or loss of the hydrogen bond with the histidine which most probably will lead to an impaired orientation of the histidine relative to the interchange cysteine and a lowering of the pK_a of the histidine in EH_2 . A distorted ion-pair interaction between the inter-

change thiolate and the protonated histidine and a lowered pK_a of the histidine lead to less stabilization of the tautomeric species II in Scheme 2 and as a consequence species III is favored. A lowered His450 pK_a also results in formation of species VII at lower pH than in wild-type enzyme as the protonated histidine is part of the majority of tautomerization species of Scheme 2.

Taken together, the results on the Glu455-mutated enzymes make it clear that the mutations lead to preference of the charge-transfer species at the EH_2 level of the enzymes and demonstrate that Glu455 is an extremely important residue in balancing the distribution of the equilibrium of electronic species at the EH_2 level in the wild-type enzyme.

The results presented here show that mutation of His450 leads to a rather simple distribution of electronic species at the EH_2 level that allows easy interpretation and has proved to be of great value for the interpretation of the complex distribution in the wild-type enzyme and Glu455-mutated enzymes. Our results on the Glu455-mutated enzymes indicate that the effect of the histidine on the charge-transfer thiol is indirect and mediated through the interchange thiol.

At present, studies are aimed at gaining more insight in the relation of the distribution of the EH_2 species in the mutated enzymes and the impact of the distribution on the separate half reactions and overall catalysis of the (mutated) enzyme(s).

We thank Dr W. G. J. Hol and Mr A. Mattevi for providing us with the coordinates of lipoamide dehydrogenase from *A. vinelandii* prior to publication. We are indebted to Dr C. H. Williams Jr for helpful discussions. This work was supported by the Dutch Foundation for Chemical Research (SON) with financial aid from the Netherlands Organization for Scientific Research (NWO).

REFERENCES

- Williams, C. H. Jr (1976) In *The enzymes* (Boyer, P. D. ed.) vol. 13, pp. 89–173, Academic Press, New York.
- Sokatch, J. R., McCully, V., Gebroski, J. & Sokatch, D. J. (1981) *J. Bacteriol.* 148, 639–646.
- Fox, B. S. & Walsh, C. T. (1982) *J. Biol. Chem.* 257, 2498–2503.
- Shames, S. L., Fairlamb, A. H., Cerami, A. & Walsh, C. T. (1986) *Biochemistry* 25, 3519–3526.
- Holmgren, A. (1980) *Experientia suppl.* 36, 149–180.
- Massey, V., Gibson, Q. H. & Veege, C. (1960) *Biochem. J.* 77, 341–351.
- Williams, C. H. Jr (1965) *J. Biol. Chem.* 240, 4793–4800.
- Reed, J. K. (1973) *J. Biol. Chem.* 248, 4834–4839.
- Matthews, R. G., Ballou, D. P., Thorpe, C. & Williams, C. H. Jr (1977) *J. Biol. Chem.* 252, 3199–3207.
- Matthews, R. G., Ballou, D. P. & Williams, C. H. Jr (1979) *J. Biol. Chem.* 254, 4974–4981.
- Wilkinson, K. D. & Williams, C. H. Jr (1979) *J. Biol. Chem.* 254, 852–862.
- Wilkinson, K. D. & Williams, C. H. Jr (1981) *J. Biol. Chem.* 256, 2307–2314.
- Sahlman, L. & Williams, C. H. Jr (1989) *J. Biol. Chem.* 264, 8033–8038.
- Sahlman, L. & Williams, C. H. Jr (1989) *J. Biol. Chem.* 264, 8039–8045.
- Massey, V. & Veege, C. (1961) *Biochim. Biophys. Acta* 48, 33–47.
- Matthews, R. G. & Williams, C. H. Jr (1976) *J. Biol. Chem.* 251, 3956–3964.
- Adamson, S. R., Robinson, J. A. & Stevenson, K. J. (1984) *Biochemistry* 23, 1269–1274.
- Mattevi, A., Schierbeek, A. J., Obmolova, G., Kalk, K. H. & Hol, W. G. J. (1991) In *Flavins and flavoproteins 1990* (Curti, B., Zanetti, G. & Ronchi, S., eds) pp. 549–556, Walter de Gruyter, Berlin, New York.
- Pai, E. F. & Schulz, G. E. (1983) *J. Biol. Chem.* 258, 1752–1757.
- Thieme, R., Pai, E. F., Schirmer, R. H. & Schulz, G. E. (1981) *J. Mol. Biol.* 152, 763–782.
- Karplus, P. A., Pai, E. F. & Schulz, G. E. (1989) *Eur. J. Biochem.* 178, 693–703.
- Reed, L. J., Koike, M., Lertich, M. E. & Leach, F. R. (1958) *J. Biol. Chem.* 232, 143–149.
- Gibson, T. J. (1984) Ph.D. Thesis, University of Cambridge, England.
- Kunkel, T. A., Roberts, J. D. & Zakour, R. A. (1987) *Methods Enzymol.* 154, 367–382.
- Westphal, A. H. & De Kok, A. (1988) *Eur. J. Biochem.* 172, 299–305.
- Sanger, F., Nicklen, S. & Coulson, A. R. (1977) *Proc. Natl Acad. Sci. USA* 74, 5463–5467.
- Van Berkel, W. J. H., Van den Berg, W. A. M. & Müller, F. (1988) *Eur. J. Biochem.* 178, 197–207.
- Benen, J. A. E., Van Berkel, W. J. H., Van Dongen, W. M. A. M., Müller, F. & De Kok, A. (1989) *J. Gen. Microbiol.* 135, 1787–1797.
- Berkel, W. J. H. van, Benen, J. A. E. & Snoek, M. C. (1991) *Eur. J. Biochem.* 197, 769–779.
- Kosower, E. M. (1966) In *Flavins and flavoproteins* (Slater, E. C., ed.) pp. 1–14, Elsevier, Amsterdam.
- Visser, A. J. W. G., Grande, H. J., Müller, F. & Veege, C. (1974) *Eur. J. Biochem.* 45, 99–107.
- Brady, A. H. & Beychok, S. (1969) *J. Biol. Chem.* 244, 4634–4637.
- Brady, A. H. & Beychok, S. (1971) *J. Biol. Chem.* 246, 5498–5503.

Chapter 3

Lipoamide Dehydrogenase from *Azotobacter vinelandii*: site-directed mutagenesis of the His450-Glu455 diad.

Kinetics of wild-type and mutated enzymes.

Jacques Benen, Willem van Berkel, Nicole Dieteren, David Arscott, Charles Williams Jr., Cees Veeger and Arie de Kok.

Summary

Three amino acid residues in the active site of lipoamide dehydrogenase from *Azotobacter vinelandii* were replaced with other residues. Histidine450, the active site base, was replaced with serine, tyrosine and phenylalanine respectively. Proline451, from X-ray analysis found to be in *cis*-conformation positioning the backbone carbonyl of His450 close to N3 of the flavin, was changed into alanine. Glutamate455, from X-ray analysis expected to be involved in modulating the pK_a of the base (histidine450), was replaced with aspartate and glutamine. The general conclusion is that mutation of the His-Glu diad impairs intramolecular electron transfer between the disulfide/dithiol and the FADH/FAD.

The wild-type enzyme functions according to a ping-pong mechanism in the physiological reaction in which the formation of NADH is rate limiting. Above pH 8.0 the enzyme is strongly inhibited by the product NADH. The pH dependence of the steady state kinetics using the NAD⁺ analog 3-acetylpyridine adenine dinucleotide [AcPyAde⁺] reveals a pK_a of 8.1 in the pK_m AcPyAde⁺ plot indicating that this pK_a is related to the deprotonation of His450 [Benen et al. (1991) *Eur. J. Biochem.* 202, 863-872] and to the inhibition by NADH.

The mutations considerably affect turnover. Enzymes Pro451->Ala, His450->Phe and His450->Tyr appear to be almost inactive in both directions. Enzyme His450->Ser is minimally active, V at the pH optimum being 0.5% of wild-type activity in the physiological reaction. Rapid reaction kinetics show that for the His450 mutated enzymes the reductive half reaction using reduced 6,8-thioctic acid amide [lip(SH)₂] is rate limiting and extremely slow when compared to the wild-type enzyme. For enzyme Pro451->Ala it is concluded that the loss of activity is due to over-reduction by lip(SH)₂ and NADH. The Glu455 mutated enzymes are catalytically competent but show strong inhibition by the product NADH (Enzyme Glu455->Asp more than Glu455->Gln). The

inhibition can largely be overcome by using AcPyAde⁺ instead of NAD⁺ in the physiological reaction.

The rapid reaction kinetics obtained for enzymes Glu455->Asp and Glu455->Gln deviate from the wild-type enzyme. It is concluded that this difference is due to cooperativity between the active sites in this dimeric enzyme. Rapid reaction kinetics of enzymes His450->Ser and Glu455->Gln show the existence of two intermediates at the 2-electron reduced level: a species with the NAD⁺ bound, the flavin reduced and the disulfide intact (oxidized) and a species with NAD⁺ bound, the disulfide reduced and the flavin oxidized. No spectral evidence is obtained for the participation of a proposed flavin C4a adduct intermediate [Thorpe, C. and Williams, C.H. Jr. (1981) *Biochemistry* 20, 1507-1513] in the reaction mechanism of enzymes His450->Ser and Glu455->Gln.

Introduction

Lipoamide dehydrogenase is the flavoprotein component of the pyruvate-, oxoglutarate- and branched chain oxo acid dehydrogenase complexes [1,2]. In the physiological direction it catalyses the oxidation of a reduced lipoyl group, that is covalently attached to the core protein of these complexes, by NAD⁺. This lipoyl group can be replaced with free lipoamide. Lipoamide dehydrogenase belongs to the family of dimeric flavoenzymes that contain a redox active disulfide bridge participating in catalysis [1]. The enzyme is composed of two identical subunits with the two active sites built by contacts between the subunits. Other members of this family are glutathione reductase [1], mercuric ion reductase [3], trypanothione reductase [4] and thioredoxin reductase [5].

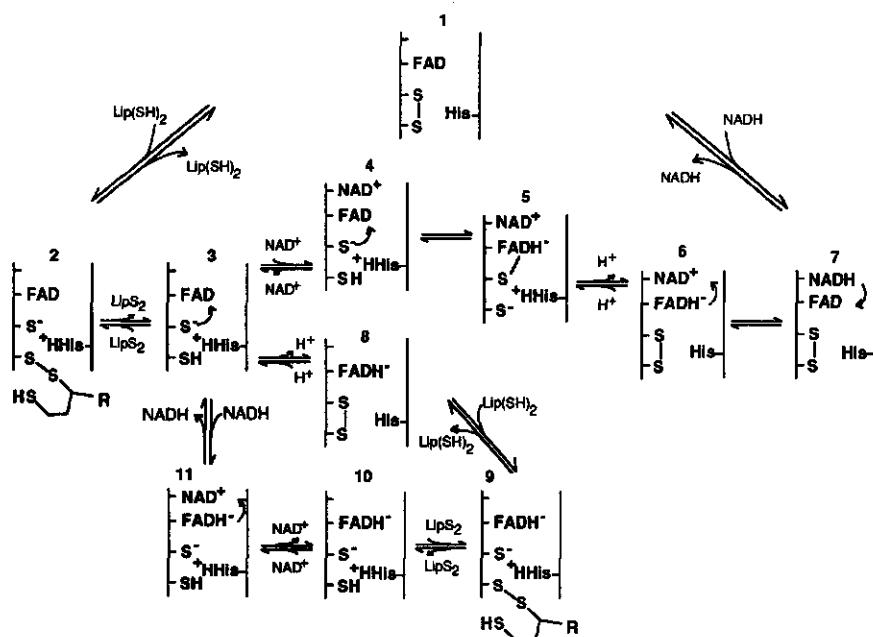
Extensive studies on lipoamide dehydrogenase have been performed on the enzymes as isolated from pig heart, rat liver and *Escherichia coli* [6-14]. All three lipoamide dehydrogenases were shown to act according to a ping-pong mechanism in the physiological reaction [6, 8, 14]. During catalysis, the enzyme shuttles between the oxidized [Eox] and the 2-electron reduced [EH₂] state [15]. The 4-electron reduced state [EH₄] was shown to be inactive and to result from over-reduction by NADH [12, 15]. The over-reduction is manifested as product inhibition. Lipoamide dehydrogenase from *E. coli* has been shown to be very susceptible to product/'dead-end' inhibition [7, 12]. The inhibition is so severe that determination of steady state kinetics was only possible in a rapid reaction spectrophotometer [14]. The nature of the dimeric structure indicates that communication between the active sites seems possible. For each enzyme a different degree of cooperativity was reported. For pig heart enzyme negative cooperativity was reported (from NAD⁺ binding studies) in mono-alkylated enzyme [16,

17] and in native enzyme [18]. For *E. coli* lipoamide dehydrogenase [14] positive cooperativity at the EH_2 level was reported while for rat liver lipoamide dehydrogenase a slight negative cooperativity at the first substrate level was reported [8]. For the related enzyme mercuric ion reductase very strong cooperativity was reported recently that was explained in terms of alternating sites activity [19].

Detailed studies on pig heart enzyme comprising both steady state and rapid reaction kinetics led to the proposal of a reaction mechanism involving a base, histidine, in the active site that becomes protonated during catalysis [9, 20, 21]. Recently, conclusive evidence for the role of the histidine was obtained by site directed mutagenesis studies on glutathione reductase [22, 23], *E. coli* [24] and *A. vinelandii* lipoamide dehydrogenase [25]. Scheme 1 depicts the proposed reaction intermediates during turnover in either direction and the formation of the EH_4 species.

Species (1) represents Eox. Species (2) has been proposed by Matthews and co-workers [9] and is known as the mixed disulfide species. After release of the oxidized substrate, species (3) is formed, the EH_2 species exhibiting the typical 530 nm charge-transfer absorbance giving rise to a red color. It has been shown for *E. coli* [11] and *A. vinelandii* lipoamide dehydrogenase [26] that this species consists of multiple electronic forms. The formation of the Michaelis complex of EH_2 and NAD^+ , species (4), has been proposed in analogy with pig heart EH_2 reacting with the NAD^+ analogs acetylpyridine adenine dinucleotide [AcPyAde^+] or nicotinamide hypoxanthine dinucleotide [10]. It was shown that these intermediates had an altered charge-transfer absorbance with a maximum at 580 nm. Species (5), the flavin C4a adduct intermediate characterized by an absorbance maximum at 384 nm, was proposed based on NAD^+ binding studies with monoalkylated pig heart enzyme [17]. This species was also identified in wild-type and a mutated mercuric ion reductase [27, 28]. After completion of the reoxidation of the disulfide the reducing equivalents reside on the FAD as depicted by species (6). This species was first described by Massey and Veeger [15] studying reduction of pig heart enzyme with NADH in the presence of arsenite. A green species was observed with an absorbance maximum at 680-700 nm. A similar green species was reported for pig heart enzyme reacting with reduced acetylpyridine adenine dinucleotide or nicotinamide hypoxanthine dinucleotide [10]. Finally FADH^- is reoxidized by NAD^+ resulting in species (7). Spectral evidence for this species, showing low long wavelength absorbance extending beyond 700 nm and a maximum at 580 nm, has only been obtained by studies of pig heart enzyme reacting with reduced acetylpyridine adenine dinucleotide or nicotinamide hypoxanthine dinucleotide [10] and very recently with Lys53- \rightarrow Arg mutated *E. coli* enzyme [29].

For *E. coli* lipoamide dehydrogenase over-reduction by a slight excess of reduced 6,8-thiodctic acid amide [$\text{lip}(\text{SH})_2$] was reported [7]. This was also shown for *A. vinelandii*



Scheme 1. Proposed reaction intermediates for lipoamide dehydrogenase. The arrows indicate charge-transfer interaction and are drawn from donor to acceptor. Explanation in text.

lipoamide dehydrogenase though at much higher concentrations of $\text{lip}(\text{SH})_2$ [26]. Species 8-10 are possible intermediates. Before reduction by $\text{lip}(\text{SH})_2$ can take place the disulfide must be in its oxidized state as shown by species (8). Analogous to reduction of Eox the disulfide can then be further reduced via the mixed disulfide intermediate, species (9). Species (10) is the fully reduced EH_4 species with virtually no absorbance in the visible region. The reduced flavin carries a negative charge on N(1) as evidenced by NMR studies [30]. Species (11) represents the NAD^+ bound EH_4 species that can be obtained by reduction of Eox with an excess of NADH via species (3) or by reacting species (10) with NAD^+ . This species is characterized by an absorbance maximum at 750 nm leading to a blue/grey color.

In a previous paper the rationale for the selection of amino acids to be mutated was outlined and the spectral properties of the wild-type and mutated enzymes were reported [26]. This paper deals with the kinetic properties and identification of several of the intermediate species as shown in Scheme 1 of *A. vinelandii* lipoamide dehydrogenase and mutated enzymes.

Materials and Methods

General. Construction of the mutated enzymes, isolation and treatment of the enzymes were performed as described [26]. NAD⁺ (grade I) NADH (grade I), NADP⁺, xanthine, xanthine oxidase (from cow milk), glucose-6-phosphate and glucose-6-phosphate dehydrogenase (from yeast, analytical grade) were from Boehringer. NAD⁺ analogs, lipS₂, dichlorophenolindophenol [Cl₂Ind] and 5,5'-dithiobis (2-nitrobenzoate) [Nbs₂] and biological buffers were obtained from Sigma Inc.. All other chemicals used were of the highest purity available. NAD⁺, AcPyAde⁺, NADH, lip(SH)₂ and enzyme concentrations were determined as described previously [26]. The thio-NAD⁺ concentration was determined as described for AcPyAde⁺.

Steady state kinetics. All activity measurements were performed on a Zeiss M4 QIII spectrophotometer at 25°C. The forward reaction lip(SH)₂/NAD⁺ was determined routinely in 50 mM sodium pyrophosphate buffer, 0.5 mM EDTA pH 8.0 [PPI/EDTA-buffer]. In a standard assay 1.0 mM NAD⁺ and 1.0 mM lip(SH)₂ were used and the formation of NADH was monitored at 340 nm. Steady state kinetics of the forward reaction of the wild-type enzyme were studied as follows. To a temperature equilibrated cuvette containing 950 µl PPI-buffer, 20 µl of each of the substrates was added followed by the addition of 10 µl of enzyme at the proper dilution. Substrate concentration combinations were chosen such as to avoid errors due to inactivation of enzyme in the time course of the experiment. Therefore the experiment was started with the lowest concentration of substrate A, where substrate B was varied, followed by the highest concentration of substrate A with B varied. Next the second lowest concentration of A was used followed by the second highest concentration of A and so on. Triplicate series were measured.

pH dependent studies were performed in buffers containing 0.5 mM EDTA and adjusted to 150 mM in ionic strength with KCl. Buffers used: pH 5.5-6.0-6.5, 100 mM Mes; pH 7.0-7.5-7.8, 100 mM Hepes; pH 8.0-8.6, 100 mM Hepps; pH 9.0-9.3 100 mM Ches. Data were analyzed according to a ping-pong mechanism.

The reverse reaction, NADH/lipS₂, was determined as described [31]. The NADH-dependent reduction of Cl₂Ind (diaphorase activity) was measured in PPI/EDTA-buffer ($\epsilon_{\text{Cl}_2\text{Ind}}$, 600 nm = 22900 M⁻¹ cm⁻¹, pH 8.0) by following the decrease of Cl₂Ind at 600 nm. The transhydrogenase reaction NADH/thio-NAD⁺ was performed according to ref. [32].

Rapid reaction kinetics. Rapid reaction kinetics were carried out using a temperature-controlled single wavelength stopped-flow spectrophotometer, type SF-51, from High Tech Scientific inc. with 1.3 ms dead time. The instrument was interfaced to

an IBM computer for data acquisition and analysis. Data were analyzed with a program from High Tech Scientific inc.. Rapid scan experiments were performed with a stopped flow instrument having a 2 cm light path cell and a dead time of 3 ms, and using a Tracor Northern diode array spectrophotometer as the detector (scan time 5.42 ms). The detector was interfaced to a Tracor Northern computer for data acquisition and analysis. All experiments were performed anaerobically at 21.0 °C in 100 mM Good buffers containing 0.5 mM EDTA adjusted to 150 mM in ionic strength with KCl. Enzyme concentrations after mixing were 26.7 μ M. Generation of 2-electron reduced enzyme [EH₂] was accomplished by reduction with a small excess of sodiumborohydride.

Rate constants at infinite substrate concentration and K_d values were determined from non-linear fitting of apparent rate constants obtained at, at least, five different substrate concentrations. Apparent rate constants represent the average of minimally four shots. In order to achieve pseudo-first order conditions the lowest substrate concentrations used were five times as high as the enzyme concentration. Since only the L-enantiomer of lip(SH)₂ reacts rapidly [6, 9], substrate concentrations were adjusted to those of the L-enantiomer. Lip(SH)₂ and lipS₂ were dissolved in buffer/ethanol to yield a final ethanol content of 5% in the mixing chamber.

Simulation of rapid reaction kinetics was performed using the program 'KINSIM' [33] run on a VAX/VMS minicomputer.

Redox potential determinations. Visible absorption spectra were recorded on a temperature controlled Aminco DW2000 spectrophotometer at 25°C. Reductions were carried out in anaerobic cuvettes in 50 mM potassium phosphate buffer pH 7.0, 0.5 mM EDTA. Redox potentials were determined in three different ways. Method one was essentially as described for pig heart enzyme [20]. Method two, the xanthine/xanthine oxidase method, was recently described by Massey [34] and was applied without modification. The co-titrants used, 30 μ M in concentration, were safranine T, phenosafranine and benzylviologen. Method three was a modification of method two. Instead of using xanthine/xanthine oxidase as an electron generating system, NADPH was generated from NADP⁺ (75 μ M) using glucose-6-phosphate dehydrogenase (2.4×10^{-4} U) and glucose-6-phosphate (400 μ M). NADPH proved useful as a reductant for lipoamide dehydrogenase since quantitative reduction could be achieved yielding spectra identical to reduction by lip(SH)₂. Furthermore NADP⁺ did not give rise to the typical long wavelength absorbance characteristic for FADH⁻/NAD⁺ charge-transfer interaction, indicating that no efficient binding occurs. For method one, the titrant was added using a gastight Hamilton syringe equipped with a dispenser. Spectra were recorded until changes were complete. For method two and three the reaction was started by the addition of enzyme (xanthine oxidase or glucose-6-phosphate

dehydrogenase) after anaerobiosis was established. In order to achieve equilibrium the amount of enzyme was chosen such as to complete reduction in a time span of 6-9 hrs. The amount of enzyme was halved to check whether equilibrium was established [34].

Results

Steady state kinetics

Wild-type lipoamide dehydrogenase. Under non-saturating conditions, the optimum pH of the reaction $\text{lip(SH)}_2/\text{NAD}^+$ is 8.0, in PPI/EDTA-buffer as found for all other lipoamide dehydrogenases [6, 7, 8]. Also the reaction $\text{lip(SH)}_2/\text{AcPyAde}^+$ shows an optimum at pH 8.0. In Fig. 1 A and 1 B the double reciprocal plots of the forward reaction $\text{lip(SH)}_2/\text{NAD}^+$ are presented. When the concentrations of lip(SH)_2 and NAD^+ are varied in fixed ratios a straight line is obtained in a double reciprocal plot (not shown). These results clearly demonstrate that *A. vinelandii* lipoamide dehydrogenase like all other lipoamide dehydrogenases studied so far functions according to a ping-pong mechanism.

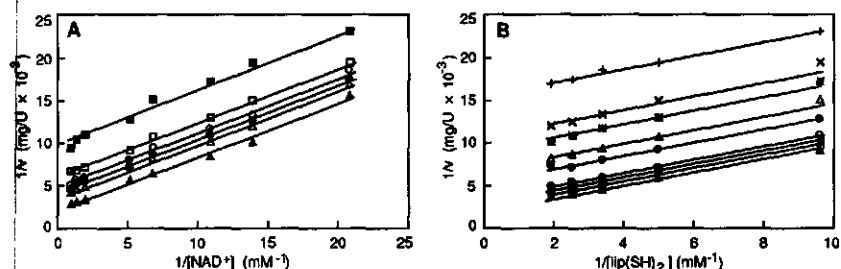


Fig. 1. Steady state kinetics of the physiological reaction of *Azotobacter vinelandii* wild-type lipoamide dehydrogenase at the optimum pH 8.0. The temperature was 25°C, for other details see Materials and Methods. A, LB-plot of the reaction $\text{lip(SH)}_2/\text{NAD}^+$ with $[\text{NAD}^+]$ varied and $[\text{lip(SH)}_2]$ fixed. Closed triangles represent the extrapolated velocities at infinite $[\text{lip(SH)}_2]$. NAD^+ concentrations (μM): 48, 72, 92, 147, 194, 511, 752 and 1044. lip(SH)_2 concentrations (μM): 104, 200, 295, 397 and 518. B, as A with $[\text{lip(SH)}_2]$ varied and $[\text{NAD}^+]$ fixed. Closed triangles represent the extrapolated velocities at infinite $[\text{NAD}^+]$.

From secondary double reciprocal plots the V and K_m values for NAD^+ and lip(SH)_2 are determined: $V = 490 \text{ U/mg}$, $k_{\text{cat}} = 420 \text{ s}^{-1}$, $K_m \text{ lip(SH)}_2 = 390 \mu\text{M}$ and $K_m \text{ NAD}^+ = 325 \mu\text{M}$. A Hill-plot constructed from the data for the wild-type enzyme reveals a coefficient of $h = 1$ with NAD^+ as a substrate excluding cooperativity at the EH_2 level. From experiments in which the lip(SH)_2 and AcPyAde^+ concentrations are varied in fixed ratios it can be concluded that the mechanism of the reaction remains ping-pong. As is clear from Table 1, the rate of reduction of AcPyAde^+ by the wild-type lipoamide

dehydrogenase is considerably lower than that of NAD⁺. From secondary double reciprocal plots the K_m values for lip(SH)₂ and AcPyAde⁺ are determined. K_m lip(SH)₂ is lowered 4-fold when compared with NAD⁺ as a substrate (see Table 1) while the K_m AcPyAde⁺ is 2-3 fold higher than the K_m NAD⁺.

To explore the effect of the pH on the activity, steady-state kinetics of wild-type enzyme was studied at different pH values (see Fig. 2 A and C) using NAD⁺ and AcPyAde⁺ as electron acceptors. Unexpectedly, strong product inhibition is observed for wild-type enzyme using NAD⁺ at high pH values. This will be discussed below. As a

Enzyme	lip(SH) ₂ / NAD ⁺			lip(SH) ₂ / APAD ⁺			NADH / Cl ₂ Ind	
	k _{cat} s ⁻¹	K _m lip(SH) ₂ μM	K _m NAD ⁺ μM	k _{cat} s ⁻¹	K _m lip(SH) ₂ μM	K _m APAD ⁺ μM	k _{cat} s ⁻¹	K _m NADH μM
Wild-type	420	390	325	100	140	1200	170	180
His450->Ser	1.6	1950	300	-	-	-	135	140
His450->Phe	0.0	-	-	-	-	-	170	150
His450->Tyr	0.0	-	-	-	-	-	170	200
Glu455->Asp	nd	-	-	2.4	30	640	160	50
Glu455->Gln	nd	-	-	1.9	240	1750	200	120
Pro451->Ala	?	-	-	-	-	-	?	-

Table 1. Steady state kinetic parameters of *Azotobacter vinelandii* wild-type and mutated enzymes. The parameters are determined at pH 8.0, the pH optimum for each enzyme, except for enzyme Glu455->Asp where the optimum was pH 7.0. nd signifies that kinetics are not studied due to strong product inhibition. A question mark (?) for enzyme Pro451->Ala signifies that the parameters can not be determined due to very transient activity (see text also). The concentration lip(SH)₂ is for the D,L-mixture.

result the K_m and V values determined at pH values above pH 8.0 are not reliable and are therefore not included in Fig. 2 A. This inhibition is not observed with AcPyAde⁺ as acceptor.

From the Log(V) plot in Fig. 2 A, a pK_a value of 6.4 is obtained for the rate limiting intermediate of wild-type enzyme. The invariance of pK_m [lip(SH)₂] and the change in the pK_m [NAD⁺] around pH 6.4 suggests that protonation of the EH₂.NAD⁺ complex is rate limiting. This is supported by rapid reaction kinetics which show that at pH 8.0 and 6.8 the reoxidation by NAD⁺ is rate limiting (see below). Almost identical pK_a values as found for the limiting protonation of the EH₂.NAD⁺ complex of wild-type enzyme were reported for pig heart [10] and *E. coli* [14] enzyme, pK_a = 6.2 and 6.7 respectively. This indicates that the enzymes obey the same mechanism of reoxidation.

Fig. 2 C shows that V for AcPyAde⁺ reduction by wild-type enzyme does not reach a maximum in the experimental pH interval. Therefore no pK_a can be assigned to a rate limiting intermediate. From the pK_m [AcPyAde⁺] plot a pK_a of 8.1 is determined representing a deprotonation of EH₂ [35]. This pK_a value may reflect deprotonation of the histidine.

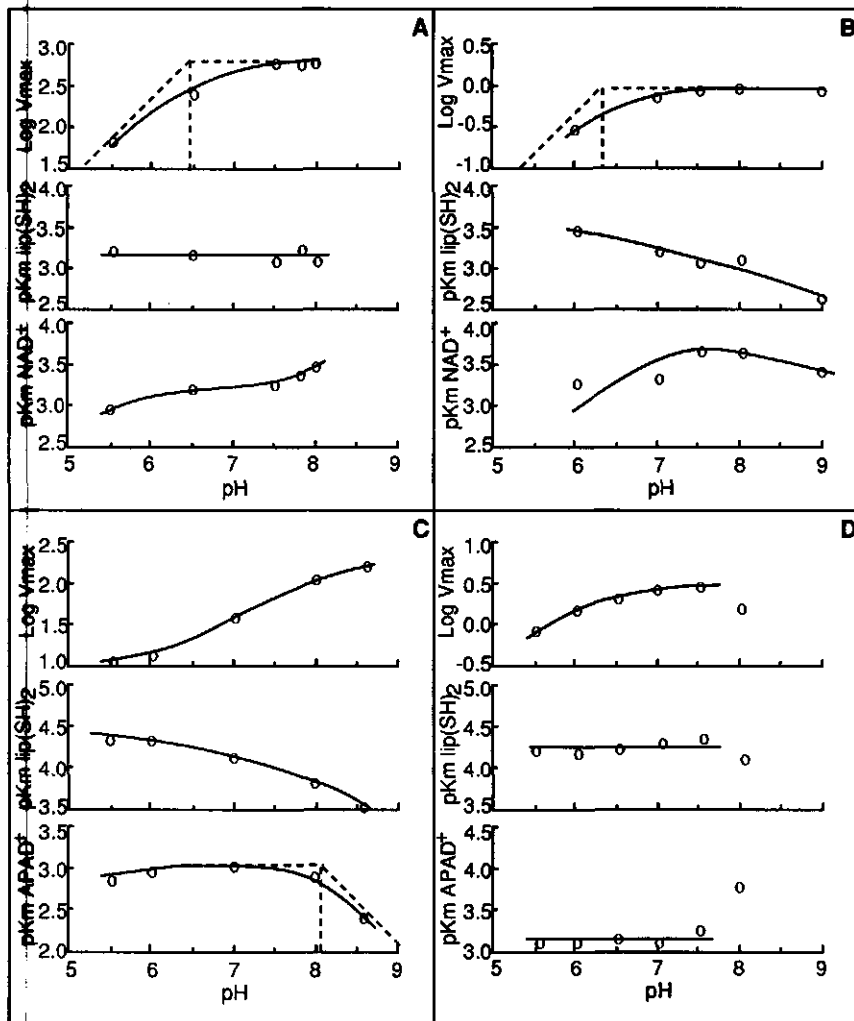


Fig. 2. pH dependence of the steady state kinetics in the physiological reaction of *Azotobacter vinelandii* wild-type lipamide dehydrogenase and mutated enzymes His450->Ser and Glu455->Asp. Conditions are described in Materials and Methods. A, wild-type enzyme using NAD^+ as electron acceptor. B, enzyme His450->Ser using NAD^+ as electron acceptor. C, wild-type enzyme using AcPyAde^+ as electron acceptor. D, enzyme Glu455->Asp using AcPyAde^+ as electron acceptor.

Mutated enzymes. Table 1 gives an overview of the specific activities in the various reactions of the wild-type and mutated enzymes. Considerable differences are observed between the wild-type and the mutated enzymes in the rate of either NAD⁺ or AcPyAde⁺ dependent oxidation of lip(SH)₂. The diaphorase activity is however almost the same in wild-type and all mutated lipoamide dehydrogenases which indicates that the binding of NADH at the *re*-side of the FAD is not appreciably affected by the mutations on the *si*-side.

His450 mutated enzymes. Changing the 'proton accepting' histidine450 [9] into tyrosine, phenylalanine or serine clearly demonstrates the important role of this residue in catalysis. With enzymes His450->Phe and His450->Tyr in either directions virtually no activity is observed. With enzyme His450->Ser almost no activity was observed in the reverse reaction, reduction of lipS₂, monitored by the oxidation of NADH in the presence of NAD⁺. About 0.5% of the wild-type activity is found in the forward reaction, lip(SH)₂/NAD⁺, at the optimum pH 8.0. A kinetic analysis as described for wild-type enzyme demonstrates that enzyme His450->Ser also functions according to a ping-pong mechanism. The K_m NAD⁺ is slightly smaller in this mutated enzyme and the K_m lip(SH)₂ is 5-fold higher than found for the wild-type enzyme.

Assuming His450 to abstract a proton from the substrate lip(SH)₂ as proposed [9], one might expect the activity of enzyme His450->Ser would increase at elevated pH values, where lip(SH)₂ (pK_{a1} = 9.35, free in solution [9]) becomes deprotonated. However V remains constant between pH 8.0 and pH 9.0. In the pH dependent studies no product inhibition by NADH is found in the experimental pH interval. From the Log(V) plot in Fig. 2 B, a pK_a value of 6.3 is obtained for the deprotonation of the rate limiting intermediate in enzyme His450->Ser.

The 0.5% of activity remaining in the forward reaction is compatible with results recently reported for His-to-Ala and His-to-Gln mutated enzymes of glutathione reductase [22, 23] and His-to-Gln in *E. coli* lipoamide dehydrogenase [24]. This suggests that the function of the imidazole as a base, can be carried out by bound solvent, albeit ineffectively. The difference in effect of either tyrosine or phenylalanine at position 450 can not be assessed via kinetics. Spectral studies showed that these enzymes still can be reduced by lip(SH)₂ though very slowly. It is therefore concluded that the rather bulky aromatic residues impose structural constraints on the enzyme that make it very difficult for lip(SH)₂ to effectively interact with the disulfide to exchange reducing equivalents.

Glu455 mutated enzymes. With enzyme Glu455->Asp very strong product (NADH) inhibition is observed in the reaction $\text{lip}(\text{SH})_2/\text{NAD}^+$. The results indicate that this enzyme is inhibited by NADH in a 'dead-end' manner. Addition of excess NAD^+ after inhibition is complete does not restore activity. Revived NADH production is only observed after the addition of an extra aliquot of enzyme. This extra enzyme portion becomes inhibited approximately as fast as the initial enzyme portion. No detailed studies were carried out to investigate this phenomenon. However the results indicate that the inhibition is more dependent on time than on the NADH concentration. In view of an increase of the dissociation constant for the monomer-dimer equilibrium upon reduction to the EH_4 level [31] it is tempting to speculate that the irreversibility of the inhibition is caused by monomerization.

The reverse reaction as well as the transhydrogenase reaction $\text{NADH}/\text{thio-NAD}^+$ are not detectable. When an electron acceptor with higher midpoint potential than NAD^+ or thio-NAD^+ is used, *in casu* AcPyAde^+ in the forward reaction, and Cl_2Ind in the diaphorase reaction, quantitative reduction of the acceptors is observed in the pH interval studied (pH 5.5-9.0) ($E'_m \text{NAD}^+/\text{NADH} = -320 \text{ mV}$ [36], $E'_m \text{thio-NAD}^+/\text{thio-NADH} = -283 \text{ mV}$ [36], $E'_m \text{AcPyAde}^+/\text{AcPyAdeH} = -258 \text{ mV}$ [36] and $E'_m \text{Cl}_2\text{Ind}/\text{Cl}_2\text{IndH}_2 = +217 \text{ mV}$ [37], pH 7.0). With AcPyAde^+ 'dead-end' inhibition is observed above pH 7.5.

Enzyme Glu455->Gln differs in catalytic behavior from enzyme Glu455->Asp. Here a somewhat less strong inhibitory effect of NADH is found. With AcPyAde^+ as acceptor no inhibition is observed.

Under non-saturating fixed substrate concentrations the optimum for the AcPyAde^+ reduction is at pH 8.0 for enzyme Glu455->Gln and is lowered to pH 7.0-7.5 for enzyme Glu455->Asp. Both Glu455 mutated enzymes function according to a ping-pong mechanism.

For both Glu455 mutated enzymes the steady-state kinetics of the reaction $\text{lip}(\text{SH})_2/\text{AcPyAde}^+$ were studied as a function of pH. Enzyme Glu455->Asp shows, as mentioned above, 'dead-end' inhibition with AcPyAde^+ . This hampers the determination of the kinetic constants above pH 7.5. Except for a change in V , the kinetic parameters of enzyme Glu455->Asp do not change significantly in the experimental pH range ($\text{pH} \leq 7.5$), Fig. 2 D. The pH dependence of steady state kinetics of enzyme Glu455->Gln is quite different from enzyme Glu455->Asp (results not shown). V changes only slightly over the experimental pH range (pH 5.5-9.0) showing an optimum at pH 8.0. The K_m for $\text{lip}(\text{SH})_2$ increases at lower pH but $K_m \text{AcPyAde}^+$ remains almost constant as in enzyme Glu455->Asp. No pK_a values are determinable for this enzyme.

Rapid reaction kinetics

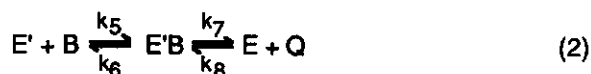
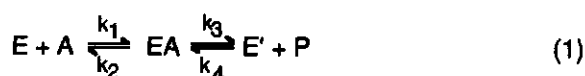
In order to get a more detailed insight into the separate half reactions, the reductive reactions with lip(SH)₂ and NADH and the oxidative reactions with NAD⁺ and lipS₂ were studied in the stopped-flow spectrophotometer.

Wild-type lipoamide dehydrogenase. At pH 7.0 and 8.0 the reduction of Eox by lip(SH)₂ and reoxidation of EH₂ by NAD⁺ and lipS₂ as monitored at 450 nm and 530 nm can essentially be described by a single-exponential function. In Table 2 the extrapolated rate constants at infinite substrate concentration and corresponding K_d values are presented.

Enzyme	Reduction level	Substrate	pH	k _a s ⁻¹	K _{d(a)} mM	k _b s ⁻¹	K _{d(b)} mM	Wavelength nm
Wild-type	Eox	lip(SH) ₂	8.0	2000	0.9			450, 530
	Eox	lip(SH) ₂	7.0	1000	0.7			530
	Eox	NADH	8.0	>3000				450, 530, 700
	EH ₂	lipS ₂	8.0	400	0.5			450, 530
	EH ₂	NAD ⁺	8.0	1000	0.37			450, 530
	EH ₂	NAD ⁺	7.0	760	0.47			450, 530
His450→Ser	Eox	lip(SH) ₂	9.3	1.9	5.0			450, 530
	Eox	lip(SH) ₂	8.6	1.5	4.3			530
	Eox	lip(SH) ₂	7.8	1.3	4.7			530
	Eox	lip(SH) ₂	7.3	1.0	3.7			530
	Eox	lip(SH) ₂	6.6	0.8	3.5			530
	Eox	NADH	8.0	>3000				450, 530, 700
	EH ₂	lipS ₂	8.0	<0.005				530
	EH ₂	NAD ⁺	8.0	4.0	0.33			530
	EH ₂	NAD ⁺	6.8	4.4	0.27			530
Glu455→Asp	Eox	lip(SH) ₂	8.0	?	?	1000	4.7	450, 530
	Eox	lip(SH) ₂	7.0	?	?	600	4.0	530
	Eox	lip(SH) ₂	5.9	230	5.4			530
	Eox	NADH	8.0	>3000				
	EH ₂	lipS ₂	8.0	?	?	12	0.55	450, 530
Glu455→Gln	Eox	lip(SH) ₂	8.6	250	2.6	60	2.5	530
	Eox	lip(SH) ₂	7.9	?	?	60	4.2	530
	Eox	lip(SH) ₂	7.3	?	?	35	3.6	530
	Eox	lip(SH) ₂	5.9	44	4.8			530
	Eox	NADH	8.0	>3000				450, 530, 700
	EH ₂	lipS ₂	8.0	<0.05				530
	EH ₂	NAD ⁺	8.0	58	0.17	14	0.30	530

Table 2. Rate constants and dissociation constants of *Azotobacter vinelandii* wild-type and mutated enzymes. For NADH reduction the rate constant of reduction of the FAD is shown. A question mark (?) signifies that the constants could not be determined due to the small absorbance changes associated at low substrate concentration (see text). K_d values for lip(SH)₂ are expressed for the L-enantiomer. Rate constants k_a and k_b are extrapolated to infinite [substrate]. The faster rate constant is k_a while the slower rate constant is k_b. The wavelength at which data were obtained is indicated in the last column.

Ping-pong enzymes obey the following equations:



for which the steady state relation

$$k_{cat} = \frac{k_3 \times k_7}{k_3 + k_7} \quad (3)$$

was derived [38]. Here k_3 and k_7 are the first order rate constants of the reaction of the first and second substrate respectively (k_a of the appropriate substrate in Table 2). A k_{cat} was calculated as 670 s^{-1} at pH 8.0 for the reaction $\text{lip(SH)}_2/\text{NAD}^+$ with data from Table 2 and equation (3). This value agrees reasonably well with k_{cat} calculated from steady state kinetics: 420 s^{-1} . Comparison of k_3 and k_7 demonstrates that, at pH 8.0, the reductive reaction by lip(SH)_2 is not rate limiting as found for the pig heart enzyme [6, 10].

The reductive reaction with NADH is extremely fast and is almost complete in the dead time of the stopped-flow instrument. Rapid scan spectra (dead time spectrum 5.42 ms after mixing) and a compilation of relative absorbance changes at 453, 530 and 700

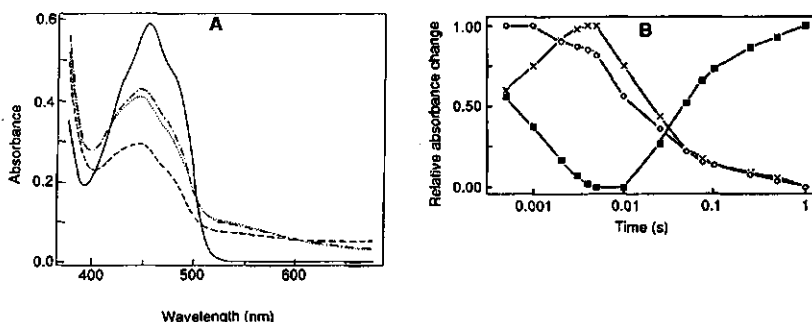


Fig. 3. Spectral changes of *Azotobacter vinelandii* wild-type lipamide dehydrogenase upon reduction by NADH in the rapid reaction instruments.

A. Reduction of wild-type enzyme by 5 molar equivalents of NADH at pH 7.8, recorded with the rapid scan instrument. Eox, —; dead time (5.42 ms after mixing), - - - -; 10.84 ms after mixing,; 542 ms after mixing, - - - - . B. Compilation of relative absorbance changes during reduction of wild-type enzyme by 10 molar equivalents of NADH in the single wavelength stopped-flow instrument. Absorbance changes at 453 nm, \circ ; absorbance changes at 530 nm, \times ; absorbance changes at 700 nm, \blacksquare .

nm collected with the single wavelength instrument are shown in Fig. 3 A and B. The absorbance at 700 nm is a monitor for the charge-transfer complex between the reduced flavin [FADH⁻] and NAD⁺ (species 6 in Scheme 1, see ref. 26 for the spectrum of this species).

Fig. 3A shows that approximately half of the total absorbance change at 453 nm takes place in 10 ms, but part B shows that only 20 % of the total absorbance change takes place in 10 ms. The fact that the 700 nm absorbance is already up at 0.5 ms indicates that a very fast phase, involving a significant decrease in absorbance at 453 nm, was largely missed. These initial changes are logically attributed to the formation of the FADH⁻/NAD⁺ charge-transfer complex. The 530 nm absorbance increases over the first 5 msec and indicates that the electrons (formally two electrons and a proton; a hydride equivalent) are passed over from the flavin to the disulfide (species 6 to 4 or 3 in Scheme 1) an effect that is more pronounced in the His450->Ser enzyme (see below). Changes occurring after 5 ms are most likely due to further reduction by the excess of NADH.

His450 mutated enzymes. The reductive reaction of Eox by lip(SH)₂ is slow (His450->Ser) to extremely slow (His450->Phe and His450->Tyr) upon mutation of the active site base. No rate constants were determined for enzymes His450->Phe and -Y. Even at the highest possible substrate concentration full reduction to EH₂ lasted 250 seconds yielding an apparent first order rate constant of $\pm 25 \times 10^{-3} \text{ s}^{-1}$. For enzyme His450->Ser the reduction by lip(SH)₂ is monophasic preceded by a lag-phase (< 300 ms). The reoxidation of EH₂ by NAD⁺ is also monophasic, however the lag-phase is not observed in these traces. The rate constants and K_d values as determined for enzyme His450->Ser are presented in Table 2. The rate constants and K_d values for the substrates L-lip(SH)₂ and L-lipS₂ should be regarded as approximations since the determined K_d values are approximately 3-4 times higher than the maximal experimental concentration of L-lip(SH)₂ or L-lipS₂ due to solubility limitations.

For the forward overall reaction of enzyme His450->Ser from equation (3) a k_{cat} of 1.0 s⁻¹ is calculated that agrees reasonably well with k_{cat} = 1.6 s⁻¹ as obtained from steady state kinetics. Contrary to the wild-type enzyme however, for enzyme His450->Ser the reductive reaction is rate limiting at both pH 6.8 and 8.0.

The rate constant for the reductive reaction by lip(SH)₂ increases only slightly with pH and the traces remain mono-exponential up to pH 9.3. The K_d for lip(SH)₂ increases with pH suggesting that the substrate binds to the mutated enzyme in its protonated state. The reoxidation reaction of His450->Ser EH₂ by lipS₂ is barely detectable at pH 8.0 indicating that the reactivity of the substrate is very poor or the affinity of the enzyme for this substrate is very low.

The reoxidation of EH_2 by NAD^+ proceeds faster in this enzyme than the reduction of Eox by $\text{lip}(\text{SH})_2$ (Table 2) although the reaction is also extremely slow when compared to wild-type enzyme. Previously we reported a pK_a of 7.5 at the EH_2 level for this enzyme for the deprotonation EH/EH_2^- [26]. This pK_a is not reflected in the pH dependence of the reoxidation rate constants.

A possible mechanism of electron transfer from the nascent thiols to the flavin involves the transient formation of a C4a adduct between the charge-transfer thiolate and the flavin [17, 27, 28], species 5 in Scheme 1. This flavin C4a adduct species exhibits characteristic absorbance at 380 nm. Therefore the reoxidation of His450->Ser EH_2 with NAD^+ was monitored at this wavelength. No absorbance changes compatible with the formation of a flavin C4a adduct species were however detected.

The kinetics of the reduction of enzyme His450->Ser by NADH are compatible with a very fast reduction of the flavin (species 6 in Scheme 1) with subsequent slow transfer of the hydride equivalent to the disulfide (species 4 and 3 in Scheme 1). Fig. 4 A and B show rapid scan spectra and a compilation of relative absorbance changes at 453, 530 and 700 nm obtained with the single wavelength instrument. The profound stabilization of the FADH/NAD^+ charge-transfer complex by a factor of 1000 is due to impaired transfer of electrons to the disulfide. This intramolecular transfer of an hydride equivalent involves partial regain of absorbance at 453 nm, loss of FADH/NAD^+ charge-transfer at 700 nm and gain of the thiolate to FAD charge-transfer absorbance at

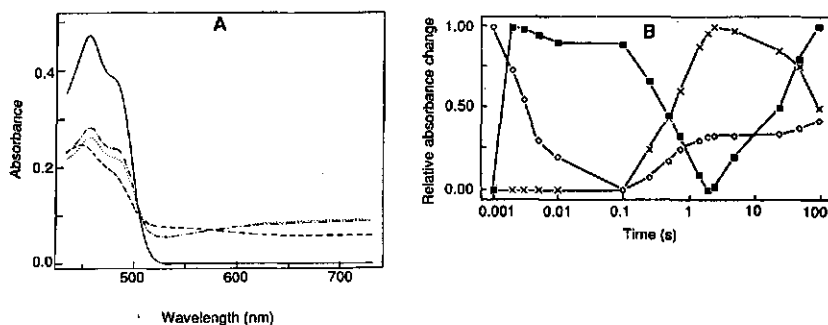


Fig. 4. Spectral changes of *Azotobacter vinelandii* His450->Ser lipoamide dehydrogenase upon reduction by NADH in the rapid reaction instruments.

A. Reduction of enzyme His450->Ser by 10 molar equivalents of NADH at pH 7.8, recorded with the rapid scan instrument. Eox, —; dead time (5.42 ms after mixing), ·····; 10.84 ms after mixing, ·····; 542 msec. after mixing, —. B. Compilation of relative absorbance changes during reduction of enzyme His450->Ser by 10 molar equivalents of NADH in the single wavelength stopped-flow instrument. Absorbance changes at 453 nm, \diamond ; absorbance changes at 530 nm, \times ; absorbance changes at 700 nm, \blacksquare .

530 nm. Following reduction of the disulfide, reaction with a second mole of NADH is very slow (species 3 to 11). Also in the reductive reaction with NADH no 380 nm absorbance is detected that would indicate the transient stabilization of a flavin C4a adduct species.

Glu455 mutated enzymes. For the Glu455 mutated enzymes the kinetic traces obtained upon reduction of Eox with lip(SH)₂ or reoxidation of EH₂ with either lipS₂ or NAD⁺ at pH > 6.0 are not mono-exponential as found for the wild-type and His450->Ser enzymes (Table 2). The introduction of a second exponential demonstrates that the reaction proceeds in at least two phases. In all three reactions studied the biphasic nature becomes more apparent at high substrate concentrations as the amplitude of the fast phase increases. Except for enzyme Glu455->Gln in the reductive reaction at pH 8.6 and in the reoxidation reaction with NAD⁺ at pH 8.0 no rate constant for the fast phase can confidently be determined due to the small absorbance changes causing variability in apparent rate constants determined at low substrate concentration. For enzyme Glu455->Gln in the reductive half reaction at pH 8.6, the contribution of the amplitude of the fast phase increases from 5 % at 250 μ M lip(SH)₂ to 30 % at 1.7 mM lip(SH)₂ and extrapolates to 50 % at infinite lip(SH)₂ concentration suggesting that only half of the enzyme reacts in the fast phase. This will be discussed below. In the oxidative reaction with NAD⁺ at pH 8.0, a similar feature is observed. The contribution of the amplitude of the fast phase increases from 25 % at [NAD⁺] = K_d to 58 % at [NAD⁺] = 10 times K_d. In this reaction no absorbance changes at 380 nm are found that indicate the formation of a C4a adduct species. The oxidative reaction of EH₂ of enzyme Glu455->Gln with lipS₂ at pH 8.0 is very slow and almost beyond detection.

Fig. 5 shows rapid scan spectra obtained from reoxidation of EH₂ of Glu455->Gln by 20 equivalents NAD⁺. EH₂ binds NAD⁺ rapidly to give a spectrum that closely resembles the absorption spectra obtained from titration of pig heart EH₂ with NAD⁺ [10] and titration of pig heart enzyme with NADH in the presence of high [NAD⁺] ref. [39]. This spectrum represents a reduced-disulfide-oxidized-flavin-NAD⁺ intermediate species (species 4 in Scheme 1). Intramolecular transfer of a hydride equivalent from the dithiol to the flavin is biphasic and relatively slow, and results in reduction of most of the flavin despite the presence of a large excess of NAD⁺. At this stage the reaction is thermodynamically blocked.

The reductive reaction of Eox Glu455->Gln with 2 equivalents NADH is shown in Fig. 6. The dead time spectrum shows that the reduction of the FAD is very fast (species 6 in Scheme 1). The subsequent intramolecular electron transfer to the disulfide is again relatively slow. Following reduction of the disulfide, reaction with a second mole of NADH is slow .

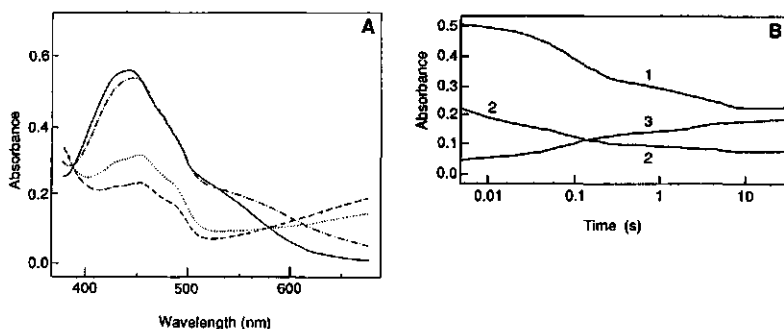


Fig. 5. Spectral changes of 2-electron reduced *Azotobacter vinelandii* Glu455->Gln lipoamide dehydrogenase upon oxidation by NAD^+ in the rapid scan instrument.

A. Oxidation of 2-electron reduced enzyme Glu455->Gln by 20 molar equivalents of NAD^+ at pH 7.8 in the rapid scan spectrophotometer. EH_2 , — ; dead time (5.42 ms after mixing), - - - - - ; 306 ms after mixing, ; 30.6 s after mixing - - - - - . B. Time dependence of absorbance changes of panel A. Curve 1, 457 nm; curve 2, 530 nm; curve 3, 670 nm. EH_2 was generated by reduction with an excess of sodium borohydride with time for the excess to self destruct.

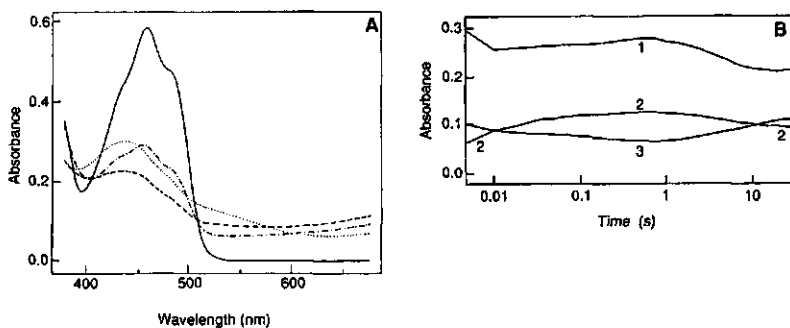


Fig. 6. Spectral changes of *Azotobacter vinelandii* Glu455->Gln lipoamide dehydrogenase upon reduction by NADH in the rapid scan instrument.

A. Reduction of enzyme Glu455->Gln by 2 molar equivalents of NADH at pH 7.8 in the rapid scan spectrophotometer. Eox, — ; dead time (5.42 ms after mixing), - - - - - ; 612 ms after mixing, ; 30.6 s after mixing - - - - - . B. Time dependence of absorbance changes of panel A. Curve 1, 457 nm; curve 2, 530 nm; curve 3, 670 nm.

Enzyme Glu455->Asp differs from Glu455->Gln in spectral properties during reduction by NADH (Table 2). At all NADH concentrations used, enzyme Glu455->Asp shows more extensive reduction of the flavin than enzyme Glu455->Gln and the subsequent reactions are less clear (results not shown)

The results obtained from the rapid reaction studies on the Glu455 mutated enzymes clearly demonstrate that the intramolecular transfer of a hydride equivalent in either direction is slowed down though not as severely as in enzyme His450->Ser. The underlying mechanism might be the same as for enzyme His450->Ser and will be discussed below.

Enzyme Pro451->Ala. The enzyme Pro451->Ala appears to be essentially inactive in both directions. Spectral studies however demonstrate that this enzyme can be reduced by both lip(SH)₂ and NADH, but rapid over-reduction to the catalytically inactive EH₄ occurs. Stopped flow studies at 530 and 450 nm show the rapid formation of a transient charge-transfer complex between thiolate and FAD upon reduction with lip(SH)₂ (within 5 s) followed by a slower reduction of the flavin (results not shown). Enzyme Pro451->Ala also becomes fully reduced by NADH in 10 ms without any detectable changes at 530 nm. The fact that the reduction by NADH is much faster than the over-reduction by lip(SH)₂ indicates that the absence of detectable activity in the physiological reaction is mainly due to the over-reduction by NADH generated after one or a few cycles of turnover.

Redox potentials. Spectral studies have suggested differences in redox potentials between wild-type and mutated enzymes [26]. The different sensitivity of the enzymes toward inhibition by NADH also indicates that differences in redox potentials may exist. Quantitative estimation of the redox potentials as measured by three different methods however failed. The main reason for this is the uncertainty as to the exact contribution of the various EH₂ species. During the reduction to EH₂ and subsequently EH₄ no isosbestic points are observed.

Although no exact redox potentials are determinable, the results obtained allow an estimation of redox potentials of the enzymes in relation to each other. The arrangement of the enzymes in order of decreasing redox potentials (E'_m EH₂/EH₄) is: Glu455->Asp, Glu455->Gln, wild-type and His450->Ser. This trend coincides with the sensitivity towards inhibition by NADH.

Several lines of evidence indicate that binding of NAD⁺ induces an increase of the redox potential of the FAD [10, 40]. Therefore the course of reduction of wild-type enzyme and enzyme Glu455->Asp by NADPH in an NADPH generating system was studied in the presence of 100 μ M AAD⁺ [10, 17, 41], a non-reducible NAD⁺ analog (K_i

AAD⁺ for wild-type enzyme in the reaction lip(SH)₂/NAD⁺ is 40 μM). The formation of NADPH is rate limiting in both the absence and presence of AAD⁺ and equal amounts of glucose-6-phosphate dehydrogenase were used. The results are very conclusive (Fig. 7, only wild-type enzyme shown): no NADPH absorbance is observed in the presence of AAD⁺ until the enzyme is almost completely reduced to EH₄.

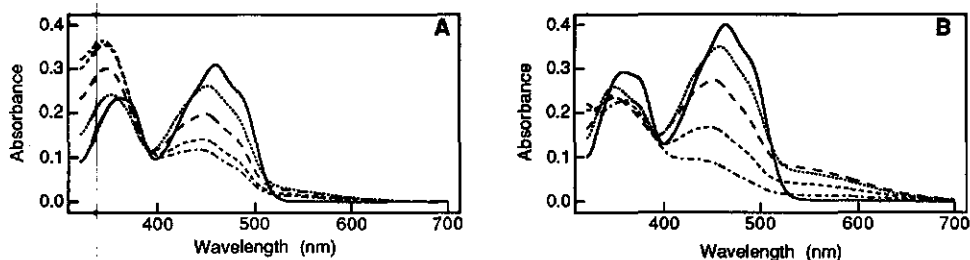


Fig. 7. Spectral changes upon reduction of *Azotobacter vinelandii* wild-type enzyme by NADPH in the absence/presence of AAD⁺. Conditions for reduction of wild-type enzyme by enzymatically formed NADPH are described in Materials and Methods. A, reduction of wild-type enzyme by NADPH. Selected spectra are shown. B, reduction of wild-type enzyme by NADPH in the presence of 100 μM AAD⁺. Selected spectra are shown. A correction was made for the contribution of AAD⁺. The same amount of glucose-6-phosphate dehydrogenase was used in A and B.

These results for the first time clearly establish that binding of a pyridine nucleotide (AAD⁺) indeed raises the EH₂/EH₄ redox potential. Additional support is obtained by the addition of AAD⁺ to EH₂ of wild-type enzyme and enzyme Glu455→Asp, generated by the addition of 5 molar equivalents of lip(SH)₂, Fig. 8. Before addition of AAD⁺ was started the EH₂ spectra were at equilibrium. Addition of 40 μM AAD⁺ results in a shift towards longer wavelength and an increase of the charge-transfer absorbance for both

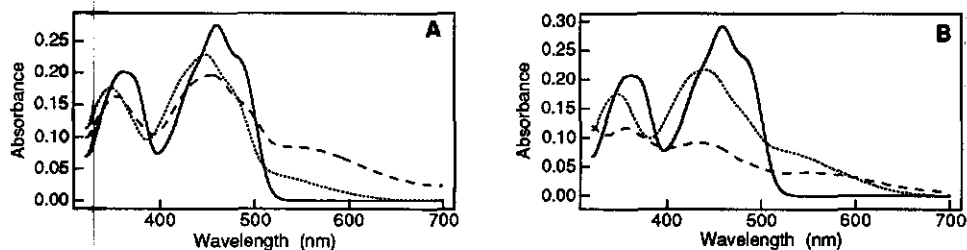


Fig. 8. The effect of addition of AAD⁺ to EH₂ of *Azotobacter vinelandii* lipoamide dehydrogenase. EH₂ was generated by the addition of 5 molar equivalents of lip(SH)₂ to the enzyme in an anaerobic cuvette at pH 7.0. Spectra shown were recorded after changes were complete. —, Eox; , EH₂; - - - - , after addition of 200 μM AAD⁺. A, Wild-type lipoamide dehydrogenase; B, Glu455→Asp lipoamide dehydrogenase.

enzymes (spectra not shown) similar to the result reported for the pig heart enzyme [10]. Subsequent additions of AAD⁺ (up to 200 μ M) have no effect on the initially obtained spectrum of wild-type enzyme after addition of 40 μ M AAD⁺. However for enzyme Glu455->Asp a bleaching of the spectrum is observed, demonstrating further reduction to EH₄ by the residual lip(SH)₂. For enzyme Glu455->Asp it is thus clear that AAD⁺ effects an increase in the redox potential of the FAD. For wild-type enzyme the further reduction to EH₄ is not observed though a profound enhancement of the 530 nm absorbance occurs which may also be related to a change of the redox potential of the FAD as was suggested by Matthews and coworkers [10] and Thorpe and Williams [17].

Discussion

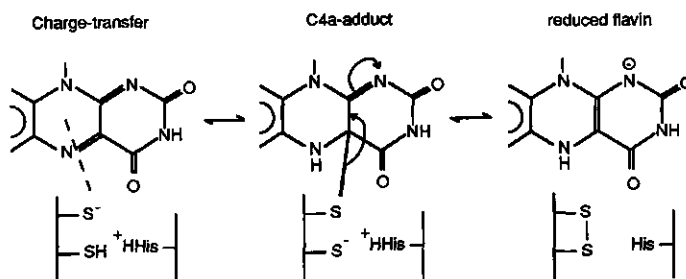
For the reductive reaction of pig heart lipoamide dehydrogenase with lip(SH)₂ a mechanism has been proposed in which a histidine functions as a proton acceptor/donor to yield the nucleophile necessary for attack of the disulfide [9, 20]. A mixed disulfide species, species 2 in Scheme 1, was postulated as an intermediate and the breakdown of this species to yield EH₂ (species 3 in Scheme 1) was assumed to be rate limiting for the pig heart enzyme [9].

The rapid reaction kinetics for the wild-type enzyme shows a 2-fold increase in reductive rate by lip(SH)₂ between pH 7.0 and 8.0 (Table 2). In this, the enzyme differs from pig heart enzyme where the rate constants were invariant between pH 5.5 and 8.0. At present we can not satisfactorily explain this discrepancy.

For pig heart enzyme it has been shown that below pH 7.6 the reoxidation reaction becomes rate limiting in overall catalysis indicating that only the EH⁻ species is capable of reacting with NAD⁺ [10]. For *A. vinelandii* enzyme the oxidation rate of EH₂ by NAD⁺ decreases from pH 8.0 to 6.8 indicating that here also EH⁻ is the reactive species since this species prevails at higher pH [26].

The reaction of wild-type and all mutated enzymes with NADH, the reverse reaction, allows the distinction of separate steps, a feature that is most prominent in enzyme His450->Ser where the rate of reduction of the disulfide by NADH is slowed by more than 1000 fold. The binding of NADH and subsequent reduction of the FAD is in all cases very fast yielding the FIH⁻·NAD⁺ species as an intermediate, species 6 in Scheme 1. The subsequent intramolecular transfer of a hydride equivalent leading to reduction of the disulfide and reoxidation of the FAD (species 4) is strongly affected by the mutations. Also, the forward reaction (species 4 to 6) is slowed by the mutations, more than 200 fold for enzyme His450->Ser.

Evidence for the formation of the proposed flavin C4a adduct intermediate (species 5) as shown in Scheme 2 is not obtained under the experimental conditions applied. A plausible explanation for this is that the rate of formation of the presumed C4a adduct is slow in either direction when compared to its breakdown. Leichus and Blanchard [42] showed recently that in the forward reaction of the pig heart enzyme the formation of the proposed species 5 is most likely the solvent isotopically sensitive transfer step under conditions of saturating $[\text{lip}(\text{SH})_2]$ and $[\text{NAD}^+]$ variable. This is in agreement with our suggestion above, that in the enzymes having either the base, His450, or its charge-relay partner, Glu455, altered, formation of the C4a adduct is slow relative to its breakdown.



Scheme 1. Formation and breakdown of the thiolate to C4a-FAD adduct. From ref [17].

However, in the reverse reaction of pig heart enzyme the formation of species 4 is most likely solvent isotopically sensitive under conditions of saturating $[\text{lipS}_2]$ and $[\text{NADH}]$ variable [41]. This is in contrast with the results obtained for the mutated enzymes where, again no C4a adduct is observed. Two possible reasons for this can be suggested. First, the decay of the C4a adduct might be faster than its formation. Second, in the absence of a base, the transfer of a hydride equivalent may become concerted. Upon opening of the disulfide to form the C4a adduct species, a negative charge develops on the interchange sulfur. It is quite possible that a protonated histidine, the base, is necessary to stabilize this negative charge, and therefore, the second possibility is probably favored.

The reoxidation reaction of EH_2 of enzyme His450- \rightarrow Ser by NAD^+ is not significantly enhanced at pH 6.8 when compared to pH 8.0. This is unexpected in light of the following. This mutated enzyme stabilizes thiolate to FAD charge-transfer. Therefore, reduction by $\text{lip}(\text{SH})_2$ requires the loss of 1 proton to reach a form analogous to species 3 without the base, EH^- . A pK_a was detected at 7.5 for the His450- \rightarrow Ser enzyme and interpreted as an EH^- to E^{2-} deprotonation [26]. This deprotonation should disfavor the reduction of NAD^+ . The almost complete absence of any reactivity at the EH_2 level of enzyme His450- \rightarrow Ser with lipS_2 at pH 8.0 agrees with the observation for pig heart

enzyme lacking reactivity of EH^- with lipS_2 [9], and our conclusion is that the main electronic species of 2-electron reduced enzyme His450->Ser is E^{2-} [26].

The reductive reaction of enzyme His450->Ser by $\text{lip}(\text{SH})_2$ is very slow and fully compatible with the mechanism proposed [1, 9]. The observed short lag-phase is in agreement with a slow formation of the proposed mixed disulfide species (assuming that this species has no absorbance) as the catalyst, the histidine, is missing. Simulation of the reaction shows that traces compatible with observed traces are only obtained when the breakdown of the mixed disulfide occurs 10-fold faster than its formation. From this we conclude that the rate limiting step in the reduction of enzyme His450->Ser by $\text{lip}(\text{SH})_2$ is the formation of the mixed disulfide intermediate.

The Glu455 mutated enzymes are quite different in their rapid reaction kinetics from wild-type enzyme. The data indicate that like the His450->Ser enzyme, intramolecular electron transfer between FAD/FADH- and the disulfide/dithiol is severely impaired. Thus, any alteration of the His-Glu diad affects not only deprotonation of the dithiol substrate, but also communication between the enzyme's two redox active couples. In addition, the Glu455 mutated enzymes differ from His450->Ser enzyme in several details of their rapid reaction kinetics. Both enzymes Glu455->Asp and -Gln show clear biphasic kinetics during reduction of Eox with $\text{lip}(\text{SH})_2$ or reoxidation of EH_2 with either lipS_2 or NAD^+ . An interesting feature of this biphasic behavior is the fact that the amplitude of the fast reaction increases with substrate concentration and that it reaches about 50 % of the total amplitude change. This indicates that only one of the active sites of enzyme Glu455->Gln is reduced at the rapid rate. Moreover, the K_d values calculated for the fast phase are equal to (enzyme Glu455->Gln with $\text{lip}(\text{SH})_2$ at pH 8.6) or lower than (enzyme Glu455->Gln EH_2 with NAD^+ at pH 8.0) those calculated for the slower amplitude change. These results strongly indicate that cooperativity between the two active sites of the enzyme occurs. It was shown previously that enzymes Glu455->Asp and -Gln show a remarkably different fluorescence quenching behavior when compared to the other (mutated) enzymes [26]. It was concluded that this was either due to an intrinsic property of these enzymes or due to cooperativity induced by the quencher. Based on the present results it is now suggested that both the fluorescence quenching behavior and the biphasic rapid reaction kinetics are due to cooperativity. Cooperativity was shown recently for the related enzyme mercuric ion reductase [19] and was shown also for (mono-alkylated) pig heart enzyme reacting with NAD^+ [16-18].

The results (Fig. 7) obtained for the reduction of wild-type enzyme by NADPH in the presence of AAD⁺ support cooperativity between the subunits. Since lipoamide dehydrogenase possesses only one NAD^+ binding site per active site, based on the extensive structure homology between glutathione reductase and lipoamide dehydrogenase from *P. putida* [43], binding of both AAD⁺ and NADPH to one active site

simultaneously can be excluded. The rise of the redox potential of the flavin of the active site reduced to EH_2 (site a) can therefore only be explained by binding of AAD^+ to the other active site (site b) or by simultaneous binding of either AAD^+ or NADP(H)^+ to site a and b. Whether site b is Eox or EH_2 is not clear.

Alteration of Glu455, the charge-relay residue in the base diad, effects profound changes in catalysis. The $\text{lip(SH)}_2/\text{NAD}^+$ activity is unmeasurable due to over-reduction by the product NADH. The $\text{lip(SH)}_2/\text{AcPyAde}^+$ activity is circa 2% of wild-type. Glu455 alters the acid-base properties of His450 [26] and positions the imidazole ring presenting its N3 toward the redox active disulfide. Both mutations can be considered conservative, Glu455→Gln and Glu455→Asp. Indeed, the almost normal rate of reduction of Glu455→Asp enzyme by lip(SH)_2 demonstrates that the aspartate can mimic the catalytic effect of the glutamate in the enzyme substrate complex. Neither the aspartate nor the glutamine residues are able however to accomplish the function of the base diad in the intramolecular transfer of electrons between FAD/FADH^- and the disulfide/dithiol. In contrast to the His450→Ser enzyme where the problem appears to be largely kinetic, the effect with enzymes Glu455→Gln and Glu455→Asp seems to be both kinetic and thermodynamic. Thus, the extent of reoxidation of 2-electron reduced enzyme Glu455→Gln by NAD^+ is very small (Fig. 5). The binding of NAD^+ raises the redox potential of FAD relative to that of the dithiol. Electrons pass, albeit slowly, to the FAD but the resulting FADH^- is not reoxidized.

Inhibition of *A. vinelandii* wild-type enzyme by NADH above pH 8.0 is not observed in pig heart enzyme while for *E. coli* enzyme this inhibition is observed at all pH values studied. For *E. coli* enzyme it was shown that the inhibition is caused by over-reduction of the enzyme from EH_2 to EH_4 by NADH and that there is a direct relation between the inhibition and the redox potential of the EH_2/EH_4 couple [12]. Like the *E. coli* enzyme [7], inhibition of the *A. vinelandii* enzyme could be circumvented in kinetic studies by using AcPyAde^+ as an electron acceptor which has a 70 mV higher midpoint potential than NAD^+ .

For pig heart enzyme it was shown that inhibition by NADH in the reverse reaction could be prevented by NAD^+ [15] implying that the relative affinity for NAD^+ and NADH is important with respect to over-reduction. Therefore, the over-reduction may not only be related to the redox potentials of the different enzymes but the relative affinities and reaction rates of NAD^+ and NADH at the EH_2 level may contribute as well. With respect to *A. vinelandii* wild-type and mutated enzymes it can be inferred from the diaphorase activity that the affinity for NADH is not very different among the enzymes. A similar conclusion is drawn from rapid reaction kinetics of Eox reacting with NADH. Furthermore, the reoxidation reaction of EH_2 by NAD^+ shows similar K_d values for

enzymes Glu455->Gln, His450->Ser and wild-type enzyme. These data taken together indicate that the over-reduction and thus susceptibility to inhibition by NADH, is directly related to differences in redox potentials. The relation between the relative redox potentials of the mutated enzymes and the susceptibility to inhibition by NADH supports this hypothesis.

Assuming that the change in the redox potential with pH for the *A. vinelandii* enzyme relative to NADH is similar to that of pig heart enzyme [20], over-reduction would be favoured at lower pH. The inhibition however becomes apparent at a pH where the histidine likely deprotonates ($pK_a = 8.1$, inferred from the pK_m AcPyAde⁺ plot). Our results show that binding of a nucleotide raises the redox potential of the EH₂/EH₄ couple. Apparently this rise is enhanced when the histidine is deprotonated. This indicates that the protonated histidine, at the EH₂ level, plays an important role in maintaining the redox potential of the active site carefully balanced to avoid over-reduction by NADH. The results of the steady state kinetic studies on the Glu455 mutated enzymes lend strong support to this hypothesis. Over the entire pH range studied strong inhibition by NADH is observed for both enzymes while it was shown previously that the pK_a of the histidine in these enzymes is considerably lowered ($pK_a \leq 6.5$) when compared to wild-type [26]. This adds a second function to His450; not only does it serve as the base for deprotonation of lip(SH)₂, it modulates the relative redox potentials of the disulfide/dithiol and FAD/FADH⁻ couples which may be reflected in the markedly diminished rates of intramolecular electron transfer in the altered enzymes.

Acknowledgments.

We thank Dr. W.G.J. Hol and Mr. A. Mattevi for providing us with the coordinates of lipoamide dehydrogenase from *Azotobacter vinelandii* prior to publication. This work was supported by the 'Dutch Foundation for Chemical Research' (SON) with financial aid from the 'Netherlands Organization for Scientific Research' (NWO), by the Health Services and Research Administration of the Department of Veterans Affairs and by grant GM21444 (CHW) from the National Institute of General Medical Sciences.

References.

1. Williams, C.H. Jr. (1991) In *Chemistry and Biochemistry of Flavoenzymes* (Müller, F., ed.) vol III, in press, CRC Press Inc., Boca Raton.

2. Sokatch, J.R., McCully, V., Gebroski, J. and Sokatch, D.J. (1981) *J. Bacteriol.* **148**, 639-646.
3. Fox, B.S. and Walsh, C.T. (1982) *J. Biol. Chem.* **257**, 2498-2503.
4. Shames, S.L., Fairlamb, A.H., Cerami, A. and Walsh, C.T. (1986) *Biochemistry* **25**, 3519-3526.
5. Holmgren, A. (1980) *Experientia suppl.* **36**, 149-180.
6. Massey, V., Gibson, Q.H. and Veeger, C. (1960) *Biochem. J.* **77**, 341-351.
7. Williams, C.H. Jr. (1965) *J. Biol. Chem.* **240**, 4793-4800.
8. Reed, J.K. (1973) *J. Biol. Chem.* **248**, 4834-4839.
9. Matthews, R.G., Ballou, D.P., Thorpe, C. and Williams, C.H. Jr. (1977) *J. Biol. Chem.* **252**, 3199-3207.
10. Matthews, R.G., Ballou, D.P. and Williams, C.H. Jr. (1979) *J. Biol. Chem.* **254**, 4974-4981.
11. Wilkinson, K.D. and Williams C.H. Jr. (1979) *J. Biol. Chem.* **254**, 852-862.
12. Wilkinson, K.D. and Williams C.H. Jr. (1981) *J. Biol. Chem.* **256**, 2307-2314.
13. Sahlman, L. and Williams, C.H. Jr. (1989a) *J. Biol. Chem.* **264**, 8033-8038.
14. Sahlman, L. and Williams, C.H. Jr. (1989b) *J. Biol. Chem.* **264**, 8039-8045.
15. Massey, V. and Veeger, C. (1961) *Biochim. Biophys. Acta* **48**, 33-47.
16. Thorpe, C. and Williams, C.H. Jr. (1976) *J. Biol. Chem.* **251**, 7726-7728.
17. Thorpe, C. and Williams, C.H. Jr. (1981) *Biochemistry* **20**, 1507-1513.
18. Muiswinkel van-Voetberg, H and Veeger, C. (1973) *Eur. J. Biochem.* **33**, 285-291
19. Miller, S.M., Massey, V., Williams, C.H. Jr., Ballou, D.P. and Walsh, C.T. (1991) *Biochemistry* **30**, 2600-2612.
20. Matthews, R. G. and Williams, C. H. Jr. (1976) *J. Biol. Chem.* **251**, 3956-3964.
21. Adamson, S. R., Robinson, J. A. and Stevenson, K. J. (1984) *Biochemistry* **23**, 1269-1274.
22. Berry, A., Scrutton, N.S. and Perham, R.N. (1989) *Biochemistry* **28**, 1264-1269.
23. Deonarian, M.P., Berry, A., Scrutton, N.S. and Perham, R.N. (1989) *Biochemistry* **28**, 9602-9607.
24. Williams, C.H. Jr., Allison, N., Russel, G.C., Prongay, A.J., Arscott, D.L., Datta, S., Sahlman, L. and Guest, J.R. (1989) *Ann. N.Y. Acad. Sci.* **573**, 55-65.
25. Benen, J.A.E., Berkel van, W.J.H. and Kok de, A. (1990) in *Flavins and Flavoproteins 1990* (Curti, B., Ronchi, S. and Zanetti, G. eds.) pp 557-564, Walter de Gruyter and Co. Berlin-New York 1991,
26. Benen, J., Berkel van, W., Zak, Z., Visser, T., Veeger, C. and Kok de, A. (1991) *Eur. J. Biochem.* **202**, 863-872.
27. Sahlman, L., Lambeir, A.M., and Lindskog, S. (1986), *Eur. J. Biochem.* **156**, 479-488.

28. Miller, S.M., Massey, V., Ballou, D., Williams, C.H. Jr., Distefano, M.D., Moore, M.J. and Walsh, C.T. (1990) *Biochemistry* 29, 2831-2841.
29. Meada-Yorita, K., Russel, G.C., Guest, J.R., Massey, V. and Williams, C.H. Jr. (1991) *Biochemistry* 30, in the press.
30. Vervoort, J. (1986) PhD Thesis, University of Wageningen, The Netherlands.
31. Berkel van, W.J.H., Regeling, A.G., Beintema, J.J. and de Kok, A. (1991) *Eur. J. Biochem.* 202, 1049-1055.
32. Broek van den, H.W.J. (1971) PhD Thesis, p. 8, University of Wageningen, The Netherlands.
33. Barshop, B.A., Wrenn, R.F. and Frieden, C. (1983) *Anal. Biochem.* 130, 134-145.
34. Massey, V. (1990) in *Flavins and Flavoproteins 1990* (Curti, B., Ronchi, S. and Zanetti, G. eds.) pp. 59-66, Walter de Gruyter and Co. Berlin-New York 1991,
35. Dixon, M. and Webb, E.C. (1979) *Enzymes*, pp. 138-164, R. Clay Ltd., Bungay, Suffolk, UK
36. Kaplan, N.O. (1960) in *The Enzymes* (Boyer, Lardy and Myrbäck eds.) vol. 3, p. 151, Academic Press, New York.
37. Clarke, W.M. (1960) *Oxidation-Reduction Potentials of Organic Systems*, The Williams and Wilkins Co., Baltimore, p. 131.
38. Palmer, G. and Massey, V. (1968) in *Biological oxidations* (Singer, T. P. ed.) part 2, p. 288, Interscience Publishers, New York.
39. Veeger, C. and Massey, V. (1963) *Biochim. Biophys. Acta* 67, 679-681.
40. Maeda-Yorita, K. and Aki, K. (1984) *J. Biochem.* 96, 683-690.
41. Fisher, T.L., Vercellotti, V. and Anderson, B.M. (1973) *J. Biol Chem.* 248, 4293-4299.
42. Leichus, B.N. and Blanchard, J.S. (1991) in *Flavins and Flavoproteins 1990* (Curti, B., Ronchi, S. and Zanetti, G. eds.) pp 589-592, Walter de Gruyter and Co. Berlin-New York
43. Mattevi, A., Obmolova, G., Sokatch, J.R., Betzel, C. and Hol, W.J.G. (1991) Submitted.

Chapter 4

Lipoamide Dehydrogenase from *Azotobacter vinelandii*. The role of the C-terminus in catalysis and dimer stabilization.

Jacques Benen, Willem van Berkel, Cees Veeger and Arie de Kok.

Summary

The 10 C-terminal residues are not visible in the crystal structure of lipoamide dehydrogenase from *Azotobacter vinelandii*, but can be observed in the crystal structures of the lipoamide dehydrogenases from *Pseudomonas putida* [Mattevi, A. *et al.*, submitted] and *Pseudomonas fluorescens*. In these structures, the C-terminus folds back towards the active site and is involved in interactions with the other subunit.

The function of the C-terminus of lipoamide dehydrogenase from *Azotobacter vinelandii* was studied by deletion of 5, 9 and 14 residues, respectively. Deletion of the last 5 residues does not influence the catalytic properties and conformational stability (thermo-inactivation and unfolding by guanidinium hydrochloride). Removal of 9 residues results in an enzyme (enzyme $\Delta 9$) showing decreased conformational stability and high sensitivity toward inhibition by NADH. These features are even more pronounced after deletion of 14 residues.

In addition tyrosine16, conserved in all lipoamide dehydrogenases sequenced thus far, and shown from the other structures to be likely involved in subunit interaction, was replaced by phenylalanine and serine. Mutation of Tyr16 also results in a strongly increased sensitivity toward inhibition by NADH. The conformational stability of both Tyr16 mutated enzymes is comparable to enzyme $\Delta 9$.

The results strongly indicate that a hydrogen bridge between tyrosine of one subunit (Tyr16 in the *A. vinelandii* sequence) and histidine of the other subunit (His470 in the *A. vinelandii* sequence), exists in the *A. vinelandii* enzyme. In the $\Delta 9$ and $\Delta 14$ enzymes this interaction is abolished. It is concluded that this interaction mediates the redox properties of the FAD via the conformation of the C-terminus containing residues 450-470.

Introduction.

Lipoamide dehydrogenase is a member of the flavoprotein disulfide oxidoreductases [1]. The homodimeric enzyme catalyzes the NAD⁺ dependent reoxidation of dihydrolipoyl groups, which are *in vivo* covalently attached to the lipoate acyl transferase component of several multienzyme complexes [2]. Each active site contains an FAD and a redox active disulfide bridge and is constituted by amino acids from both subunits [3, 4, 5].

For lipoamide dehydrogenase from *Azotobacter vinelandii* the crystal structure of the oxidized state has been determined at 0.22 nm resolution [4]. The geometry of the active site is highly identical to the active site of human glutathione reductase [4]. Unfortunately, no crystal structure of reduced *A. vinelandii* lipoamide dehydrogenase or mutated enzymes is available.

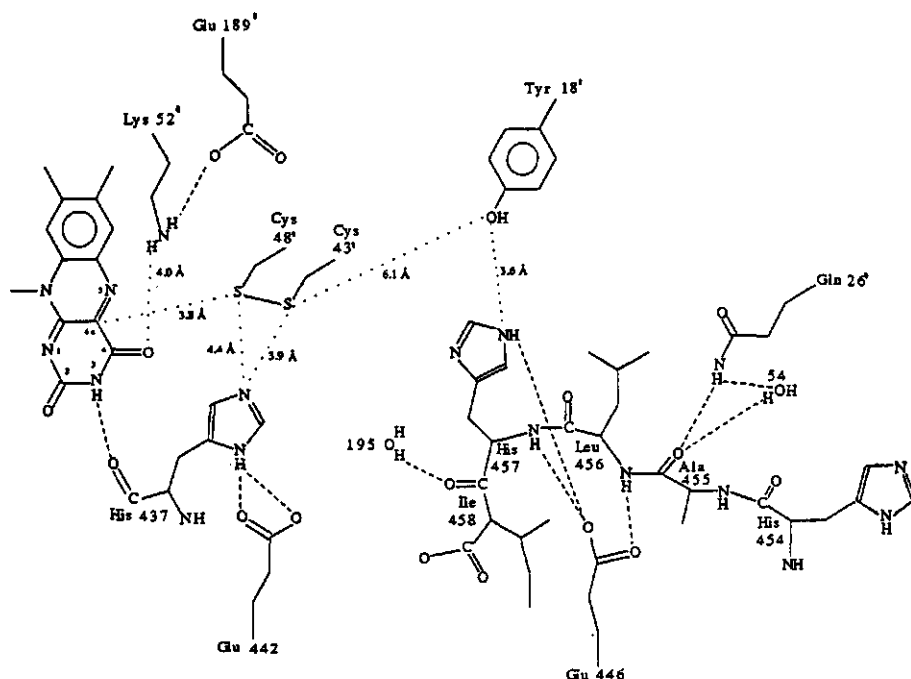


Fig. 1. Schematic picture of the interactions made by the C-terminal residues at the si-side of the flavin of lipoamide dehydrogenase from *Pseudomonas putida*.

Residues of the opposite subunit are indicated by a prime symbol following their sequence number. H-bonds ($d < 0.34$ nm) are shown by dashed lines, while the dotted lines indicate distances between residues directly or indirectly involved in catalysis. Corresponding numbering of relevant conserved residues of *A. vinelandii* enzyme in brackets: Tyr18' (16'), Glu26' (24'), Cys43' (48'), Cys48' (53'), Lys52' (57'), Glu189' (194'), His437 (450), Glu442 (455), Glu446 (459), His457 (470). This figure was kindly provided by Mr. A. Mattevi.

Lipoamide dehydrogenase from *A. vinelandii* contains a 15 amino acid C-terminal extension compared to glutathione reductase [6, 7]. The last 10 residues are disordered and not visible in the electron density map [4]. It was suggested that these residues constitute a mobile structure on the outside of the molecule and might serve in the interaction with the core component of the 2-oxo acid complexes, the acyl transferase. Deletion mutagenesis experiments however have shown that this hypothesis is not correct [8]. Furthermore it was shown that deletion of 9 or 14 of the C-terminal residues (enzymes designated $\Delta 9$ and $\Delta 14$) strongly affects catalysis [8]. A possible clue to the role of the C-terminal residues is given by the recently elucidated X-ray structures of lipoamide dehydrogenase from *Pseudomonas putida* [5] and *P. fluorescens* [Mattevi and HqI, personal communication]. In these enzyme structures, the C-terminus folds partly back into the protein structure comprising the active site. The relevant part of the structure is shown in Fig. 1.

These new structures also show that a tyrosine (Tyr16 in the *A. vinelandii* enzyme), which is strictly conserved in all lipoamide dehydrogenases sequenced thus far, could be involved in interaction with the C-terminus of the other subunit.

Here we report on the characterization of the C-terminal deletion enzymes, $\Delta 5$, $\Delta 9$ and $\Delta 14$ and the mutated enzymes Tyr16 \rightarrow Phe, Tyr16 \rightarrow Ser. Based on the results presented in this paper it is concluded that in *A. vinelandii* enzyme the C-terminus conformation is similar to that observed in the *Pseudomonas* enzymes. Based on this feature a coherent explanation of the effects of the mutations is discussed.

Materials and Methods.

General. All biochemicals, bacterial strains and vectors used were described elsewhere [9, 10]. The mixed oligonucleotide allowing mutagenesis of Tyr16 into Phe and Ser was synthesized according to [9].

Construction of plasmids. The construction of plasmid pJAB1000, carrying the wild type *lpd*-gene was described in [8]. A partial restriction map is shown in Fig. 2. The procedure for mutagenesis of Tyr16 was identical to the one described in [9], except for the cassette. The cassette was obtained by digestion of pJAB1000 with the restriction endonucleases *Sph*I and *Kpn*I. The *Sph*I/*Kpn*I fragment, encoding the N-terminal part of the *lpd*-gene, containing Tyr16, was cloned into *Sph*I/*Kpn*I digested M13mpb18 and subjected to mutagenesis. After screening for the desired mutations by sequencing the cassette was excised by digestion with *Hind*III and *Kpn*I. Before religating the mutated cassette into pJAB1000 the two *Kpn*I sites, one immediately downstream of the

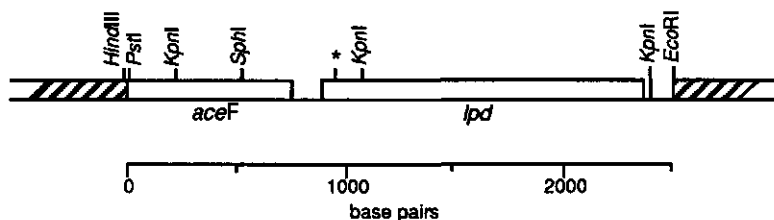


Fig. 2. Partial restriction map of the plasmid pJAB1000 carrying the *lpd*-gene from *Azotobacter vinelandii*, encoding lipoamide dehydrogenase, and part of the *aceF*-gene encoding acetyl transferase. The asterisk (*) indicates the position of Tyr16.

lpd-gene and the other upstream, were destroyed. The upstream *KpnI* site was destroyed by digestion of pJAB1000 with *PstI* and *SphI*. The sticky ends were filled with T4-DNA polymerase and religated yielding plasmid pEH1. From this plasmid the downstream *KpnI* site was removed by partially digesting pEH1 with *KpnI* and filling the sticky end with T4-DNA polymerase. After checking for the desired change the *HindIII/KpnI* fragment of the altered pEH1 (plasmid pEH12) was replaced with the mutated cassette yielding an intact *lpd*-gene carrying either the Tyr16->Phe or Tyr16->Ser mutation.

The construction of enzymes lacking the C-terminal residues (enzymes $\Delta 5$, $\Delta 9$ and $\Delta 14$) was described previously [8].

Analytical methods. Purification of mutated enzymes was according to [9]. Spectral studies and stopped flow kinetics were performed in 100 mM Hepes, 0.5 mM EDTA, 150 mM ionic strength pH 8.0 (Hepes/EDTA buffer), as described [10]. Steady state kinetics were studied according to [10] in 100 mM Hepes, 0.5 mM EDTA, 150 mM ionic strength pH 7.0. Thermoinactivation was determined as described in [11] using lip(SH)₂ and 3-acetylpyridine dinucleotide [AcPyAde⁺] as substrates in activity determinations for the Tyr16 mutated enzymes and NADH and dichlorophenolindophenol for enzymes $\Delta 5$, $\Delta 9$ and $\Delta 14$. Unfolding experiments were performed according to [11].

Calculation of the fractional contribution of the different enzyme species, the oxidized enzyme (Eox), the 2-electron reduced enzyme (EH₂) and the 4-electron reduced enzyme (EH₄) as shown in Fig. 4, to the mixed spectra in Fig. 5 is performed as follows. It is assumed that the EH₂ spectra in Fig. 3 as obtained after reduction with borohydride represent fully formed (100 %) EH₂. The EH₄ spectrum was obtained by reducing the enzyme with 1 M dithiothreitol. A species in which the FAD is reduced and the disulfide oxidized as a result of translocation of the electrons in EH₂ (designated FIH⁻) is

spectrally indistinguishable from EH_4 . Since Eox and FIH^-/EH_4 do not absorb at 540 nm, the extinction at 540 nm of the mixed spectra in Fig. 5 can directly be used to calculate the fraction of EH_2 . Since Eox and EH_2 are isosbestic in the region of 445 nm any decrease in extinction of the mixed spectra at this wavelength when compared to the extinction of Eox and EH_2 is a result from the formation of FIH^- and/or EH_4 . At the isosbestic point (see table 2) the fractional contribution of $\text{FIH}^- + \text{EH}_4$ can be calculated in the following way:

$$\epsilon_{\lambda\text{mixed}} = F_{\text{Eox}} \times \epsilon_{\lambda\text{ox}} + F_{\text{EH}_2} \times \epsilon_{\lambda\text{EH}_2} + (F_{\text{FIH}^-} + F_{\text{EH}_4}) \times \epsilon_{\lambda\text{EH}_4} \quad (1)$$

in which $\epsilon_{\lambda\text{mixed}}$ is the extinction of the mixed spectrum at the exact wavelength (λ) of isosbesticity of Eox and EH_2 , F denotes the fractional contribution of the species indicated and the extinctions of Eox , EH_2 and EH_4 at wavelength λ are given by $\epsilon_{\lambda\text{ox}}$, $\epsilon_{\lambda\text{EH}_2}$ and $\epsilon_{\lambda\text{EH}_4}$ respectively and are derived from Fig. 4. Since $\epsilon_{\lambda\text{ox}}$ and $\epsilon_{\lambda\text{EH}_2}$ are equal at the isosbestic point and $(F_{\text{Eox}} + F_{\text{EH}_2}) = (1 - (F_{\text{FIH}^-} + F_{\text{EH}_4}))$, equation (1) can be written as:

$$\epsilon_{\lambda\text{mixed}} = \epsilon_{\lambda\text{EH}_2} \times (1 - (F_{\text{FIH}^-} + F_{\text{EH}_4})) + (F_{\text{FIH}^-} + F_{\text{EH}_4}) \times \epsilon_{\lambda\text{EH}_4} \quad (2)$$

resulting in equation (3):

$$F_{\text{FIH}^-} + F_{\text{EH}_4} = \frac{\epsilon_{\lambda\text{EH}_2} - \epsilon_{\lambda\text{mixed}}}{\epsilon_{\lambda\text{EH}_2} - \epsilon_{\lambda\text{EH}_4}} \quad (3)$$

Calculation of the individual fractions of FIH^- and EH_4 is possible by studying the electron distribution in an equilibrating system at the start and at the end of the equilibrium, provided that no extra input of electrons takes place during equilibration. In case of the present study this calculation, with data presented in Table 2, is only done for reduction with 1 molar equivalent of $\text{lip}(\text{SH})_2$ (see below) where it can be assumed that no further reduction occurs. Reduction with 2 molar equivalents of $\text{lip}(\text{SH})_2$ shows a clear decrease of Eox after equilibration indicating that further reduction has occurred.

As an example the calculation of the fractional contribution of FIH^- and EH_4 is given for enzyme $\text{Tyr16} \rightarrow \text{Phe}$. As mentioned above the FIH^- species originates from electron transfer from the dithiol to the flavin. It is assumed that no further reduction by residual $\text{lip}(\text{SH})_2$ occurs. The total fraction of electrons present for enzyme $\text{Tyr16} \rightarrow \text{Phe}$ immediately after reduction is either 0.65 or 0.69. ($\text{EH}_2 + \text{FLH}^-$ or EH_4). After equilibration the fraction of Eox has increased by 0.06 due to disproportionation at the expense of EH_2 . Consequently the fraction of EH_4 is 0.06 ($2\text{EH}_2 \rightarrow \text{Eox} + \text{EH}_4$) and the fraction of electrons herein is 0.12. Together with the fraction electrons in EH_2 this adds

up to 0.35. When it is assumed that the remainder is in fact FLH⁻ this constitutes a fraction of 0.30 (0.36-0.06 EH₄). The total of the fractions of electrons in EH₂, EH₄ and FLH⁻ then is 0.65 which is exactly the same as the total immediately after reduction when it is assumed that here only is FLH⁻ is present. In an identical way the distribution of electrons for enzymes Tyr16->Ser and Δ9 can be calculated.

Results

Kinetics of the mutated enzymes. Previously it was reported that deletion of the 9 C-terminal residues (enzyme Δ9), results in strongly decreased activity in the forward reaction [8]. This appeared to be caused by inhibition by NADH. Here activity could only be optimally detected with AcPyAde⁺ as a substrate as observed with Glu455 mutated enzymes [10]. Enzyme Δ5 has kinetic properties essentially identical to wild type enzyme while enzyme Δ14 is virtually inactive (results not shown). The Tyr16 mutated enzymes also show severe inhibition by the product NADH in the forward reaction while in the reverse reaction, NADH/lipS₂, no activity is observed in a standard assay. Using AcPyAde⁺ as an electron acceptor, the Tyr16 mutated enzymes show an optimum at pH 7.0 instead of pH 8.0 as found for the wild-type enzyme [10]. Table 1 shows the kinetic parameters of the Tyr16 mutated enzymes and the wild-type enzyme at pH 7.0. The Lineweaver-Burk plots of the Tyr16 mutated enzymes are parallel (not shown), demonstrating that the mechanism is still ping-pong. Mutation of Tyr16 into Phe or Ser only slightly affects the rate of turnover (Table 1). The reductive half reaction with

Enzyme	V	K _m AcPyAde ⁺	K _m lip(SH) ₂
	U/mg	μM	μM
wild-type	40	1000	70
Tyr16->Phe	20	800	80
Tyr16->Ser	14	1100	90

Table 1. *Steady state kinetics of wild-type and mutated enzymes Tyr16->Phe and Tyr16->Ser of Azotobacter vinelandii lipoamide dehydrogenase.* The kinetics were determined with lip(SH)₂ and AcPyAde⁺ as substrates in 100 mM Hepes, 0.5 mM EDTA, 150 mM ionic strength pH 7.0, at 25 °C. The data were analyzed according to a ping-pong mechanism.

lip(SH)₂ is also only slightly affected. Rapid reaction kinetics of the lip(SH)₂ reduction at pH 8.0 result in rate constants of 2150 s⁻¹ and 850 s⁻¹ for enzyme Tyr16->Phe and Tyr16->Ser respectively with dissociation constants of 1.9 mM and 1.5 mM for L-lip(SH)₂. For wild-type enzyme this rate constant at pH 8.0 is 2000 s⁻¹ and K_d = 0.9 mM [10]. These results indicate that Tyr16 is not or only slightly involved in lip(SH)₂ binding.

Spectral properties of the mutated enzymes. For the mutated enzymes Δ9, Tyr16->Phe and -Ser the visible absorption spectra of Eox are very similar to the wild-type enzyme. In all three cases the absorbance maximum is 1 nm red shifted to 458 nm. Enzyme Δ5 is spectrally indistinguishable from wild-type enzyme. The absorption spectrum of enzyme Δ14 shows less vibrational fine structure and the absorbance maximum is 4 nm blue shifted to 453 nm (results not shown).

Fig. 3 shows the spectra of enzymes Tyr16->Phe, Tyr16->Ser and Δ9 as obtained after reduction with NADH. With enzymes Tyr16->Phe and Δ9 reduction of the flavin is complete with only 1.5 molar equivalents (Meqs) of NADH added. The addition of 1.0

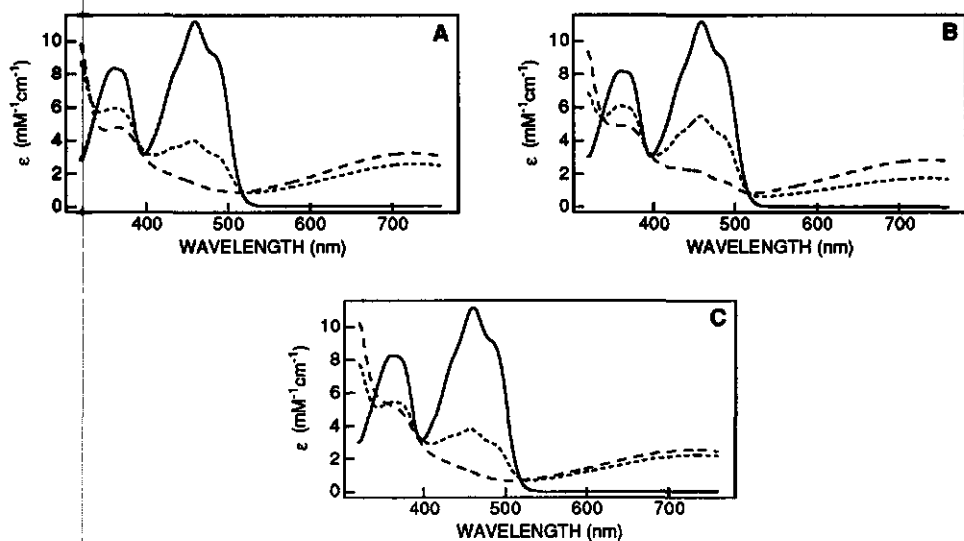


Fig. 3. Visible absorption spectra of the mutated *Azotobacter vinelandii* lipamide dehydrogenases Tyr16->Phe, Tyr16->Ser and Δ9 upon NADH reduction.

All three enzymes were reduced with 1.0 (.....) and 1.5 (2.0 in case of Tyr16->Ser) (----) molar equivalents of NADH. (—) Eox. The spectra shown are those recorded when changes were complete (after 15 to 20 min.). A, enzyme Tyr16->Phe; B, enzyme Tyr16->Ser; C enzyme Δ9. The experiments were conducted in Hepes buffer pH 8.0 at 25 °C.

Meq of NADH results in more than 70% reduction of the FAD. These data demonstrate that the reducing equivalents mainly reside on the flavin, favoring the species $\text{F}^{\text{H-}}$, instead of being mainly transferred to the disulfide as found for the wild-type [9], pig heart [12, 13] and mutated enzyme His450->Ser [9]. Addition of up to 1.0 mM NAD^+ to enzyme reduced with 1.5 Meqs of NADH does not result in any reoxidation of the FAD. This failure of NAD^+ to reoxidize the enzyme to EH_2 or Eox is also reflected in the steady state kinetics.

For enzyme Tyr16->Ser the spectra obtained upon NADH reduction are somewhat different from those of enzymes Tyr16->Phe and $\Delta 9$. With this enzyme slightly more than 2.0 Meqs of NADH are needed for complete reduction (Fig. 3B). The low 340 nm absorbance demonstrates that almost all NADH is oxidized in the process of reduction, indicating formation of EH_4 . Again, addition of 1.0 mM of NAD^+ to the fully reduced enzyme did not result in any reoxidation.

Previously it was shown that enzymes that are easily reduced by NADH and which

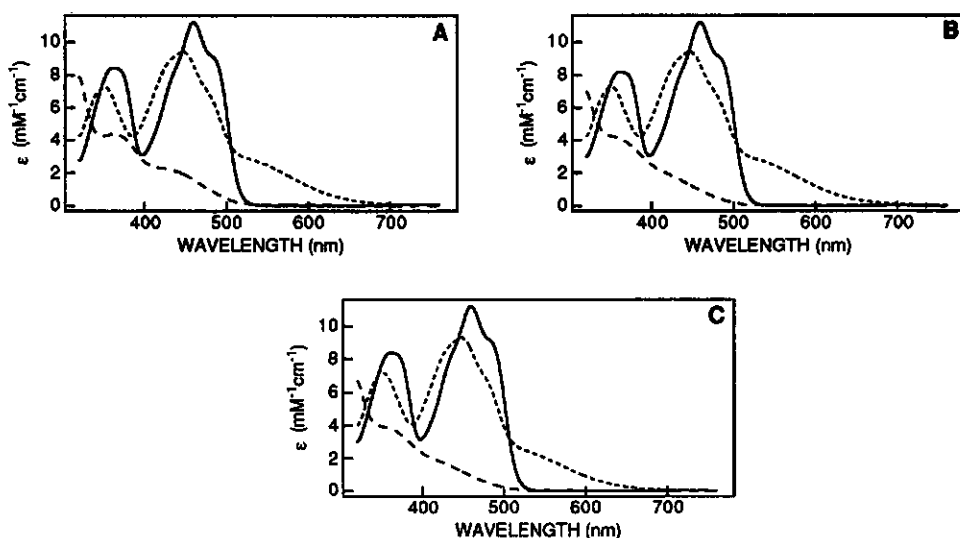


Fig. 4. Visible absorption spectra of the mutated *Azotobacter vinelandii* lipamide dehydrogenases Tyr16->Phe, Tyr16->Ser and $\Delta 9$ after reduction with borohydride or dithiothreitol.

The spectra of the borohydride reduction shown (.....) were recorded immediately after addition of the reductant. Dithiothreitol reduction (---) was accomplished with 1.0 M of reductant. The spectra of the dithiothreitol reduction shown are those recorded when changes were complete. (—) Eox. A, enzyme Tyr16->Phe; B, enzyme Tyr16->Ser; C enzyme $\Delta 9$. The experiments were conducted in Hepes buffer pH 8.0 at 25 °C.

show strong inhibition by NADH during turnover have a higher redox potential of the FAD (E_m EH_2/EH_4) [10, 14, 15]. In analogy to this it is suggested that the redox potential of the FAD of the Tyr16 mutated enzymes and enzyme $\Delta 9$ is likely to be higher than that of the wild-type enzyme.

Fig. 4 shows the spectra of enzymes Tyr16->Phe, Tyr16->Ser and $\Delta 9$ as obtained by reduction with either excess of borohydride or dithiothreitol. Upon reduction with borohydride the three enzymes initially form the typical EH_2 spectrum with the reducing equivalents resting on the dithiol. The EH_2 species shown in Fig. 4, recorded immediately after addition of the reductant, are thus only transiently stable. The least stable is enzyme $\Delta 9$ and the most stable is enzyme Tyr16->Phe. The spectra of enzymes Tyr16->Phe, Tyr16->Ser and $\Delta 9$ are retained for approximately 15-20, 5-10 and 2-3 minutes respectively after which slow reduction of the FAD occurs.

In Fig. 5 spectra of enzymes Tyr16->Phe, Tyr16->Ser and $\Delta 9$ respectively are presented as obtained after reduction with $\text{lip}(\text{SH})_2$. Upon reduction of these enzymes with a small excess of $\text{lip}(\text{SH})_2$ over-reduction to EH_4 and/or formation of FIH^- and/or disproportionation is observed. Typical for those three enzymes is the fact that the 530 nm charge-transfer absorbance during $\text{lip}(\text{SH})_2$ reduction never reaches values as high as found when using borohydride. Also the blue shift of the absorbance maximum is less,

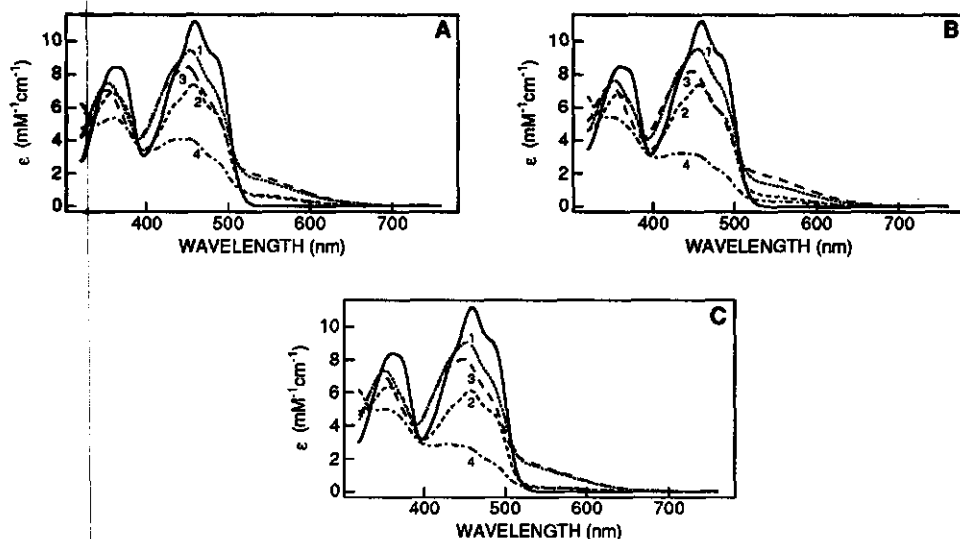


Fig. 5. Visible absorption spectra of the mutated *Azotobacter vinelandii* lipoamide dehydrogenases Tyr16->Phe, Tyr16->Ser and $\Delta 9$ upon $\text{Lip}(\text{SH})_2$ reduction.

The spectra shown are those recorded immediately after the addition of 1.0 (....., 1) or 2.0 (---, 3) molar equivalents of $\text{lip}(\text{SH})_2$ and after changes are complete (after 2 hours) after the addition of 1.0 (- - - -, 2) or 2.0 (- · - · - ·, 4) molar equivalents. (—) Eox. A, enzyme Tyr16->Phe; B, enzyme Tyr16->Ser; C enzyme $\Delta 9$. The experiments were conducted in Hepps buffer pH 8.0 at 25 °C.

suggesting that still Eox is present. Stopped flow studies show that for all three enzymes the 530 nm absorbance rapidly increases mono-exponentially followed by a slow decrease at a rate compatible with the rate of over-reduction/ disproportionation observed in the absorption spectra. This demonstrates that during recording of absorption spectra no initial high absorption at 530 nm is missed.

The spectra shown in Fig. 5 are those obtained immediately after mixing with 1 or 2 Meqs of lip(SH)₂ and after changes are complete (after 2 hours). When it is assumed that the EH₂ spectra shown in Fig. 3 represent fully formed EH₂ with maximal thiolate to FAD charge-transfer it is possible to calculate the mole fractions of Eox, EH₂ and FIH⁻+EH₄ in each of the spectra shown in Fig. 5 (see Materials and Methods). The calculated fractions are presented in Table 2. It is clear that in each case the initial amount of EH₂ formed decreases. After reduction with 1.0 Meq of lip(SH)₂, the decrease is mainly associated with an increase of FIH⁻+EH₄ and only a small increase of Eox in case of enzyme Tyr16->Phe and Δ9. The small increase of Eox relative to FIH⁻+EH₄ indicates that no significant disproportionation occurs. This can be due to either further reduction of Eox and EH₂ by residual lip(SH)₂ present, or intramolecular electron transfer from the dithiol to the FAD.

For enzyme Tyr16->Phe the distribution of FIH⁻ and EH₄ species, after the reduction with one equivalent of lip(SH)₂ before and after equilibration, is outlined in the Materials and Methods section. In an identical way the fractional contribution of FIH⁻ and EH₄ of

Meqs [†] lip(SH) ₂	Tyr16->Phe					Tyr16->Ser					Δ9				
	Eox	EH ₂	FIH ⁻ / EH ₄ [#]	FIH ⁻ ⊙	EH ₄ ⊙	Eox	EH ₂	FIH ⁻ / EH ₄ [#]	FIH ⁻ ⊙	EH ₄ ⊙	Eox	EH ₂	FIH ⁻ / EH ₄ [#]	FIH ⁻ ⊙	EH ₄ ⊙
1.0	0.35	0.61	0.04	0.04	0.00	0.44	0.52	0.04	0.04	0.00	0.26	0.68	0.06	0.06	0.00
1.0 final	0.41	0.23	0.36	0.30	0.06	0.44	0.24	0.32	0.32	0.00	0.40	0.14	0.46	0.32	0.14
2.0	0.17	0.70	0.13	-	-	0.14	0.71	0.15	-	-	0.12	0.73	0.15	-	-
2.0 final	0.03	0.26	0.71	-	-	0.11	0.13	0.76	-	-	0.07	0.12	0.81	-	-

Table 2. Fractional contribution of oxidized, two- and four- electron reduced species to lip(SH)₂ reduced Tyr16->Phe, Tyr16->Ser and Δ9 mutated *Azotobacter vinelandii* lipoamide dehydrogenases.

Spectral data are presented in Fig. 4. Analysis is described under Materials and Methods.

[†] Meqs: molar equivalents added. [#] Fractional contribution of FIH⁻+EH₄. ⊙ Fractional contribution of FIH⁻ and EH₄ calculated as described under Materials and Methods assuming that no further reduction occurred. Final designates that changes in the spectrum were complete after the amount of lip(SH)₂ added. Eox and EH₂ of enzymes Tyr16->Phe, Tyr16->Ser and Δ9 are isosbestic at 445.4, 445.4 and 444.7 nm respectively.

enzymes Tyr16->Ser and $\Delta 9$ is calculated (Table 2). For all three mutated enzymes the calculated total fraction of electrons after equilibration is exactly the same as in the initial spectra. From this it is concluded that intramolecular electron transfer from the dithiol to the FAD is dominant in these 2-electron reduced mutated enzymes. For *E. coli* enzyme the existence of the FLH⁻ species was demonstrated [14], although this species was only present in small quantities. The occurrence of translocation suggests that the redox potentials of the disulfide and the FAD are relatively close, however the slow rate at which the electron transfer occurs suggests that this feature is related to slow structural changes.

Conformational stability. Recent conformational stability studies on wild-type lipoamide dehydrogenase from *A. vinelandii* have shown that over-reduction of the enzyme to EH₄ by NADH or dithionite promotes subunit dissociation thereby strongly increasing the sensitivity towards limited proteolysis, thermoinactivation and unfolding agents [11].

Except for enzyme $\Delta 5$, the thermal stability of the mutated enzymes is decreased with respect to wild-type enzyme. Table 3 shows that the melting temperatures (t_m) of both Tyr16 mutated enzymes and enzyme $\Delta 9$ are clearly lower than the corresponding value of the wild type enzyme. For enzyme $\Delta 14$, thermostability is strongly decreased yielding a t_m value which is only slightly higher as found for the monomeric wild type

Enzyme	t_m	C_m Gdn/HCl
	°C	M
wild-type ¹⁾	80	2.45
$\Delta 5$	80	2.40
Tyr16->Phe	72	2.15
Tyr16->Ser	72	2.10
$\Delta 9$	65	2.05
$\Delta 14$	45	0.85
apoenzyme ¹⁾	40	0.75

Table 3. Conformational stability of mutated lipoamide dehydrogenase from *A. vinelandii*. The melting temperatures (t_m) and midpoint concentrations of unfolding (C_m Gdn/HCl) were determined as described in ref. 11. (see also Fig. 6).

¹⁾ from ref. 11.

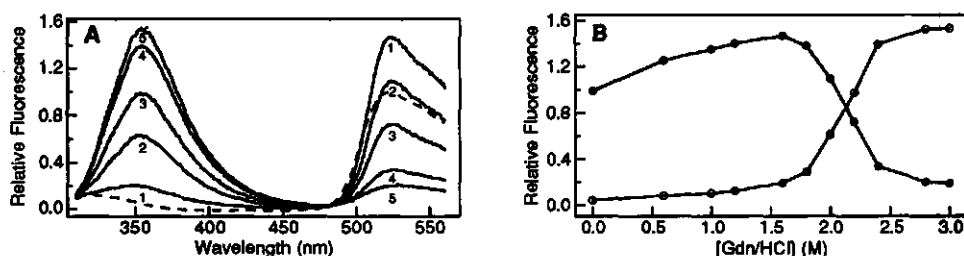


Fig. 6. Tryptophan fluorescence emission spectra of Tyr16->Ser lipoamide dehydrogenase from *A. vinelandii* in Gdn/HCl.

2 μ M enzyme was incubated for 30 min in 100 mM K_2HPO_4 , pH 7.0 and various concentrations of Gdn/HCl at 25 °C. The excitation wavelength was 295 nm. To the relative fluorescence of the native enzyme at 524 nm, a value of 1.0 is assigned. (A) Fluorescence spectrum in the absence (---) and in the presence of 1.6 (1), 2.0 (2), 2.2 (3), 2.4 (4) and 2.8 M Gdn/HCl (5), respectively (—). (B) Relative fluorescence at 355 (○) and 524 (●) nm as a function of the unfolding agent.

apoenzyme [11]. The high flavin fluorescence of *A. vinelandii* lipoamide dehydrogenase is an intrinsic property of the dimeric enzyme [11]. Except for enzyme $\Delta 14$, this property is conserved in the mutated enzymes. For enzyme $\Delta 14$, flavin fluorescence is strongly decreased and the flavin ring is more accessible to solvent [16].

Lipoamide dehydrogenase from *A. vinelandii* contains a single tryptophan residue (Trp199) [17]. Both Trp199 and flavin can be used as internal probes to study the unfolding of the (mutated) enzyme by guanidinium hydrochloride (Gdn/HCl) [11]. As an example, the unfolding of enzyme Tyr16->Ser as a function of Gdn/HCl concentration is recorded in Fig. 6. From the midpoint concentrations of Gdn/HCl required for unfolding (C_m) it is clear that the conformational stability of the mutated enzymes is decreased when compared to wild type enzyme (Table 3). Enzyme $\Delta 14$ deviates most showing a C_m value only slightly higher than that reported for the monomeric wild type apoenzyme [11].

The dissociation constant for wild type dimeric enzyme is below 1 nM [11]. For enzymes $\Delta 9$ and $\Delta 14$, K_d values of 5 nM and 2.5 μ M respectively were reported [8]. Therefore it is concluded that the decreased conformational stability of the mutated enzymes is a consequence of deteriorated subunit interaction.

Discussion

Recently the crystal structures of lipoamide dehydrogenase from *Pseudomonas fluorescens* [Mattevi, personal communication] and lipoamide dehydrogenase from the

N-terminal sequence

<i>A. vinelandii</i>	SQKFDVIVIGAGPGGYVAAIKSAQLGLKTA	(30)
<i>P. fluorescens</i>	*****V*****RA*****	(30)
<i>P. putida</i>	QQTITQTTLLI**A*****RAG***IP*E	(32)

C-terminal sequence

<i>A. vinelandii</i>	(447)	VFAHPALSEALHEAALAVSGHAIHVNRKK-	(476)
<i>P. fluorescens</i>	(447)	**S**T*****N*****I*****R	(477)
<i>P. putida</i>	(434)	IH***T*G**VQ****RAL***L*I	(458)

Fig. 7. Sequence alignment of the N- and C- termini of lipamide dehydrogenase from *Azotobacter vinelandii* [17], *Pseudomonas fluorescens* [18] and *Pseudomonas putida* [19].

An asterisk (*) indicates a residue identical to that in *A. vinelandii* lipamide dehydrogenase.

branched-chain oxo acid dehydrogenase complex from *Pseudomonas putida* with NAD⁺ bound [5] were elucidated to 0.28 nm and 0.245 nm resolution respectively. In both structures the C-terminal part folds back into the protein and is in contact with the N-terminal part of the other subunit (Fig. 1). Tyr18', the equivalent of Tyr16' of the *A. vinelandii* enzyme, is fairly well positioned to form a hydrogen bond with a histidine of the C-terminal part of the other subunit [4]. In view of the impressive sequence homology of the three lipamide dehydrogenases, especially in the N- and C-terminal region (see Fig. 7), and the overlapping results obtained with the Tyr16 mutated enzymes and enzyme Δ9, it is concluded that also in the native *A. vinelandii* wild-type enzyme the C-terminus folds back into the cavity, visible in the structure. Recent further refinement of the *A. vinelandii* structure shows that indeed density is present that could account for the back folded C-terminus [Mattevi, personal communication]. The properties of the mutated enzymes strongly indicate that the interaction between Tyr16' and His470 stabilizes the subunit interaction which is of utmost importance for optimal catalysis, preventing the enzyme from inhibition/over-reduction by NADH. The question arises whether the observed differences in susceptibility toward inhibition/over-reduction between the *E. coli*, *A. vinelandii* and pig heart wild-type enzymes is linked to the dimer stability.

Since the residues involved in the subunit interaction are relatively far away from the active site, it is puzzling how the dimer interaction modulates the redox properties of the active site. It is now tempting to speculate that the observed diminished subunit interaction leads to an increased redox potential of the FAD mediated via the conformation of the C-terminus comprising residues 450-470. The isoalloxazine of the

FAD is located at the interface of the two subunits. Only one contact with the isoalloxazine, to N-3, is provided by the subunit whose C-terminus flanks the active site: the backbone carbonyl oxygen of His450 [4] (His437 in Fig. 1). This carbonyl oxygen is positioned by the *cis*-proline451. Disturbance of this contact leads to altered redox properties of the flavin as shown by studies of enzyme Pro451->Ala [9, 10]. The strong over-reduction/inhibition of the Glu455 mutated enzymes [10] may occur in a similar way since these enzymes also show decreased melting temperatures (67-70°C).

Acknowledgements

We thank Dr. W. Hol and Mr. A. Mattevi for preparing Fig. 1 and for making data available to us prior to publication. We also thank Mss. E. Hissink and M. de Kort for technical assistance. This work was supported by the 'Dutch Foundation for Chemical Research' (SON) with financial aid from the 'Netherlands Organization for Scientific Research' (NWO).

References

1. Williams, C. H. Jr. (1991) in *Chemistry and Biochemistry of Flavoenzymes* (Müller, F., ed) vol 3, in press, CRC Press Inc., Boca Raton.
2. Reed, L. J. (1974) *Acc. Chem. Res.* 7, 40-46.
3. Schierbeek, A. J., Swarte, M. B. A., Dijkstra, B. W., Vriend, G., Read, R. J., Hol, W. G. J., Drenth, J. and Betzel, C. (1989) *J. Mol. Biol.* 206, 365-379.
4. Mattevi, A., Schierbeek, A. J. and Hol, W. G. J. (1991) *J. Mol. Biol.* 220, 975-994.
5. Mattevi, A., Obmolova, G., Sokatch, J. R., Betzel, C. and Hol, W. J. G. (1991) submitted.
6. Greer, S. and Perham, R. N. (1986) *Biochemistry* 25, 2736-2742.
7. Krauth-Siegel, R. L., Enders, B., Henderson, G. B., Fairlamb, A. H. and Schirmer, R. H. (1987) *Eur. J. Biochem.* 164, 123-128.
8. Schulze, E., Benen, J. A. E., Westphal, A. H. and De Kok, A. (1991) *Eur. J. Biochem.* 200, 29-34.
9. Benen, J., Van Berkel, W., Zak, Z., Visser, T., Veeger, C. and De Kok, A. (1991) *Eur. J. Biochem.* 202, 863-872.
10. Benen, J., Van Berkel, W., Dieteren, N., Arscott, D., Williams, C. Jr., Veeger, C. and de Kok, A. (1992) submitted to *Eur. J. Biochem.*
11. Berkel van, W. J. H., Regelink, A. G., Beintema, J. J. and De Kok, A. (1991) *Eur. J. Biochem* 202, 1049-1055.

12. Massey, V. and Veeger, C. (1961) *Biochim. Biophys. Acta* 48, 33-47.
13. Veeger, C and Massey, V. (1963) *Biochim. Biophys. Acta* 67, 679-681.
14. Wilkinson, K. D. and Williams C. H. Jr. (1979) *J. Biol. Chem.* 254, 852-862.
15. Wilkinson, K. D. and Williams C. H. Jr. (1981) *J. Biol. Chem.* 256, 2307-2314.
16. Benen, J. A. E., Van Berkel, W. J. H. and De Kok, A. (1991) in *Flavins and Flavoproteins 1990* (Curti, B., Ronchi, S. and Zanetti, G. eds.) pp 557-564, Walter de Gruyter and Co. Berlin-New York.
17. Westphal, A. H. and De Kok, A. (1988) *Eur. J. Biochem.* 172, 299-305.
18. Benen, J. A. E., Van Berkel, W. J. H., Van Dongen, W. M. A. M., Müller, F., and De Kok, A. (1989) *J. Gen. Microbiol.* 135, 1787-1797.
19. Burns, G., Brown, T., Hatter, K. and Sokatch, J. R. (1989) *Eur. J. Biochem.* 179, 61-69.

Chapter 5

Molecular Cloning and Sequence Determination of the *lpd* Gene Encoding Lipoamide Dehydrogenase from *Pseudomonas fluorescens*

By JACQUES A. E. BENEN,¹ WILLEM J. H. VAN BERKEL,¹
WALTER M. A. M. VAN DONGEN,¹ FRANZ MÜLLER² AND
ARIE DE KOK^{1*}

¹ Department of Biochemistry, Agricultural University of Wageningen, Dreijenlaan 3,
NL-6703 HA Wageningen, The Netherlands

² Sandoz AG, Agro Division, Toxicological Section, CH-4002 Basle, Switzerland

(Received 9 December 1988; revised 17 March 1989; accepted 5 April 1989)

The *lpd* gene encoding lipoamide dehydrogenase (dihydrolipoamide dehydrogenase; EC 1.8.1.4) was isolated from a library of *Pseudomonas fluorescens* DNA cloned in *Escherichia coli* TG2 by use of serum raised against lipoamide dehydrogenase from *Azotobacter vinelandii*. Large amounts (up to 15% of total cellular protein) of the *P. fluorescens* lipoamide dehydrogenase were produced by the *E. coli* clone harbouring plasmid pCJB94 with the lipoamide dehydrogenase gene. The enzyme was purified to homogeneity by a three-step procedure. The gene was subcloned from plasmid pCJB94 and the complete nucleotide sequence of the subcloned fragment (3610 bp) was determined. The derived amino acid sequence of *P. fluorescens* lipoamide dehydrogenase showed 84% and 42% homology when compared to the amino acid sequences of lipoamide dehydrogenase from *A. vinelandii* and *E. coli*, respectively. The *lpd* gene of *P. fluorescens* is clustered in the genome with genes for the other components of the 2-oxoglutarate dehydrogenase complex.

INTRODUCTION

Lipoamide dehydrogenase (dihydrolipoamide dehydrogenase; EC 1.8.1.4) is the flavo-protein component (E3) of the multienzyme complexes that catalyse the oxidative decarboxylation of pyruvate (pyruvate dehydrogenase complex; PDC), 2-oxoglutarate (2-oxoglutarate dehydrogenase complex; OGDC) and branched-chain oxoacids (branched chain oxoacid dehydrogenase complex; BCOADC) to acyl-CoA (Williams, 1976; Sokatch *et al.*, 1981). Lipoamide dehydrogenase catalyses the reoxidation of reduced lipoyl groups that are covalently bound to the dihydrolipoamide acyltransferase components (E2) of the complexes.

Lipoamide dehydrogenase belongs to the family of FAD-containing pyridine nucleotide oxidoreductases. Other members of this family are glutathione reductase (Williams, 1976), mercuric reductase (Fox & Walsh, 1982), thioredoxin reductase (Holmgren, 1980) and trypanothione reductase (Shames *et al.*, 1986). Common characteristics of these enzymes are (1) they are all dimeric and (2) they all contain one redox-active disulphide bridge per subunit which participates in catalysis.

From several organisms genes encoding lipoamide dehydrogenase have been cloned and sequenced: from *Escherichia coli* (Stephens *et al.*, 1983) and recently from man (small-cell carcinoma) and pig (adrenal medulla) (Otulakowski & Robinson, 1987), from bakers' yeast (Browning *et al.*, 1988; Ross *et al.*, 1988) and from *Azotobacter vinelandii* (Westphal & de Kok, 1988).

Abbreviations: PDC, pyruvate dehydrogenase complex; OGDC, 2-oxoglutarate dehydrogenase complex; BCOADC, branched-chain oxoacid dehydrogenase complex; ORF, open reading frame.

In *E. coli* and *A. vinelandii* only one copy of the *lpd* gene is present. In *E. coli* the gene belongs to the *ace* operon together with the genes encoding pyruvate dehydrogenase (EC 1.2.4.1) (E1) and dihydrolipoamide acetyltransferase (EC 2.3.1.12) (E2) of the PDC (Langley & Guest, 1977; Guest *et al.*, 1981); in *A. vinelandii*, on the other hand, the *lpd* gene was found to be located downstream of the gene encoding dihydrolipoamide succinyltransferase (EC 2.3.1.61) (E2) of the OGDC (Westphal & de Kok, 1988; Hanemaaijer *et al.*, 1988). In both organisms the *lpd* genes can be transcribed independently from the genes for the other components in the respective clusters by use of separate promoters. In *Saccharomyces cerevisiae* (Dickinson *et al.*, 1986) and in man, PDC and OGDC contain identical lipoamide dehydrogenases. In man this lipoamide dehydrogenase is also found in BCOADC (Otulakowski *et al.*, 1988).

In *Pseudomonas putida* and *P. aeruginosa*, on the other hand, two different lipoamide dehydrogenases have been found (Sokatch *et al.*, 1981; McCully *et al.*, 1986) and their respective genes have been mapped in *P. putida* (Sykes *et al.*, 1985). One lipoamide dehydrogenase (*lpd-val*), encoded by *lpdv*, is part of the BCOADC; the second (*lpd-glc*), encoded by *lpdg*, is part of the OGDC, of the glycine oxidation system (Sokatch & Burns, 1984) and most likely of the PDC. The *lpdv* gene is part of a cluster comprising the genes encoding the BCOADC and the *lpdg* gene is part of the cluster encoding the OGDC.

Sequence homology between carboxy-terminal peptides containing the active-site histidine residue of *lpd-val* from *P. aeruginosa* and *P. putida* and lipoamide dehydrogenase from *E. coli* has already been demonstrated by McCully *et al.* (1986) and extends to other lipoamide dehydrogenases. Therefore, a detailed structure-function analysis of lipoamide dehydrogenases, some of them cooperating in different complexes and others being specific for one complex, is very interesting. Of great value to this is the determination of the three-dimensional structure of *A. vinelandii* lipoamide dehydrogenase, which is in progress (Schierbeek *et al.*, 1989). Here we report on the molecular cloning and sequence determination of the gene encoding lipoamide dehydrogenase of the OGDC of *P. fluorescens*. Some general properties of the highly expressed, purified enzyme are described as well.

METHODS

Bacterial strains, vectors and growth conditions. *E. coli* TG2 (Gibson, 1984), a *recA* version of TG1 [$\Delta(lac-pro)$ *thi supE* (Res⁻ Mod⁻ (k)) *F'(traD36 proA⁺ B⁺ lacI^q ZAM15)*] was used throughout as a host for cloning and grown in YT medium. The *P. fluorescens* strain used in this study was that described by Howell *et al.* (1972) and was grown in YT-medium or in minimal medium containing 20.0 mM-K₂HPO₄, 20.0 mM-NH₄Cl, 80.0 mM-NH₄NO₃, 85 μ M-MgSO₄, 15.5 mM-*p*-hydroxybenzoate and 0.1 mg FeCl₃ l⁻¹, pH 7.0. Plasmids pUC9 (Vieira & Messing, 1982), pUC18 and pUC19 (Yanisch-Perron *et al.*, 1985) and pTZ18R (Pharmacia) were used for cloning; M13mp9 and M13mp18 were used for nucleotide sequencing (Norlander *et al.*, 1983; Yanisch-Perron *et al.*, 1985).

Materials. Restriction endonucleases were obtained from Anglian Biotechnology, Boehringer or Bethesda Research Laboratories (BRL). T4 DNA ligase and *E. coli* DNA polymerase I (Klenow fragment) were obtained from BRL. Universal sequencing primer, 7-deaza-dGTP and calf intestinal phosphatase were from Boehringer. Low- and high-gelling-temperature agarose were from Seakem. [α -³²P]dATP (3000 Ci mmol⁻¹; 11.1 TBq mmol⁻¹) was purchased from New England Nuclear (NEN). Goat anti-rabbit IgG conjugated to alkaline phosphatase was from Promega Biotec. Sera against purified lipoamide dehydrogenase from *A. vinelandii* and *E. coli* were kindly provided by Mr A. H. Westphal (Westphal & de Kok, 1988). Chromatography resins were from Pharmacia. All chemicals used were of analytical grade.

Isolation of chromosomal and plasmid DNA. *P. fluorescens* was grown at 30 °C in 1 litre of minimal medium to an OD₆₀₀ of 1.5–2.0. Cells were harvested by centrifugation (10 min, 6000 g) and washed once with 100 ml 20% (w/v) sucrose, 150 mM-NaCl, 100 mM-EDTA, pH 7.6 (SSE). The pellet was resuspended in 20 ml SSE and lysozyme (10 mg) was added, followed by incubation at 37 °C for 1 h. Next, 5 mg proteinase K was added, followed by another incubation at 37 °C for 1 h. The lysate was extracted five times with phenol, phenol/chloroform/isoamyl alcohol (25:24:1, by vol.) and repeatedly extracted with chloroform/isoamyl alcohol (24:1, v/v) (Maniatis *et al.*, 1982), until upon centrifugation no pellicle was formed at the interface. Finally, the DNA was precipitated with ethanol, dissolved in 10 mM-Tris/HCl, pH 8.0, 0.1 mM-EDTA and stored at 4 °C with a drop of chloroform added. Large-scale plasmid DNA isolations were performed as described by Westphal & de Kok (1988) and small-scale isolations as described by Birnboim & Doly (1979).

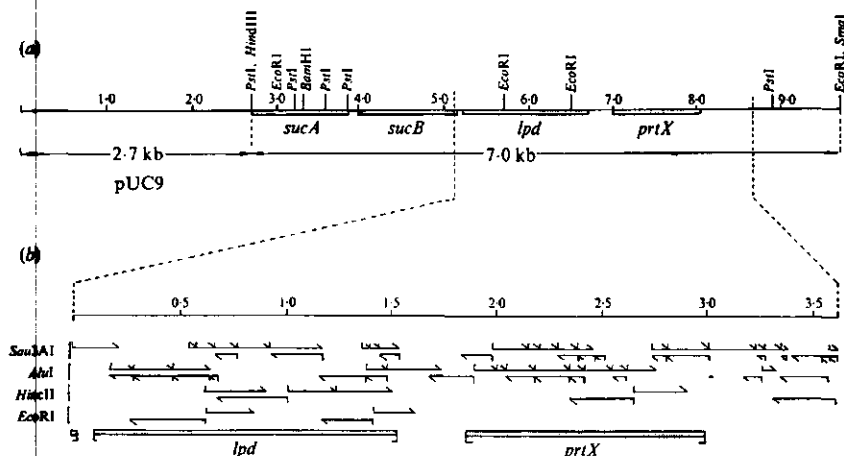


Fig. 1. (a) Physical map of plasmid pCJB94 with the genes for 2-oxoglutarate dehydrogenase (*sucA*), dihydroliipoamide succinyltransferase (*sucB*), liipoamide dehydrogenase (*lpd*) and an ORF encoding a polypeptide with yet unknown function (*prtX*). (b) The insert of plasmid pJB201 and the strategy for determination of the nucleotide sequence of subcloned fragments of pJB201 in M13 vectors. The arrowheads show the direction and extent to which *Sau*3AI, *A*luI, *H*incII and *E*coRI fragments of pJB201 were sequenced. Numbers in panel (a) and at the top of panel (b) indicate the length of the fragments (in kb).

Construction and screening of a *P. fluorescens* gene library in *E. coli*. Construction of a *P. fluorescens* gene library in *E. coli* and screening for clones that produce *P. fluorescens* liipoamide dehydrogenase was performed essentially according to the procedure used for the isolation of the *A. vinelandii* *lpd* gene as described by Westphal & de Kok (1988) with the following slight modifications. Instead of 9–23 kb partial *Sau*3AI fragments, 7–15 kb *Sau*3AI fragments of genomic *P. fluorescens* DNA were ligated into *Bam*HI-digested pUC9 and instead of 125 I-labelled protein A, goat anti-rabbit IgG conjugated to alkaline phosphatase was used for detection of bound antibodies. As a source of primary antibodies, serum raised against *A. vinelandii* liipoamide dehydrogenase was used.

Plasmid pCJB94 was isolated from a clone that appeared positive upon initial screening and which produced high amounts of liipoamide dehydrogenase. The *lpd* gene was subcloned from this plasmid. Therefore, plasmid pCJB94 was partially digested with restriction enzyme *Sau*3AI, the digested DNA was fractionated on a 1.2% (w/v) low-gelling-temperature agarose gel and fragments of 3.0–4.0 kb were isolated and ligated into the *Bam*HI site of pTZ18R. After transformation of *E. coli* TG2 cells with the recombinant plasmids, the same screening procedure was applied as described above. Out of several positive clones *E. coli* TG2(pJB201) was chosen for sequence analysis of the cloned gene.

Nucleotide sequence determination and analysis. The insert of plasmid pJB201 was isolated and digested with several restriction enzymes. The resulting fragments were cloned in M13-derived vectors for sequence determination with the dideoxy chain-termination method of Sanger *et al.* (1977) according to the strategy displayed in Fig. 1. Because of the high G + C content, 7-deaza-dGTP was used instead of dGTP. Sequence data were compiled and analysed with a VAX computer using the programs of Staden (1982, 1984).

Western blotting. This was done as described by Westphal & de Kok (1988) with the same modification, with respect to detection of bound antibodies, as mentioned above.

Southern blotting. Digests of *P. fluorescens* DNA and plasmids pCJB94 and pJB201 were fractionated in a 0.6% (w/v) agarose gel in 89 mM-Tris/borate, 2 mM-EDTA, pH 8.3, followed by transfer of the DNA to nitrocellulose according to Southern (1975). Isolated insert of pJB201 was nick-translated using [32 P]dATP and used as a probe (Rigby *et al.*, 1977). Hybridization was carried out at 65 °C for 16 h in 6 × SSC, 5 × Denhardt's solution and 0.1% (w/v) SDS (Maniatis *et al.*, 1982). The blot was washed at 65 °C in buffers containing 0.1% (w/v) SDS and 6 × SSC, 1 × SSC and 0.1 × SSC, respectively, each wash lasting 45 min.

Enzyme purification. *P. fluorescens* liipoamide dehydrogenase was isolated from *E. coli* TG2(pCJB94), applying essentially the same procedure as used for the isolation of liipoamide dehydrogenase from *A. vinelandii* cloned in *E. coli* TG2 (Westphal & de Kok, 1988). Briefly, cell-free extract was treated with protamine sulphate to remove nucleic acids and large complexes. After centrifugation, the supernatant was made 50% saturated with

ammonium sulphate, clarified by centrifugation and applied to a Sepharose 6B column for hydrophobic interaction chromatography. The enzyme, firmly bound at the top of the matrix, was eluted with 45% saturated ammonium sulphate in 50 mM-potassium phosphate, pH 7.0, 0.5 mM-EDTA. FPLC analytical gel filtration was done as described by Van Berkel *et al.* (1988).

Lipoamide dehydrogenase activity was assayed as described by Van den Broek (1971) using 1 M-potassium phosphate, pH 7.0, instead of 0.8 M-sodium citrate, pH 6.5, as the buffer.

RESULTS AND DISCUSSION

Isolation of E. coli clones that produce P. fluorescens lipoamide dehydrogenase

Genomic *P. fluorescens* DNA was partially digested with restriction endonuclease *Sau3AI*. Fragments of 7–15 kb were isolated and ligated into the *Bam*HI site of pUC9. The recombinant plasmids were used to transform *E. coli* TG2. Of the resulting clones, 1900 were screened with antiserum raised against lipoamide dehydrogenase from *A. vinelandii*. One clone, *E. coli* TG2(pCJB94), reacted strongly with the antiserum: this clone had a bright yellow appearance, suggesting that a large amount of a flavoprotein was produced. Cell-free extract of *E. coli* TG2(pCJB94) showed a lipoamide dehydrogenase activity which was 30-fold higher than that of cell-free extract of *E. coli* TG2(pUC9). SDS-polyacrylamide gel electrophoresis (SDS-PAGE) of this cell-free extract revealed large amounts of a polypeptide with an apparent molecular mass of 56 kDa which was not detectable in *E. coli* TG2(pUC9) (results not shown).

The *P. fluorescens* lipoamide dehydrogenase produced by *E. coli* TG2(pCJB94) was purified from cell-free extract of this clone following essentially the same procedure as described by Westphal & de Kok (1988) for purification of lipoamide dehydrogenase from *A. vinelandii* cloned in *E. coli* (Table 1). The *P. fluorescens* lipoamide dehydrogenase was eluted from the Sepharose 6B column at 45% ammonium sulphate saturation instead of 25% as found for the *A. vinelandii* enzyme. This indicates that *P. fluorescens* lipoamide dehydrogenase is less hydrophobic than *A. vinelandii* lipoamide dehydrogenase. SDS-PAGE of the purified protein showed a polypeptide with an apparent molecular mass of 56 kDa that was virtually free of contaminating polypeptides (Fig. 2a, lane 2). The mobility of this purified polypeptide on SDS-PAGE is different from *E. coli* lipoamide dehydrogenase, which has an apparent molecular mass of 50 kDa (Fig. 2a, lane 1).

The subunit composition of the purified enzyme was estimated by gel filtration. The enzyme eluted as one symmetrical peak from a Superose 12 column. The apparent molecular mass of the protein as estimated from the distribution coefficient was 110 kDa, indicating that, like other lipoamide dehydrogenases, the enzyme is a dimer in its native state. The molecular mass as determined here is in agreement with the reported molecular mass of lipoamide dehydrogenase holoenzyme purified from *P. fluorescens* by Scouten & McManus (1971).

The amino acid sequence of the 22 amino-terminal residues of the purified protein was determined by automated Edman degradation. This sequence was different from the N-terminal sequence of *E. coli* lipoamide dehydrogenase, but was found to coincide with the sequence derived from the nucleotide sequence of the gene found in the cloned *P. fluorescens* fragment (*vide infra*), omitting the initiating formylmethionine. This demonstrates that the purified lipoamide dehydrogenase was synthesized under the direction of the cloned *P. fluorescens* DNA fragment.

Western blots of purified lipoamide dehydrogenases from *E. coli*, *A. vinelandii* and *P. fluorescens* [obtained from *E. coli* TG2(pCJB94)] were incubated with antiserum raised against lipoamide dehydrogenases from *E. coli* or *A. vinelandii* (Fig. 2b, c). Cloned *P. fluorescens* lipoamide dehydrogenase reacted with antiserum against *A. vinelandii* lipoamide dehydrogenase (Fig. 2c) but not with serum against the *E. coli* enzyme (Fig. 2b). It can also be concluded from Fig. 2 that purified *P. fluorescens* lipoamide dehydrogenase as isolated from *E. coli* TG2(pCJB94) was not detectably contaminated with endogenous *E. coli* lipoamide dehydrogenase.

A purification table of a large-scale isolation of the cloned *P. fluorescens* lipoamide dehydrogenase is presented in Table 1. From this table it can be estimated that the cloned enzyme accounts for approximately 15% of the total cellular protein of *E. coli* TG2(pCJB94).

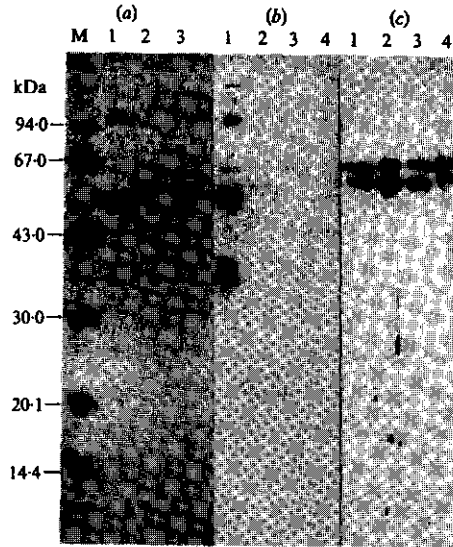


Fig. 2. Electrophoretic profiles of purified lipamide dehydrogenases in a 12.5% (w/v) polyacrylamide gel with 0.1% SDS. (a) Staining with Coomassie brilliant blue R; (b, c) Western blots of purified lipamide dehydrogenases incubated with antisera against *E. coli* lipamide dehydrogenase (b) or *A. vinelandii* lipamide dehydrogenase (c). Lanes 1, *E. coli* lipamide dehydrogenase purified from isolated pyruvate dehydrogenase complex; lanes 2, *P. fluorescens* lipamide dehydrogenase purified from *E. coli* TG2(pCJB94); lanes 3, purified *A. vinelandii* lipamide dehydrogenase; lanes 4, sample buffer; lane M: molecular mass markers. The band at approximately 60 kDa in all four lanes in (c) results from reaction of antiserum against *A. vinelandii* lipamide dehydrogenase with some component present in the sample buffer. The bands at 100 kDa and 40 kDa in *E. coli* lipamide dehydrogenase represent residual pyruvate dehydrogenase and a degradation product of the latter.

Table 1. Purification of *P. fluorescens* lipamide dehydrogenase from *E. coli* TG2(pCJB94)

Step	Volume (ml)	Protein (mg)	Specific activity* (U mg ⁻¹)	Total activity* (U)	Yield (%)
Cell-free extract	860	5525	19.2	107 500	100
Protamine sulphate supernatant	900	3240	32.7	106 200	98
50% ammonium sulphate supernatant	1240	936	88.7	83 040	77
Sephacrose 6B (pooled fractions)	215	512	127.1	65 575	61

* 1 U = 1 μ mol NADH oxidized min⁻¹.

Using standard assay conditions, the specific activity of the purified enzyme (127 U mg⁻¹; 1 U = 1 μ mol NADH oxidized min⁻¹) is comparable to the specific activity of cloned *A. vinelandii* lipamide dehydrogenase.

Nucleotide sequence and analysis of the *P. fluorescens* *lpd* gene

The *lpd* gene from *P. fluorescens* was subcloned from the 7 kb insert of pCJB94. From one of the resultant clones, *E. coli* TG2(pJB201) (Fig. 1), plasmid was isolated and the 3.6 kb insert used for sequence analysis.

The sequencing strategy is shown in Fig. 1; all sequence data were derived from gel-readings from at least two independently sequenced fragments. The final 3610 bp sequence was compiled

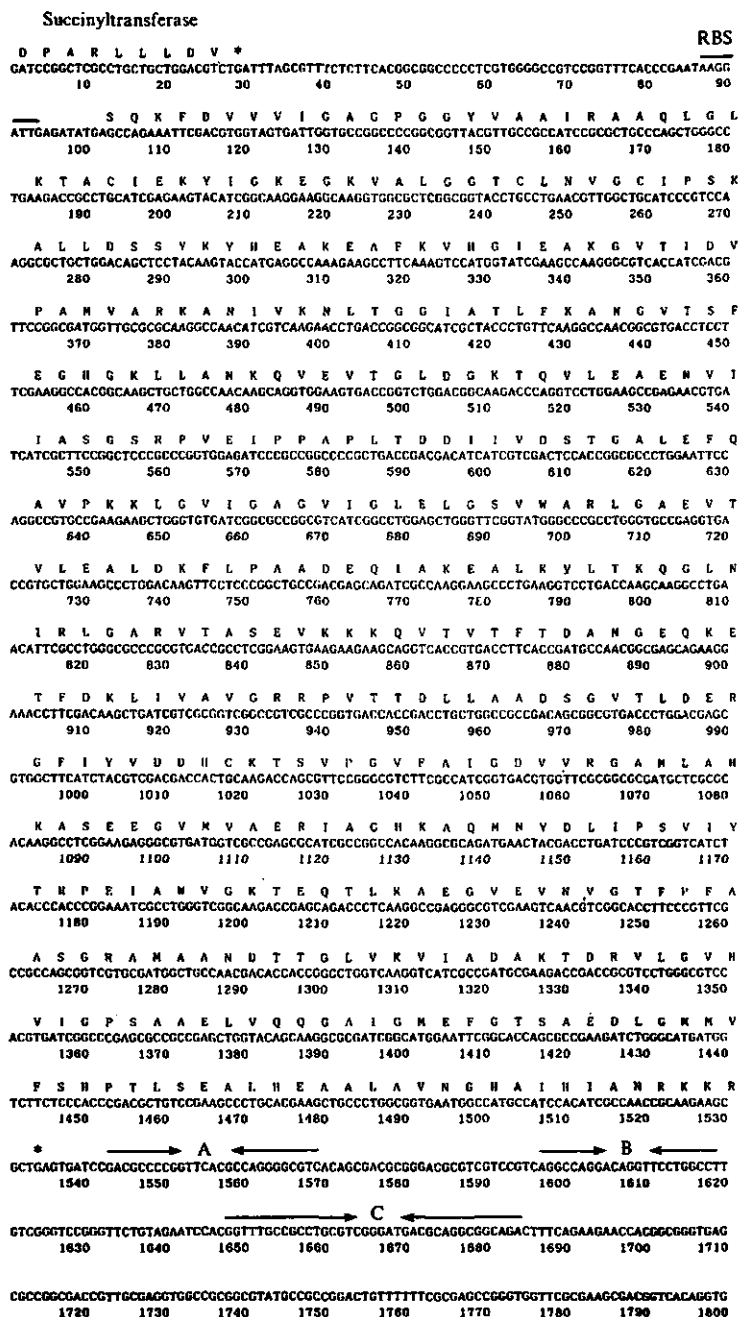


Fig. 3. Nucleotide sequence of the *P. fluorescens* *lpd* gene with the derived amino acid sequence in one-character code. Indicated are a putative ribosome-binding site, RBS (overlined) and three possible terminators, A, B and C (arrows). Asterisks represent stop codons. The initiating formylmethionine is omitted.

from overlapping sequence files, 78% of the data (93% of the coding region of the *lpd* gene) being derived from gel-readings of both strands. The insert of pJB201 (3610 bp) was found to comprise two open reading frames (ORFs), one between bp 99 and 1532 and the second between bp 1863 and 2990. The first ORF (bp 99–1532; Fig. 3) could be identified as coding for lipoamide dehydrogenase. Identification was based on (1) the extensive homology of the derived amino acid sequence of the polypeptide encoded by this gene with lipoamide dehydrogenase from both *A. vinelandii* (Westphal & de Kok, 1988) and *E. coli* (Stephens *et al.*, 1983) showing 84% and 42% homology, respectively (Fig. 4), and (2) the identity of the derived amino-terminal amino acid sequence with that of the protein purified from *E. coli* TG2(pCJB94).

The derived amino acid sequence of *P. fluorescens* lipoamide dehydrogenase (Fig. 3) contains 477 amino acid residues excluding formylmethionine. The calculated molecular mass is 50033 Da (50830 Da when FAD is included). Apparently, the molecular mass as determined by SDS-PAGE (56 kDa) is overestimated by 10%. A similar observation was reported for lipoamide dehydrogenase from *A. vinelandii* (Westphal & de Kok, 1988).

Upstream of the *lpd* gene no consensus *E. coli*-type promoter sequence could be identified in pJB201. Expression of *P. fluorescens* lipoamide dehydrogenase from plasmid pJB201 is dependent on the *lacZ* promoter of the cloning vector. This was confirmed by cloning the insert in inverted direction towards the *lacZ* promoter in pUC19. The start codon AUG is preceded by a potential ribosome-binding site (bp 87–94).

The nucleotide sequence downstream of the *lpd* gene contains three regions of dyad symmetry. Free energy calculations (Tinoco *et al.*, 1973) for the mRNA transcripts of the regions of dyad symmetry suggest that they may form very stable stem-and-loop structures: region A, $\Delta G = -109 \text{ kJ mol}^{-1}$; region B, $\Delta G = -84 \text{ kJ mol}^{-1}$; and region C, $\Delta G = -148 \text{ kJ mol}^{-1}$. The indicated stem-and-loop structures might serve as transcription terminators.

Homology between lipoamide dehydrogenases

The primary structures of lipoamide dehydrogenases from *E. coli* (Stephens *et al.*, 1983), *A. vinelandii* (Westphal & de Kok, 1988) and *P. fluorescens* (this study) are aligned in Fig. 4. Indications about functional domains in lipoamide dehydrogenases were first obtained by Rice *et al.* (1984). They compared the primary structures of *E. coli* lipoamide dehydrogenase and human glutathione reductase and fitted the primary structure of lipoamide dehydrogenase into the three-dimensional structure of glutathione reductase. Schierbeek *et al.* (1989) determined the three-dimensional structure of lipoamide dehydrogenase from *A. vinelandii* by X-ray crystallography. The overall folding of the polypeptide chain of *A. vinelandii* lipoamide dehydrogenase appears to be very similar to that of glutathione reductase, with the same four-domain structure. In the primary structure several features appear to be conserved in the enzymes: the ADP-binding folds of the cofactors FAD and NAD(P)⁺ (positions 5–35 and 182–210, respectively, relative to *P. fluorescens* lipoamide dehydrogenase), the region around the active-site disulphide bridge (positions 44–60) and the region around the active-site histidine (positions 448–455). These conserved regions are indicated in Fig. 4; they are also conserved in *P. fluorescens* lipoamide dehydrogenase.

Besides the primary structures of the bacterial lipoamide dehydrogenases shown in Fig. 4, sequences of eukaryotic lipoamide dehydrogenases have been published: those of porcine adrenal medulla and human small-cell carcinoma (Otulakowski & Robinson, 1987) and of bakers' yeast (Browning *et al.*, 1988; Ross *et al.*, 1988). Also in the primary structures of these eukaryotic lipoamide dehydrogenases the above-mentioned features are conserved (not shown).

Localization of *lpd* genes in the genome: *P. fluorescens*, *E. coli* and *A. vinelandii* compared

In pCJB94 the *lpd* gene is preceded by the genes for the other two components of the OGDC (Fig. 1). Immediately upstream of the *lpd* gene, the gene for dihydrolipoamide succinyltransferase (*sucB*) was detected; this gene has now been subcloned and sequenced and is highly homologous to the dihydrolipoamide succinyltransferase of *A. vinelandii* (A. H. Westphal, personal communication) and *E. coli* (Spencer *et al.*, 1984). Also the gene for the third component of the OGDC, 2-oxoglutarate dehydrogenase (*sucA*), could be identified (results not

	I	10	20	30	40	II	50	60
Pflip	SQKFDVVVIG	ACPGGYAAI	RAAQGLKTA	CIRKVIKFG	KVALGCTCLN	VGCIPSKALI		
Avlip	*****	*****	NS*****	L*****	*****	*****		
Eclip	STEITQ**L*	***A**S**	*C*D**E**V	IV**NT---	*****	*****		
	70	80	90	100	110	120		
Pflip	DSSYKVEAK	EAFKVICFA	KGVITDVPAN	VARKANIVKN	LTGGIATLFX	ANGVTSFEGH		
Avlip	*****F***H	*S*LI***ST	GE*A*****J	I***DQ**R*	***V*S**I*	*****L*****		
Eclip	HVA-**VI*EA	K*LAE***VF	GEPKT*IDKI	RTM*EKVINQ	****L*GNA*	GRKVKVNGNL		
	130	140	150	160	170	180		
Pflip	GKLLANKQVE	VTGLDCKTQV	LEAENVIIAS	GSRPVEIPPA	PLTDDIIVDS	TGALEFQAVP		
Avlip	*****G*K**	***AA**SS**	*DT*****I**	*K*****	*VDQ*VI***	*****D*N**		
Eclip	**FTGANTL*	*E*EN*KT-*	INFDNA***A	*****IQL*FI	*HE*PR**M*	*D**I*KE**		
	190	200	210	220	230	240		
Pflip	KKLGVIAGCV	IGLEIGSVMA	RLGAELTVLE	ALDKFLPAD	EQLAKALKV	LTKQGLNIRL		
Avlip	G*****	*****	*****	*M*****V*	*V*****Q*J	*****L*		
Eclip	ER*L*M*G*I	****MGT**VI	A**SQID*V*	MF*QVI****	KD*V*VFT*R	IS*-K*LM*		
	250	260	270	280	290	300		
Pflip	GARVASEVK	KKQVTYFTD	ANGE-QKETF	DKLIVAVGR	PVITDLAAD	SGVTLDERGF		
Avlip	*****GT***	N*****K*V*	*E*-KSQA*	*****	*****	*****		
Eclip	ETK***V*A*	EDGIY*TMEG	KKAPAEPRQV	*AVL**I*V	*NGKN*D*GK	A**EV*D**		
	309	319	329	339	349	359		
Pflip	IYVDHCKTS	VPGVFAIGDV	VRGANLAHKA	SEEGVNVAR	IAGHKAQMN	DLIPSVIYTH		
Avlip	*****V*A**	*****V*****	*****V*****	*****V*****	*****V*****	*****V*****		
Eclip	I***KQLR*N	**HI*****I	*GDP*****G	VH**HVA**V	***K*HYFDP	KV***IA**E		
	369	379	389	399	409	419		
Pflip	PEIAWVGKTE	QTLKAEVVEV	NVGTFRFTTS	GRAMAANDTT	OLYKVIADRK	TORVLGVHVI		
Avlip	*****G*****	*A*****AJ	***V*P*AA*	*****A*	*F*****A*	*****A*****		
Eclip	**V*****L**	KEA*EK*ISY	ETA**PWAA*	***I*SDCAD	*MT*L*F*KE	SH**I*GAIV		
	429	439	449	IV	459	469		
Pflip	GPSAAELVQQ	GAIGMEFGTS	AEDLGMNVFS	NPTLSALHE	AALAVNGHAI	RIANRKKR		
Avlip	*****	*****	*****A	*****A	*****S*****	*****		
Eclip	*TNGG**LGE	IGLAI*M*CD	***I*ALTIHA	*****H*SVGL	**EVPE*SIT	DLP*P*AKKK		

Fig. 4. Comparison of the amino acid sequence of the lipoamide dehydrogenases of *P. fluorescens* (Pflip), *A. vinelandii* (Avlip; Westphal & de Kok, 1988) and *E. coli* (Eclip; Stephens *et al.*, 1983). Identical residues are indicated by asterisks. Boxed residues indicate the ADP-binding site of FAD (I), the redox-active disulphide bridge (II), the ADP-binding site of NAD⁺ (III) and the region around the active-site histidine (IV).

shown). In order to investigate whether another copy of the *lpd* gene is present in *P. fluorescens*, genomic *P. fluorescens* DNA was hybridized with the cloned *lpd* gene (Fig. 5). Only one DNA fragment was found to hybridize with the cloned *lpd* gene in *Bam*HI-, *Pst*I- and *Hind*III-digested *P. fluorescens* DNA (Fig. 5, lanes 1, 2 and 3, respectively). In accordance with the presence of two *Eco*RI sites in the insert of pJB201 (Fig. 2), three fragments were found to hybridize in *Eco*RI-digested genomic DNA (Fig. 5, lane 4). From this experiment we obtained no indication of the presence of a second *lpd* gene in the *P. fluorescens* genome with sufficient sequence homology to the cloned gene to be detected under the hybridization conditions applied. This suggests that, if another *lpd* gene is present, as in other pseudomonads (Sokatch *et al.*, 1981; McCully *et al.*, 1986), only limited sequence homology exists between those *lpd* genes.

These results indicate that in *P. fluorescens*, as in *A. vinelandii*, but contrary to *E. coli*, the *lpd* gene forms part of the OGDC cluster. Surprisingly, the homology in genetic organization between *P. fluorescens* and *A. vinelandii* also extends downstream of the *lpd* gene. Downstream of

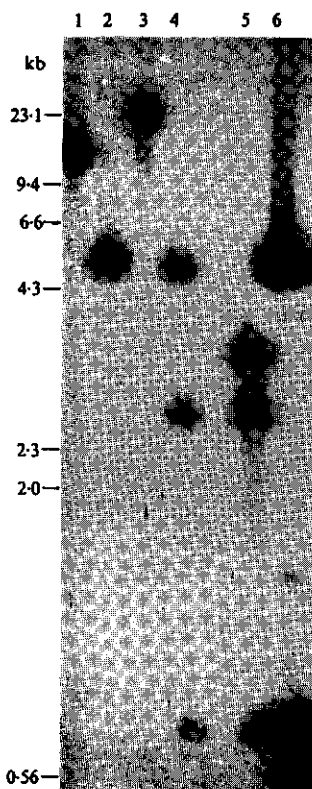


Fig. 5. Autoradiograph of a Southern blot containing *P. fluorescens* chromosomal DNA digests (lane 1, *Bam*HI; lane 2, *Pst*I; lane 3, *Hind*III; lane 4, *Eco*RI) and *Eco*RI digests of pCJB94 (lane 5) and pJB201 (lane 6) hybridized with the 32 P-labelled insert of pJB201.

the *lpd* gene large ORFs are found in both organisms (position 1863–2990 in the sequence of pJB201, *prtX* in Fig. 1) which might encode polypeptides that are 85% homologous when compared to each other. This indicates that the organization of the OGDC clusters of *A. vinelandii* and *P. fluorescens* is very similar. Formal proof that, as in *A. vinelandii*, no *lpd* gene is present in the PDC cluster of *P. fluorescens*, has to await the analysis of the genes of the PDC cluster.

We are grateful to Dr R. Amons for the determination of the N-terminal sequence with the gas-phase sequenator and to Mr E. Keukens and Ms M. C. Snoek for technical assistance. We thank Ms M. F. van Eijk for editing the typescript and Mr M. M. Bouwmans for drawing the figures. This investigation was supported by the Netherlands Foundation for Chemical Research (SON), with financial aid from the Netherlands Organization for Scientific Research (NWO).

REFERENCES

- BURROUGHS, H. C. & DOLY, J. (1979). A rapid alkaline extraction procedure for screening recombinant plasmid DNA. *Nucleic Acids Research* **7**, 1513–1523.
- BROWNING, K. S., UHLINGER, D. J. & REED, L. J. (1988). Nucleotide sequence for yeast dihydrolipamide dehydrogenase. *Proceedings of the National Academy of Sciences of the United States of America* **85**, 1831–1834.

- DICKINSON, J. R., ROY, D. J. & DAWES, J. W. (1986). A mutation affecting lipamide dehydrogenase, pyruvate dehydrogenase and 2-oxoglutarate dehydrogenase activities in *Saccharomyces cerevisiae*. *Molecular and General Genetics* **204**, 103-107.
- FOX, B. S. & WALSH, C. T. (1982). Mercuric reductase - purification and characterization of transposon-encoded flavoprotein containing an oxidation-reduction-active disulfide. *Journal of Biological Chemistry* **257**, 2498-2503.
- GIBSON, T. J. (1984). *Studies on the Epstein-Bar virus genome*. PhD thesis, University of Cambridge, UK.
- GUEST, J. R., COLE, S. T. & JEYASEELAN, K. (1981). Organization and expression of the pyruvate dehydrogenase complex genes of *Escherichia coli* K12. *Journal of General Microbiology* **127**, 65-79.
- HANEMAAIJER, R., JANSSEN, A., DE KOK, A. & VEEGER, C. (1988). The dihydrolipoyltransacetylase component of the pyruvate dehydrogenase complex of *Azotobacter vinelandii*. *European Journal of Biochemistry* **174**, 593-599.
- HOLMGREN, A. (1980). Pyridine nucleotide-disulfide oxidoreductases. *Experientia, Supplement* **36**, 149-180.
- HOWELL, L. G., SPECTOR, T. & MASSEY, V. (1972). Purification and properties of *p*-hydroxybenzoate hydroxylase from *Pseudomonas fluorescens*. *Journal of Biological Chemistry* **247**, 4340-4350.
- LANGLEY, P. & GUEST, J. R. (1977). Biochemical genetics of the α -ketoacid dehydrogenase complexes of *Escherichia coli* K12: isolation and biochemical properties of deletion mutants. *Journal of General Microbiology* **99**, 263-276.
- MANIATIS, T., FRITSCH, E. F. & SAMBROOK, J. (1982). *Molecular Cloning: a Laboratory Manual*. Cold Spring Harbor, NY: Cold Spring Harbor Laboratory.
- MCCULLY, V., BURNS, G. & SOKATCH, J. R. (1986). Resolution of branched chain oxoacid dehydrogenase complex of *Pseudomonas aeruginosa* PAO. *Biochemical Journal* **233**, 737-742.
- NORRANDER, J., KEMPE, T. & MESSING, J. (1983). Construction of improved M13 vectors using oligodeoxynucleotide-directed mutagenesis. *Gene* **26**, 101-106.
- OTULAKOWSKI, G. & ROBINSON, B. H. (1987). Isolation and sequence determination of cDNA clones for porcine and human lipamide dehydrogenases. *Journal of Biological Chemistry* **262**, 17313-17318.
- OTULAKOWSKI, G., ROBINSON, B. H. & WILLARD, H. F. (1988). Gene for lipamide dehydrogenase maps to human chromosome 7. *Somatic Cell and Molecular Genetics* **14**, 411-414.
- RICE, D. W., SCHULZ, G. E. & GUEST, J. R. (1984). Structural relationships between glutathione reductase and lipamide dehydrogenase. *Journal of Molecular Biology* **174**, 483-496.
- RIGBY, P. W. J., DIECKMANN, M., RHODES, C. & BERG, P. (1977). Labeling deoxyribonucleic acid to high specific activity *in vitro* by nick translation with DNA polymerase I. *Journal of Molecular Biology* **113**, 237-251.
- ROSS, J., REID, G. A. & DAWES, J. W. (1988). The nucleotide sequence of the *LPD1* gene encoding lipamide dehydrogenase in *Saccharomyces cerevisiae*: comparison between eukaryotic and prokaryotic sequences for related enzymes and identification of potential upstream control sites. *Journal of General Microbiology* **134**, 1131-1139.
- SANGER, F., NICKLEN, S. & COULSON, A. R. (1977). DNA sequencing with chain terminating inhibitors. *Proceedings of the National Academy of Sciences of the United States of America* **74**, 5463-5467.
- SCHIERBEEK, A. J., SWARTE, B. M. A., DIJKSTRA, B. W., VRIEND, G., READ, R. J., HOL, W. J. G., DRENTH, J. & BETZEL, C. (1989). Structure of lipamide dehydrogenase from *Azotobacter vinelandii* determined by a combination of molecular and isomorphous replacement techniques. *Journal of Molecular Biology* **206**, 365-379.
- SCOUTEN, W. H. & McMANUS, I. R. (1971). Microbial lipamide dehydrogenase - purification and some characteristics of the enzyme derived from selected microorganisms. *Biochimica et biophysica acta* **227**, 248-263.
- SHAMES, S. L., FAIRLAMB, A. H., CERAMI, A. & WALSH, C. T. (1986). Purification and characterization of trypanothione reductase from *Crithidia fasciculata*, a newly discovered member of disulfide containing flavoprotein reductase. *Biochemistry* **25**, 3519-3526.
- SOKATCH, J. R. & BURNS, G. (1984). Oxidation of glycyl by *Pseudomonas putida* requires a specific lipamide dehydrogenase. *Archives of Biochemistry and Biophysics* **228**, 660-666.
- SOKATCH, J. R., MCCULLY, V., GEBROSKI, J. & SOKATCH, D. J. (1981). Isolation of a specific dehydrogenase for a branched chain ketoacid dehydrogenase from *Pseudomonas putida*. *Journal of Bacteriology* **148**, 639-646.
- SOUTHERN, E. M. (1975). Detection of specific sequences among DNA fragments separated by gel electrophoresis. *Journal of Molecular Biology* **98**, 503-517.
- SPENCER, M. E., DARLISON, M. G., STEPHENS, P. E., DUCKENFIELD, J. K. & GUEST, J. R. (1984). Nucleotide sequence of the *sucB* gene encoding the dihydrolipoyl succinyl transferase of *Escherichia coli* K12 and homology with the corresponding acetyl transferase. *European Journal of Biochemistry* **141**, 361-374.
- STADEN, R. (1982). Automation of the computer handling of gelreading data produced by the shotgun method of DNA sequencing. *Nucleic Acids Research* **10**, 4731-4751.
- STADEN, R. (1984). A computer program to enter DNA gelreading data into a computer. *Nucleic Acids Research* **12**, 499-503.
- STEPHENS, P. E., LEWIS, H. M., DARLISON, M. G. & GUEST, J. R. (1983). Nucleotide sequence of the lipamide dehydrogenase gene of *Escherichia coli* K12. *European Journal of Biochemistry* **135**, 519-527.
- SYKES, P. J., MENARD, J., MCCULLY, V. & SOKATCH, J. R. (1985). Conjugative mapping of pyruvate, 2-ketoglutarate and branched chain ketoacid dehydrogenase genes in *Pseudomonas putida* mutants. *Journal of Bacteriology* **162**, 203-208.
- TINOCO, I., JR, BOKER, P. N., DENGLER, B., LEVINE, M. D., UHLENBECK, O. C., CROTHERS, D. M. & GRALLA, J. (1973). Improved estimation of secondary structure in ribonucleic acids. *Nature New Biology* **246**, 40-41.
- VAN BERKEL, W. J. H., VAN DEN BERG, W. A. M. &

- MÜLLER, F. (1988). Large scale preparation and reconstitution of apo-flavoproteins with special reference to butyryl-CoA dehydrogenase from *Megasphaera elsdenii*: hydrophobic interaction chromatography. *European Journal of Biochemistry* 178, 197-207.
- VAN DEN BROEK, H. W. J. (1971). *Pyridine nucleotide transhydrogenase*. PhD thesis, Agricultural University of Wageningen, The Netherlands.
- VIEIRA, J. & MESSING, J. (1982). The pUC plasmids, an M13mp7 derived system for insertion mutagenesis and sequencing with synthetic universal primers. *Gene* 19, 259-268.
- WESTPHAL, A. H. & DE KOK, A. (1988). Lipoamide dehydrogenase from *Azotobacter vinelandii*; molecular cloning, organization and sequence analysis of the gene. *European Journal of Biochemistry* 172, 299-305.
- WILLIAMS, C. H., JR (1976). Flavin containing dehydrogenases. In *The Enzymes*, vol. 13, pp. 89-173. Edited by P. D. Boyer. New York: Academic Press.
- YANISCH-PERRON, C., VIEIRA, J. & MESSING, J. (1985). Improved M13 phage cloning vectors and host strains: nucleotide sequences of the M13mp18 and pUC19 vectors. *Gene* 33, 103-119.

Chapter 6

Lipoamide dehydrogenase from *Pseudomonas fluorescens*.

Some spectral properties and conformational stability

Jacques Benen, Willem van Berkel and Arie de Kok.

Summary

Lipoamide dehydrogenase from *Pseudomonas fluorescens* is characterized with respect to some spectral properties and with respect to the conformational stability of the several redox states.

The visible spectrum of the oxidized enzyme is characteristic of a flavin in an apolar environment. Reduction of the enzyme by NADH shows that the reducing equivalents mainly reside on the disulfide. Excess NADH does not fully reduce the enzyme to the four-electron reduced level. The enzyme is not inhibited by the product NADH.

The oxidized enzyme is thermostable showing a melting temperature of 86 °C. The thermal stability drastically decreases upon reduction. The oxidized and lip(SH)₂ reduced enzyme are insensitive to unfolding by urea. Unfolding of NADH-reduced enzyme by urea is inhibited in the presence of NAD⁺. It is concluded that over-reduction results in a decreased stability of the dimer.

Introduction

The gene encoding lipoamide dehydrogenase from *Pseudomonas fluorescens* has recently been cloned and expressed in *Escherichia coli* [1]. The enzyme shows 84 % amino acid sequence identity with lipoamide dehydrogenase from *Azotobacter vinelandii*. The crystal structures of three lipoamide dehydrogenases have been determined at present, from *A. vinelandii* at 0.22 nm resolution [2] and from *P. putida* [3] and from *P. fluorescens* [Mattevi, personal communication] at 0.25 and 0.28 nm resolution respectively. The three structures appear to be almost identical. In the *Pseudomonas* structures the last ten amino acid residues, which were initially not visible in the electron density map of *A. vinelandii* enzyme, appear to fold back into the protein structure that constitutes the active site. Apart from the, for *A. vinelandii* enzyme,

nine established intersubunit hydrogen bonds, this backfolded C-terminus makes additional contacts with the other subunit [3]. Site-specific mutagenesis experiments with the *A. vinelandii* enzyme have shown that the C-terminus adopts a similar conformation in this enzyme (Chapter 4) [4]. In contrast to the high degree of amino acid and structural identity the *A. vinelandii* and *P. fluorescens* enzyme differ strongly with respect to FAD induced dimerization of the apoenzyme [5] indicating differences in the enzyme's structures which are not revealed at the current level of resolution.

Lipoamide dehydrogenases, as isolated from different sources, strongly differ with respect to inhibition by the product NADH [6-8]. This inhibition is mainly due to over-reduction to the four-electron reduced state (EH₄), as first demonstrated with the *E.coli* enzyme [9]. For lipoamide dehydrogenase from *A. vinelandii* it was shown that over-reduction strongly promotes subunit dissociation and that dimerization is the driving force for the conformational stability of the protein [10]. Interestingly, both product inhibition and conformational stability are affected by mutations located in the vicinity of the interface [4].

Preliminary experiments in our laboratory indicated that lipoamide dehydrogenase from *P. fluorescens* is insensitive to product inhibition despite the conservation of amino acids at the C-terminus. In this Chapter some catalytic properties and conformational stability of lipoamide dehydrogenase from *P. fluorescens* are reported.

Materials and Methods

Biochemicals and concentration determinations have been described in Chapters 2 and 3 [8, 10]. Lipoamide dehydrogenase from *P. fluorescens*, as cloned in *E. coli*, was isolated according to Chapter 5 [1]. Thermoinactivation and unfolding experiments were performed essentially as described elsewhere [11]. Absorption spectra under anaerobic conditions were recorded at 25 °C on an Aminco DW-2000 spectrophotometer, essentially as reported earlier. Rapid reaction and steady-state kinetics were studied as reported previously [8] with one slight modification: for steady state kinetics stock solutions of dihydrolipoamide (lip(SH)₂) were prepared in pure methanol.

Results

Spectral properties. Fig. 1 shows the visible absorption spectra of lipoamide dehydrogenase from *P. fluorescens* before and after anaerobic reduction with one and two molar equivalents of NADH. At pH 8.0, the flavin absorption spectrum of the

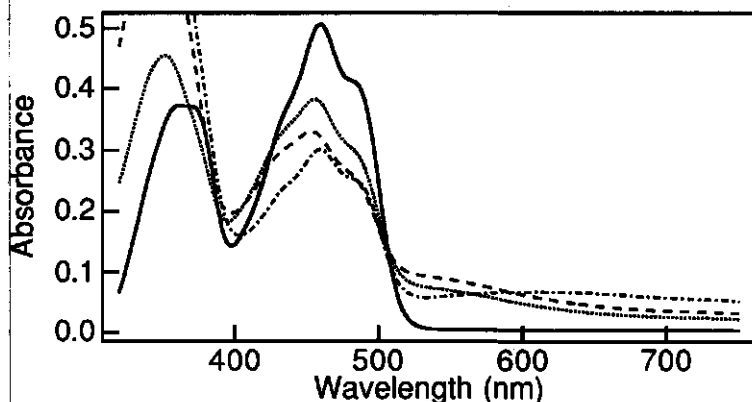


Fig 1. Visible absorption spectra of *Pseudomonas fluorescens* lipoamide dehydrogenase. Spectra were recorded at 25°C in 100 mM Hepes, 0.5 mM EDTA, pH 8.0, 150 mM ionic strength, before (— : Eox) and after the addition of 1.0 (· · · · ·) and 2.0 molar equivalents of NADH (---) and after the addition of 4.0 mM NAD⁺ (- · - · -) to 2 molar equivalents of NADH reduced enzyme. Spectra shown were recorded when changes were complete.

oxidized enzyme is very similar to those reported for lipoamide dehydrogenases from other sources. Addition of one equivalent of NADH yields a spectrum resembling that reported for the pig heart enzyme [12]. The relatively high absorbance at 530 nm and the low absorbance around 700 nm demonstrate that the reducing equivalents mainly reside on the disulfide, characteristic for the 2-electron reduced enzyme (EH₂). Full reduction of the enzyme to the four-electron reduced state [EH₄] can not be accomplished by NADH as also reported for the pig heart enzyme [12]. This suggests that the redox potentials of the EH₂/EH₄ couples of both enzymes are very alike and more negative than those reported for lipoamide dehydrogenase from *A. vinelandii* and *E. coli* [10, 13]. This is also indicated by kinetic studies: in the forward reaction, at pH 8.0, no significant inhibition by NADH is observed.

Upon addition of a large excess of NAD⁺ to stoichiometric NADH-reduced enzyme, a species is formed exhibiting maximal charge-transfer absorbance at 650-700 nm (Fig. 1). A similar species was reported for pig heart enzyme [12]. From work on *A. vinelandii* mutated lipoamide dehydrogenase [8] it is concluded that this is a species with NAD⁺ bound, the flavin oxidized and with the disulfide reduced.

Conformational stability. Fig. 2 shows the thermostability of lipoamide dehydrogenase from *P. fluorescens* in the absence and presence of reducing agents. The oxidized enzyme is highly thermostable yielding a midpoint temperature of thermal

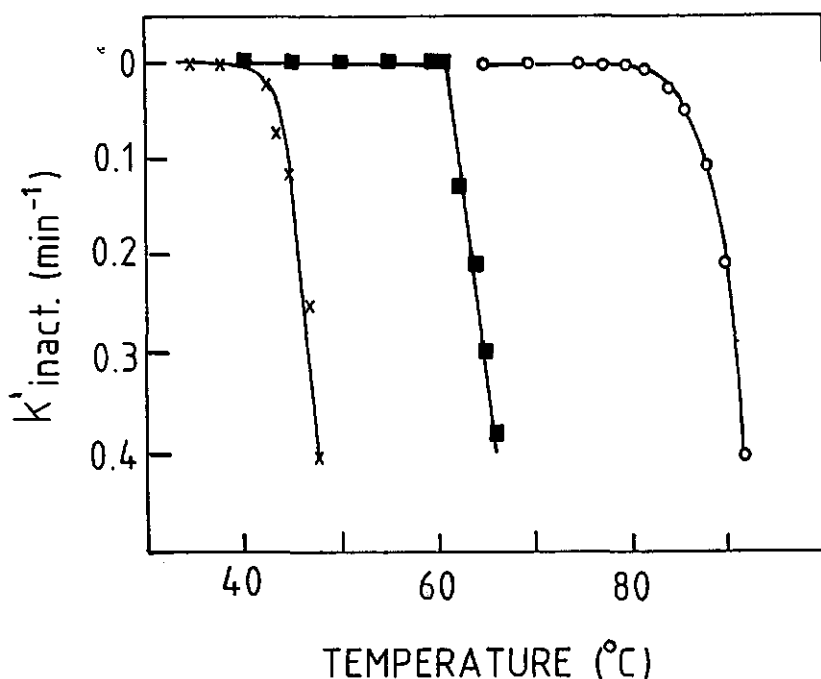


Fig 2. Thermostability of *Pseudomonas fluorescens* lipamide dehydrogenase in the absence and presence of reducing agents. The apparent first-order rate constant for enzyme inactivation is plotted as a function of the incubation temperature. 2.0 μ M enzyme was incubated at different temperatures. For other details see Materials and Methods. Oxidized enzymes (○), in the presence of 1 mM lip(SH)₂ (■), in the presence of 1 mM dithionite (x).

denaturation (t_m) of 86 °C. This value is 6°C higher than that reported for the *A. vinelandii* enzyme [11]. Upon reduction with excess dithionite or NADH, thermostability strongly decreases, yielding apparent t_m values (44 and 47 °C, respectively) in the same range as reported for the monomeric apoenzyme [5]. Reduction with excess lip(SH)₂ gives rise to a very sharp break in the melting curve at 61 °C (Fig. 2). This sharp break is also observed in similar studies with *A. vinelandii* enzyme [11] and ascribed to over-reduction to the EH₄ state at elevated temperatures.

The oxidized forms of lipamide dehydrogenase from pig heart and *A. vinelandii* are highly resistant towards unfolding by urea [11, 14]. Unfolding of these enzymes by urea is induced upon reduction by NADH.

Inactivation of the *P. fluorescens* enzyme in 7 M urea, pH 7.0, follows first-order kinetics. As can be concluded from Table 1, in urea, both oxidized and lip(SH)₂-reduced enzyme are very slowly inactivated, whereas rapid inactivation occurs when the enzyme is reduced with dithionite or to some lesser extent, with excess NADH. The

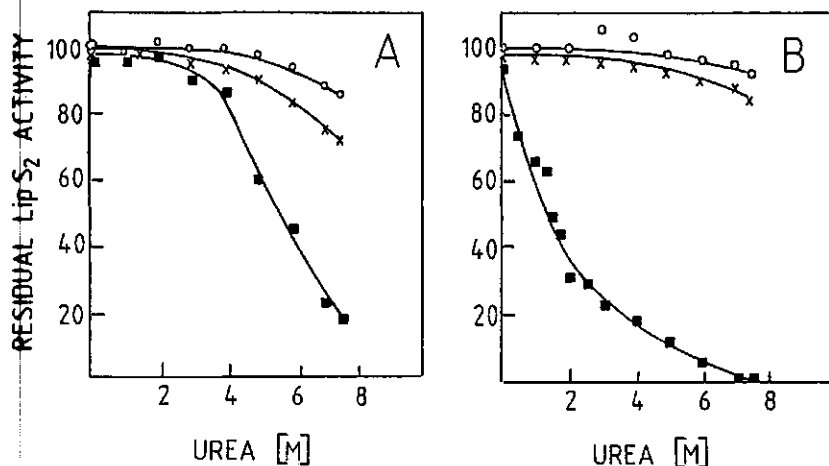


Fig. 3. Inactivation of *Pseudomonas fluorescens* and *Azotobacter vinelandii* lipoamide dehydrogenase by urea either in the absence or presence of reducing agents. 2.0 μ M enzyme was incubated in 100 mM K_2HPO_4 , pH 7.0 and various concentrations of urea at 25 $^{\circ}C$. The residual lipoamide activity after 30 min incubation is plotted against the concentration urea. A, *P. fluorescens* lipoamide dehydrogenase. B, *A. vinelandii* lipoamide dehydrogenase. Oxidized enzymes (o), in the presence of 1 mM lip(SH)₂ (x), in the presence of 1 mM NADH (■).

Reductant	$k'_{inact.} \times 10^3 \text{ min}^{-1}$
none	4.1
lip(SH) ₂	5.9
NADH/NAD ⁺	7.6
NADH	150
dithionite	230

Table 1. Inactivation of *Pseudomonas fluorescens* lipoamide dehydrogenase in urea. The enzyme was incubated at 25 $^{\circ}C$ in 7 M urea, pH 7.0, either in the absence or presence of 1 mM reducing agent (and 1 mM NAD⁺, when indicated).

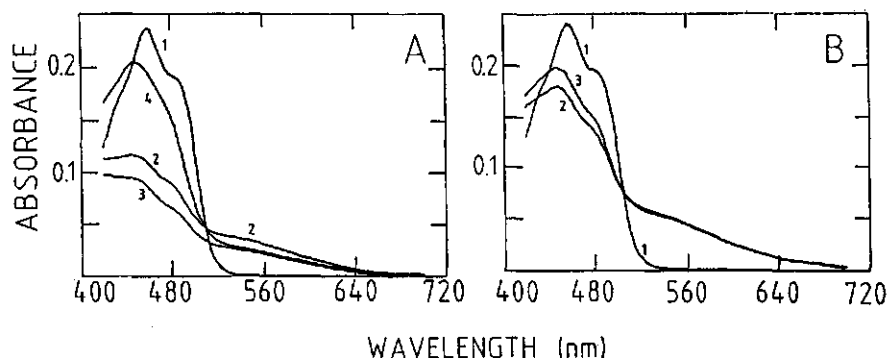


Fig. 4. Absorption spectra of anaerobically NADH-reduced *Pseudomonas fluorescens* lipamide dehydrogenase in the presence of urea. 20 μ M enzyme in 100 mM K_2HPO_4 , pH 7.0, in the presence of 3 M urea was anaerobically reduced with 1 mM NADH at 25 $^{\circ}C$. Spectra were recorded at time intervals as indicated below. After 30 min incubation, air was admitted and spectra were recorded again. (A) Eox (1); 1 min after NADH reduction (2); 20 min after NADH reduction (3); after air-inlet (4). (B) Eox in the presence of 1 mM NAD^+ (1); 20 min after NADH reduction (2); after air-inlet (3).

rates of inactivation are somewhat lower than those reported for *A. vinelandii* enzyme [11]

Fig. 3 A shows the conformational stability of oxidized and reduced enzyme species at various urea concentrations. The oxidized and lip(SH)₂ reduced enzyme are relatively urea-insensitive (cf. Table 1) while the activity of NADH reduced enzyme becomes affected above 4 M urea. The apparent midpoint concentration of urea inactivation (C_m urea) for this species is 5.5 M and much higher than the value observed for the *A. vinelandii* enzyme (C_m urea = 1.5 M, Fig. 3B).

In urea, the shape of the absorption spectrum of the oxidized enzyme remains virtually unchanged with a gradual shift of the absorption maximum from 457 nm (no urea) to 460 nm (7 M urea). Comparable effects were reported for pig heart lipamide dehydrogenase [14]. This indicates that in the oxidized state urea induces a small change in the polarity of the microenvironment of the isoalloxazine ring of the protein bound FAD.

As already mentioned above, in the absence of urea, full reduction to EH_4 by NADH is not observed. Fig. 4 shows the spectral properties of lipamide dehydrogenase from *P. fluorescens* after reduction by excess NADH and in the presence of NAD^+ and 3.0 M urea. In 3 M urea, reduction by excess NADH leads to reduction of the flavin to the same extent as found for Eox, however the 700 nm absorbance is lost (Fig. 4A). This loss of 700 nm absorbance is most likely due to an urea induced change in the polarity of the active site, rather than to loss of NAD^+ binding (see below). After reoxidation by

air inlet, a typical EH_2 spectrum is obtained indicating that under the conditions used, the dimeric structure of the enzyme is retained. Gelfiltration of this particular sample over Bio-gel P-6DG reveals the presence of about 15 % free FAD. For *A. vinelandii* enzyme (C_m urea = 1.5 M), under identical conditions, full reduction to EH_4 occurs and more than 90% of FAD is released after reoxidation (not shown).

In 3 M urea and excess of NAD^+ , over-reduction of the *P. fluorescens* enzyme by NADH is almost completely blocked (Fig. 4B). The absorption spectrum, showing an intense charge transfer band at 530 nm remains virtually unchanged, even after reoxidation. The relatively high extinction at 530 nm might again be due to an urea-induced effect on the polarity of the active site. Under the same conditions, the *A. vinelandii* is only slightly protected from over-reduction by NADH; gelfiltration of the reoxidized *A. vinelandii* sample reveals the presence of about 80% free FAD (not shown). The above results clearly confirm earlier conclusions that over-reduction of lipoamide dehydrogenase to EH_4 promotes subunit dissociation [11].

Discussion

The results described in this Chapter show that, despite their very high degree of sequence homology and structural identity, *P. fluorescens* and *A. vinelandii* lipoamide dehydrogenase differ with respect redox properties. The most striking differences are observed upon reduction with excess NADH. With lipoamide dehydrogenase from *P. fluorescens*, binding of NAD^+ shifts the distribution of two-electron reduced species in favor of the disulfide reduced enzyme, whereas in the *A. vinelandii* enzyme the electrons mainly reside on the flavin. There is thus a clear relation between the redox potential of the couple EH_2/EH_4 and the sensitivity toward urea denaturation: the lower the couple, the lower the sensitivity toward urea denaturation. The higher thermostability of the *P. fluorescens* enzyme when compared to the *A. vinelandii* enzyme, as reflected in all redox states, is ascribed to a higher dimer stability of the *P. fluorescens* enzyme.

Site-specific mutagenesis experiments on the *A. vinelandii* enzyme [4] indicate that small structural changes in the vicinity of the subunit interface may lead to drastic effects on enzyme catalysis. The catalytic properties and conformational stability of the mutated enzymes strongly suggest that the interaction of the C-terminus with the other subunit influences the redox properties of the active site. Recent results on the crystal structure of lipoamide dehydrogenase from *A. vinelandii* indicate that in this enzyme the C-terminus also folds back into the protein. Refinement of the crystal structure of lipoamide dehydrogenase from *P. fluorescens* is therefore of utmost importance. Together with

site-specific mutagenesis experiments, this will yield valuable information on the structural features involved in the regulation of the redox properties of this type of flavoenzymes.

Acknowledgements.

This work was supported in part by the Netherlands Foundation of Chemical Research (S.O.N.) with financial aid from the Netherlands Organization for Scientific Research (N.W.O.).

References

1. Benen, J. A. E., Van Berkel, W. J. H., Van Dongen, W. M. A. M., Müller, F., and De Kok, A. (1989) *J. Gen. Microbiol.* 135, 1787-1797.
2. Mattevi, A., Schierbeek, A. J. and Hol, W. G. J. (1991) *J. Mol. Biol.* 220, 975-994.
3. Mattevi, A., Obmolova, G., Sokatch, J. R., Betzel, C. and Hol, W. J. G. (1991) submitted.
4. Benen, J., Van Berkel, W., Veeger, C. and De Kok, A. (1992) submitted.
5. Van Berkel, W. J. H., Benen, J. A. E. and Snoek, M. C. (1991) *Eur. J. Biochem.* 197, 769-779.
6. Massey, V., Gibson, Q. H. and Veeger, C. (1960) *Biochem. J.* 77, 341-351.
7. Williams, C. H. Jr. (1965) *J. Biol. Chem.* 240, 4793-4800.
8. Benen, J., Van Berkel, W., Dieteren, N., Arscott, D., Williams, C. Jr., Veeger, C. and de Kok, A. (1992) submitted.
9. Wilkinson, K. D. and Williams C. H. Jr. (1981) *J. Biol. Chem.* 256, 2307-2314.
10. Benen, J., Van Berkel, W., Zak, Z., Visser, T., Veeger, C. and De Kok, A. (1991) *Eur. J. Biochem.* 202, 863-872.
11. Berkel van, W. J. H., Regelink, A. G., Beintema, J. J. and De Kok, A. (1991) *Eur. J. Biochem* 202, 1049-1055.
12. Veeger, C and Massey, V. (1963) *Biochim. Biophys. Acta* 67, 679-681.
13. Wilkinson, K. D. and Williams C. H. Jr. (1979) *J. Biol. Chem.* 254, 852-862.
14. Massey, V., Hofmann, T. and Palmer, G. (1962) *J. Biol. Chem.* 237, 3820-3828

General discussion

The work described in this thesis mainly focussed on mechanistic studies on lipoamide dehydrogenase from *Azotobacter vinelandii* as approached by site directed mutagenesis. This enzyme was chosen as a subject of investigation to enhance our knowledge about the pyruvate dehydrogenase complex of which this enzyme is a constituent. For many years this complex, particularly the acetyl transferase core component, has been a major subject of investigation in our laboratory. At the start of the investigations described in this thesis the genes encoding the components of the complex from *Azotobacter vinelandii* were cloned in our laboratory by Westphal and Haanemaayer and initial progress had been made on the elucidation of the crystal structure by Schierbeek from the crystallography group at the Groningen University, headed by Prof. Hol. Refinement studies, ultimately resulting in a resolution of 0.22 nm, were performed by Mattevi. Biochemical knowledge of this particular enzyme was however scarce.

In the sixties and seventies considerable progress was made on the elucidation of the reaction mechanisms of the pig heart and *E. coli* lipoamide dehydrogenases by careful kinetic and spectral studies and by means of chemical modification. The enzymes were found to contain a flavin and a redox active disulfide bridge. The two redox active groups allow the distinction of three redox states: the oxidized enzyme (Eox), the 2-electron reduced enzyme (EH₂) and the 4 electron reduced enzyme (EH₄). Only Eox and EH₂ are kinetically important, EH₄ constitutes an inactive species. The kinetical patterns of these enzymes in the forward direction, reoxidation of dihydrolipoamide (lip(SH)₂) with NAD⁺ as electron acceptor, were in general compatible with a ping pong mechanism. A major finding of these studies was the discovery of a base in the active site, later identified as a histidine. The postulated function of the histidine is the activation of the substrate dihydrolipoamide (lip(SH)₂) by proton abstraction resulting in facilitated nucleophilic attack on the disulfide bridge. This base also appeared to be involved in the distribution of electronic species at the, catalytically important, EH₂ level of these enzymes.

In order to understand the role of the histidine in catalysis, we replaced this histidine (His450) by several other residues: phenylalanine, serine and tyrosine. Apart from these, for catalysis seemingly 'drastic' mutations, additional mutated enzymes were prepared in which supposedly either the position of the histidine was altered (enzyme Pro451->Ala) or its chemical properties (enzymes Glu455->Asp and Glu455->Gln), as judged from the crystal structure of the highly homologous glutathione reductase. In glutathione reductase Pro468 (the equivalent of Pro451) is in the *cis*-conformation and directs His467 (the equivalent of His450) toward the active site

disulfide bridge and Glu472 (the equivalent of Glu455) forms a short strong hydrogen bond with His450 and thus might modulate its pK_a . These features were later shown to be identical in the structure of *A. vinelandii* lipoamide dehydrogenase.

A detailed analysis of the spectral and kinetic properties of the wild-type and mutated enzymes is described in Chapters 3 and 4 respectively.

The mutations all affect turnover, which will be discussed below. They also considerably affect the visible absorbance and fluorescence properties especially at the EH_2 level. Remarkable is the strong increase of absorbance attributed to the thiolate to FAD charge-transfer complex at high pH (530 nm absorption) in all mutated enzymes when compared to wild-type enzyme (enzyme Pro451->Ala only transiently forms the EH_2 species).

An increase in charge-transfer absorbance can be the result of several factors or a combination thereof:

- 1) a smaller distance between the charge-donor (thiolate) and charge-acceptor (FAD),
- 2) a lower dielectrical constant,
- 3) an increase of the difference in redox potential between the charge-donor and charge-acceptor and
- 4) an increase in the concentration of donor or acceptor.

In case of factors 1-3, the charge-transfer absorbance not only increases, but also the maximum shifts to longer wavelength. In case of factor 4, the maximum remains unchanged. For the Glu455 mutated enzymes and enzyme His450->Ser no significant shift of the thiolate to FAD charge-transfer absorbance maximum is observed, whereas in enzymes His450->Phe and -Tyr a clear red-shift occurred. It is therefore concluded that the increased charge-transfer absorbance in the mutated enzymes is primarily due to an increased concentration of thiolate as a result of a higher degree of deprotonation of the charge-transfer thiol relative to the wild type enzyme (FAD is constant) due to pK_a changes of the participating groups, with an additional micropolarity effect in the enzymes His450->Phe and -Tyr. Based on this conclusion the pH profiles of the thiolate to FAD charge-transfer absorbance as presented in chapter 2, Fig. 4 were interpreted.

The model for the distribution of electronic species developed for *E. coli* and pig heart EH_2 , takes only two deprotonation steps into account, the histidine and the charge-transfer thiol. The interchange thiol remains protonated at high pH. This model predicts that upon removal of the active site base the pH dependence of the thiolate to FAD charge-transfer absorbance would mainly obey one pK_a , of the charge-transfer thiol. Our results with the His450 mutated enzymes however clearly show that the pH dependence of the thiolate to FAD charge-transfer is governed by two pK_a values.

In view of the pig heart model the low pK_a , equal in all three His450 mutated enzymes, must be assigned to the charge-transfer thiol. The high pK_a must then be assigned to at least one group that

- 1) influences the charge-transfer absorbance (for more than 55% in enzyme His450->Phe to more than 75% in enzyme His450->Ser),
- 2) whose pK_a is affected by polarity of the side-chain engineered and
- 3) accounts for the largest drop in fluorescence despite the fact that at the pK_a of this group at least 95 % of the charge-transfer thiol is deprotonated.

There is however no direct structural evidence for a residue that could fulfill all three requirements. Therefore we have developed a new model for the *A. vinelandii* lipoamide dehydrogenase in which the interchange thiol as a third deprotonatable group participates.

In this model the low pK_a found for the His450 mutated enzymes is assigned to the interchange thiol with the charge-transfer absorbance as a result of tautomerization with the charge-transfer thiol. The high pK_a , associated with the 3 marked effects mentioned above, is logically assigned to the charge-transfer thiol (in effect, both prototropic tautomers). In the wild-type enzyme, where three pK_a values were found, the low pK_a is assigned to the interchange thiol, the intermediate pK_a to the charge-transfer thiol and the high pK_a to the protonated histidine. For the Glu455 mutated enzymes it is concluded that, at low pH, co-titration of all three residues occurs due to a lowered pK_a of His450 and loss of the orienting effect of Glu455 on the histidine toward the interchange thiolate. Despite the fact that the microscopic pK_a model presented explains the observed macroscopic pK_a values it should be kept in mind that the assignments made are still disputable and other residues might contribute as well. Therefore the model should be regarded as a working hypothesis.

The steady state kinetics of the forward reaction reaction of the wild-type enzyme is compatible with a ping-pong bi bi mechanism. Previous studies in our laboratory had shown that this enzyme functions according to a ternary complex mechanism. At present we cannot satisfactorily explain this discrepancy. The Glu455- and Tyr16- (Chapter 4) mutated enzymes and enzyme His450->Ser also function according to a ping pong bi bi mechanism indicating that this mechanism is indeed correct. It should be noted that the steady state kinetics of the Glu455- and Tyr16 mutated enzymes was studied with another electron acceptor, *in casu*, 3-acetylpyridine dinucleotide (APAD⁺). This was done because these enzymes show strong inhibition by the product NADH.

The steady-state kinetics of the His450 mutated enzymes clearly shows the important function of this histidine as a catalyst. Enzymes His450->Phe and His450->Tyr appear to be almost inactive in both directions. Enzyme His450->Ser is

still, though minimally, active: V at the pH optimum being 0.5% of wild-type activity in the physiological reaction. Rapid reaction kinetics shows that for these enzymes the reductive half reaction using lip(SH)_2 is rate limiting and extremely slow when compared to the wild type enzyme. This important function of the histidine was also reported in the course of our investigations from site directed mutagenesis studies of *E. coli* lipoamide dehydrogenase and *E. coli* glutathione reductase. Enzyme Pro451->Ala is essentially inactive in both directions and it is concluded that the loss of activity is due to over-reduction to EH_4 by lip(SH)_2 and NADH.

It is shown for the Glu455 mutated enzymes that the activity in the forward reaction is considerably lower than for the wild-type enzyme. Rapid reaction studies with lip(SH)_2 showed that the rate of the reductive reaction of enzyme Glu455->Asp was halved and for enzyme Glu455->Gln this reaction was decreased approximately 10 fold. This indicates that in the substrate bound enzyme Glu455->Asp the histidine still can act as a base. This function is clearly hampered in substrate bound enzyme Glu455->Gln.

The reduction of the flavin of the wild-type enzyme and His450- and Glu455 mutated enzymes by NADH proceeds very fast. In the wild-type enzyme this reduction is followed by a fast reduction of the disulfide with concomitant reoxidation of the FAD. In the mutated enzymes this intramolecular transfer of a hydride equivalent is severely affected. Also the transfer of a hydride equivalent from the dithiol to the FAD, effected by NAD^+ , is severely diminished. These properties of the mutated enzymes have enabled the spectral identification of species 4 and 6 of the reaction intermediates as presented in Scheme 1 in chapter 3. Species 5 in this scheme is the so-called flavin C4a adduct species with a covalent bond between the charge-transfer thiolate and C4a of the flavin. We have obtained no spectral evidence for the participation of the proposed flavin C4a adduct species during studies of the transfer of a hydride equivalent in the mutated enzymes from species 4 to 6 or *vice versa*.

This questions the existence of the C4a adduct species as a catalytic relevant intermediate. The effect of the mutations on catalysis in chapter 3 are interpreted in the light of the currently 'established' involvement of this C4a adduct species. For the reverse direction of transfer of a hydride equivalent (from species 6 to 4) it is concluded that this intermediate is probably not involved and direct hydride transfer occurs from the reduced flavin to the disulfide. Similarly, as a result of microscopic reversibility, in the direction 4 to 6 it can be concluded that hydride transfer can account for the lack of identification of the C4a adduct species.

One might argue that the mutations alter the mechanism of transfer of a hydride equivalent from participation of the C4a adduct species to direct hydride transfer or a concerted reaction. Before doing this one must consider the following. The flavin C4a

adduct species has until now never been reported in any (mutated) lipoamide dehydrogenase except for pig heart enzyme where the interchange thiol was alkylated. Only in wild type mercuric reductase this species has been observed upon reduction with NADPH at low pH. Other reports on the C4a adduct were with mercuric reductase of which the interchange thiol is replaced by alanine and with thioredoxin reductase of which the flavin was replaced by 1-deaza-FAD. The majority of reports on the C4a adduct species is thus with enzymes that are far from 'healthy'. Interestingly too in this respect is the fact that no C4a adduct formation was reported in monoalkylated glutathione reductase and no reports of this species were made on *E. coli* glutathione reductase or *E. coli* lipoamide dehydrogenase in which the interchange thiol was mutated. Therefore it is proposed here that in wild-type lipoamide dehydrogenase the C4a adduct is not a relevant catalytic intermediate and the electron transfer from disulfide/dithiol to FAD/FADH⁻ occurs via hydride transfer.

For the Glu455 mutated enzymes strong inhibition by NADH was observed indicating that the redox potential of the EH₂/EH₄ couple was higher than in the wild-type enzyme. Therefore the quantitation of the redox potentials was investigated. These studies were however frustrated as discussed in chapter 3. Nevertheless it could be concluded that the redox potential of the EH₂/EH₄ couple of these enzymes is higher than in the wild-type enzyme. Spectral studies with these enzymes showed that EH₂ generated by reduction by lip(SH)₂ is rather stable and does not result in easy reduction of the FAD (in contrast to the Tyr16 mutated enzymes and enzyme Δ9, cf chapter 4 and below). Addition of AAD⁺ (a non-reducible NAD⁺ analog) to EH₂ of enzyme Glu455->Asp resulted in reduction of the FAD, strongly indicating that binding of a nucleotide increases the redox potential of the FAD relative to that of the disulfide bridge. Similar results were obtained for this enzyme and the wild-type enzyme in a study in which reduction was performed with enzymatically generated NADPH in the presence and absence of AAD⁺. For both the wild type enzyme and the Glu455 mutated enzyme the binding of a nucleotide thus increases the redox potential of the FAD. Why is it then that in enzyme Glu455->Asp strong inhibition is observed and not in wild-type enzyme?. A possible explanation is that the redox potential of the FAD-nucleotide complex is higher in enzyme Glu455->Asp than it is in the wild-type enzyme. This is supported by two lines of evidence. First, the addition of AAD⁺ to EH₂ of both enzymes results in reduction of FAD only in enzyme Glu455->Asp and second, transhydrogenation from NADH to thio-NAD⁺ was only observed with wild-type enzyme. Apparently, the redox potential of APAD⁺ is high enough to accept electrons from the reduced FAD in enzyme Glu455->Asp. Initially it was thought that the His450, which is influenced by Glu455 is directly involved in modulation of the redox potential

of the FAD. However, the results obtained with the Tyr16 mutated enzymes and C-terminal deletion mutants described in Chapter 4, show that the increased redox potential of the EH_2/EH_4 couple of these mutated enzymes is directly related to a diminished subunit interaction. Evidence is obtained that this may be the case for the Glu455 mutated enzymes too in addition to a possible role for His450.

The 10 C-terminal residues are not visible in the crystal structure of lipoamide dehydrogenase from *A. vinelandii*, but can be observed in the crystal structures of lipoamide dehydrogenase from *Pseudomonas putida* and *Pseudomonas fluorescens*. In these structures, the C-terminus folds back towards the active site and is involved in interactions with the other subunit.

The function of the C-terminus of lipoamide dehydrogenase from *Azotobacter vinelandii* was studied by deletion of 5, 9 and 14 residues, respectively. Tyrosine 16, conserved in all lipoamide dehydrogenases sequenced thus far, and shown from the other structures to be likely involved in subunit interaction, was replaced by phenylalanine and serine.

Deletion of the last 5 residues does not influence the catalytic properties and conformational stability (thermo-inactivation and unfolding by guanidinium hydrochloride). Removal of 9 residues results in an enzyme (enzyme $\Delta 9$) showing decreased conformational stability and high sensitivity toward inhibition by NADH. These features are even more pronounced after deletion of 14 residues.

Mutation of Tyr16 also results in a strongly increased sensitivity toward inhibition by NADH and results in slow translocation of reducing equivalents from the dithiol to the FAD demonstrating that EH_2 is not 'stable'. Similar conclusions can be drawn for enzyme $\Delta 9$. The conformational stability of both Tyr16 mutated enzymes is comparable to enzyme $\Delta 9$.

The results strongly indicate that a hydrogen bridge between tyrosine of one subunit (Tyr16 in the *A. vinelandii* sequence) and histidine of the other subunit (His470 in the *A. vinelandii* sequence), also exists in the *A. vinelandii* enzyme. In the $\Delta 9$ and $\Delta 14$ enzymes this interaction is missing. It is concluded that this interaction mediates the redox properties of the FAD via the conformation of the C-terminus comprising residues 450-470.

Chapter 5 describes the molecular cloning and sequence determination of lipoamide dehydrogenase from *P. fluorescens*. The derived amino acid sequence shows a very high degree of sequence identity in comparison to the *A. vinelandii* sequence especially in the region of residues which constitute the active site.

Despite the high sequence homology and high degree of structural identity differences between the *A. vinelandii* and *P. fluorescens* lipoamide dehydrogenases

are manifest as presented in Chapter 6. The spectral differences are in accord with the conclusion that the redox potential of the couple EH_2/EH_4 in the nucleotide bound enzyme is lower in the *P. fluorescens* enzyme. Due to the fact that NADH does not fully reduce the enzyme to the EH_4 level (the redox potential of the FAD is lower in the *P. fluorescens* enzyme) the conformational stability of NADH reduced enzyme is much higher than found for *A. vinelandii* enzyme. The temperature stability of the *P. fluorescens* enzyme is higher than the *A. vinelandii* enzyme and therefore strongly suggests a general relation between the dimer stability and the redox properties. A relation which may also extend to other lipoamide dehydrogenases.

Samenvatting

Levende organismen, van bacteriën tot complexe meercelligen, vertonen twee kenmerkende eigenschappen: ze planten zich voort en ze vertonen al dan niet waarneembare activiteit. Teneinde deze eigenschappen tot uiting te brengen bedient een organisme zich van allerlei organische verbindingen die variëren in complexiteit. Tot de meest complexe verbindingen horen het DNA en de eiwitten. Het DNA bevat erfelijke informatie die in pakketjes, genaamd genen, lineair gerangschikt zijn in het DNA. Voor het merendeel van de genen geldt dat de informatie die erin besloten ligt, codeert voor een eiwit. Een eiwit bestaat uit een keten van relatief eenvoudige bouwstenen, de aminozuren, waarvan in het algemeen 20 verschillende gebruikt worden om een eiwit samen te stellen. Met deze 20 aminozuren is in een lange keten, in principe, een oneindig aantal variaties te maken. Welke aminozuren op welke plaats door de cellulaire eiwit-fabriekjes genaamd ribosomen in de groeiende eiwitketen ingebouwd moeten worden, ligt besloten in het gen coderend voor dat eiwit. De aminozuursketen, het eiwit, is op een voor ieder eiwit karakteristieke wijze tot een kluwen samengevouwen.

Eiwitten kunnen grofweg verdeeld worden in twee categorieën. Tot de eerste categorie behoren de enzymen en tot de tweede categorie worden hier alle andere eiwitten gerekend. Deze tweede categorie omvat onder andere signaleiwitten en structurele eiwitten. De enzymen zorgen ervoor dat reacties die onder normale omstandigheden niet of nauwelijks plaatsvinden, snel en efficiënt verlopen. Ze worden hierbij niet zelf omgezet. Met andere woorden: enzymen zijn katalysatoren. Voor elke natuurlijke organische verbinding is er zowel een synthese route als een afbraak route via enzymen.

Een voorbeeld. Suiker in droge vorm is stabiel aan de lucht en dus reageert de suiker niet met de aanwezige zuurstof. In steriel water is suiker eveneens stabiel. Suiker is, zoals bekend, een prima energie leverancier voor in levende organismen. De energie die opgeslagen zit in de opgeloste suiker wordt in de levende cel vrij gemaakt door de suiker met behulp van enzymen in verschillende stappen af te breken. In zuurstof afhankelijke organismen reageren deze afbraakproducten vervolgens met zuurstof tot de uiteindelijke bouwstenen van de suiker, water en kooldioxide. Deze eindproducten kunnen dan weer door planten met behulp van enzymen weer worden omgezet in suiker onder invloed van zonlicht, dat voor de noodzakelijke energie zorgt.

Enzymen zijn zeer specifiek voor wat betreft hun substra(a)t(en), zoals een sleutel past op een slot. De reactie vindt plaats in het zogenaamde 'actieve centrum'. Naast enzymen die reacties met één substraat katalyseren, zijn er ook enzymen die twee of

meerdere substraten met elkaar laten reageren. De volgorde van binding van de substraten aan het enzym is bepalend voor het mechanisme volgens welk het enzym werkt. Zo wordt er bijvoorbeeld onderscheid gemaakt tussen een geordend en een groeps-overdracht mechanisme (ook wel ping-pong mechanisme genoemd). In het geordend mechanisme binden eerst de twee substraten, steeds in vaste volgorde, waarna de reactie plaatsvindt en beide producten vervolgens loslaten. In geval van een groeps-overdracht mechanisme bindt altijd eerst één substraat waarbij een groep van het substraat overgedragen wordt op het enzym en het veranderde substraat, nu product genaamd, loslaat. Vervolgens bindt het tweede substraat. Hierop wordt dan de tijdelijk op het enzym geparkeerde groep overgedragen, gevolgd door loslaten van het tweede product. De enzym gekatalyseerde reacties zijn in het algemeen omkeerbaar, dus uitgaande van de producten is het vaak mogelijk de oorspronkelijke substraten terug te vormen. Dit hangt af van de relatieve concentraties van de substraten en producten en van de 'kinetische karakteristieken' van het enzym

In beginsel is het zo dat als beide substraten in, t. o. v. het enzym, hoge concentraties aanwezig zijn en er geen producten aanwezig zijn bij de start van de reactie, na een korte aanloop fase (meestal minder dan een seconde) gedurende langere tijd een lineair verband is in de tijd tussen de gebruikte substraat concentraties en de waargenomen snelheid van productvorming. Dit wordt dan de snelheid bij een gegeven substraatconcentratie genoemd. Naarmate een substraatconcentratie hoger wordt loopt de snelheid op. Dit blijft echter niet eeuwig doorgaan. Op een gegeven moment is het zo dat een toename in de substraatconcentratie niet meer resulteert in een toename van de snelheid. Dit heet de maximale snelheid (V_{max}) en is kenmerkend voor ieder enzym. Door de afhankelijkheid van de snelheid van het enzym van beide substraten nauwkeurig te bestuderen is het mogelijk inzicht te krijgen of er bijvoorbeeld sprake is van een geordend mechanisme of van een groeps-overdracht mechanisme. Omdat er onder condities gewerkt wordt waarbij de snelheid in principe onveranderlijk is in de tijd bij een gegeven combinatie van substraten, is noodzakelijkerwijs de snelheid van binding van de substraten en snelheid van loslaten van de producten gelijk. Met andere woorden de concentraties van vrij enzym, substraat gebonden enzym en product gebonden enzym zijn constant in de tijd en dus 'statisch'. Deze toestand wordt in Engelse bewoordingen 'steady state' genoemd.

Bestudering van deze steady-state is vergelijkbaar met het beschrijven van de karakteristieken van een auto waarbij gedurende de tests steeds met een andere constante snelheid gereden werd. Deze karakteristieken zullen zeker interessant zijn maar echt leuk wordt het pas als ook de acceleratie van de auto bekeken wordt. Dit geldt evenzeer voor enzymen. De acceleratie fase van de auto is vergelijkbaar met

de aanloop fase tot de steady-state kinetiek van het enzym. Deze fase wordt de 'pre-steady state' fase genoemd. Omdat deze pre-steady state fase slechts zo kort duurt, is het noodzakelijk hiervoor geavanceerde apparatuur te gebruiken. De informatie die uit de nauwkeurige analyse van de pre-steady state fase gehaald wordt, geeft inzicht in de snelheid van binding van ieder van de substraten en producten en maakt het soms mogelijk om tussenstappen in de omzetting van substraat naar product of omgekeerd te identificeren als iedere tussenstap andere meetbare eigenschappen heeft.

Na dit intermezzo terug naar de suiker afbraak. Suikerafbraak door organismen onder zuurstofloze condities leidt tot de vorming van eenvoudige zuren (bv. zuurkool en spierpijn) of alcohol. Hierbij wordt echter maar een klein gedeelte van de in de suiker aanwezige energie benut. In aanwezigheid van zuurstof is het mogelijk tot 600% meer energie uit de suiker te halen door 'verbranding' tot water en kooldioxide. Dit proces is veel complexer dan dat onder zuurstofloze condities en omvat dan ook een geweldige grotere hoeveelheid en variëteit aan enzymen.

Een van de sleutel enzymen in dit proces is het pyruvaat dehydrogenase. Dit enzym is onderdeel van een enzymcomplex bestaande uit drie verschillende enzymen. Het substraat van dit complex, pyruvaat, is de directe voorloper van de producten zoals verkregen onder zuurstofloze suikerafbraak. Het complex neemt dus het substraat voor deze zuurstofloze routes weg. De drie enzymen die deel uitmaken van dit complex zijn het pyruvaat dehydrogenase, het transacetylase en het lipoamide dehydrogenase. Het pyruvaat dehydrogenase splitst kooldioxide af van pyruvaat en draagt het resterende deel van het substraat, een acetylgroep, over op een lipoylgroep van het transacetylase. Het transacetylase koppelt vervolgens de acetylgroep aan Coenzym A, dat afgeleid is van het vitamine panthotheenzuur (uit de groep van de B-vitamines). Het acetyl-Coenzym A is de verbinding die in een complex van reacties wordt omgezet tot water en kooldioxide. Ook is het mogelijk met deze verbinding andere voor het organisme noodzakelijke verbindingen te maken. Nadat het transacetylase het acetyl-Coenzym A heeft afgegeven, resteert een lipoylgroep die niet in de juiste toestand is om opnieuw een acetylgroep te ontvangen. De toestand waarin de lipoylgroep verkeert heet de 'gereduceerde' vorm. De juiste toestand om opnieuw een acetylgroep te ontvangen heet de 'geoxideerde' vorm. Het omzetten van de lipoylgroep van de gereduceerde in de geoxideerde vorm vindt plaats door het lipoamide dehydrogenase. In feite doet het lipoamide dehydrogenase niets anders dan twee elektronen (e^-) van de lipoylgroep afpakken en deze overdragen op NAD^+ (afgeleid van vitamine B1). Teneinde de electro-neutraliteit te handhaven zijn hierbij twee protonen betrokken (H^+). Op de lipoylgroep worden door lipoamide dehydrogenase dus twee -SH groepen (dithiol) omgezet in een -S-S-

groep (disulfide) en ontstaat vrij $\text{NADH} + \text{H}^+$. Dit type van reacties wordt redox reacties genoemd. De reactie van lipoamide dehydrogenase verloopt volgens een groeps-overdracht mechanisme en kan dus als twee deelreacties worden voorgesteld:



In het algemeen bevatten enzymen die redox reacties katalyseren een extra groep zijnde een metaalatoom of prosthetische groep, of beide. Lipoamide dehydrogenase bevat als extra groep een flavine molecuul. Dit flavine is afgeleid van vitamine B2 en heeft in zijn geoxideerde toestand een fel gele kleur. Uit de literatuur is bekend dat lipoamide dehydrogenase naast het flavine nog een tweede redoxactieve groep bevat: een disulfide-brug. Deze brug is analoog met de disulfide-brug van de lipoylgroep en kan dus ook geopend worden. Het verschil met de lipoylgroep zit in het feit dat de twee SH groepen in het enzym afkomstig zijn van de twee aminozuren, cysteïnes, die een dusdanige positie ten op zichte van elkaar hebben dat de brug vorming mogelijk is. De twee redoxactieve groepen, het flavine en de disulfide-brug, zorgen ervoor dat het enzym in principe drie redoxtoestanden kent: de geoxideerde vorm (Eox), de 2-electronen gereduceerde vorm (EH_2) en de 4-electronen gereduceerde vorm (EH_4). Aangetoond is dat voor katalyse alleen de vormen Eox en EH_2 relevant zijn. De vorming van EH_4 bleek niet productief. De twee electronen die in de katalyse betrokken zijn gaan over in paren. Eerst wordt de disulfide-brug gereduceerd en vervolgens worden de electronen gezamenlijk overgedragen op het flavine. Voor bestudering van het gezuiverde enzym wordt als substraat gebruik gemaakt van gereduceerd lipoamide (lip(SH)_2) in plaats van de lipoylgroep van het transacetylase.

Het feit dat de twee electronen overgaan in paren resulteert in een volledig gereduceerd flavine. Dit gereduceerde flavine is kleurloos. Dus zou men slechts één kleurverandering in het enzym verwachten, van geel naar kleurloos. Reductie van het enzym zoals geïsoleerd uit varkenshart tot het EH_2 niveau gaf echter duidelijk de vorming van een rood-gekleurd enzym te zien. Aanvankelijk werd dit geïnterpreteerd als een 1-electron gereduceerd flavine (dat ook rood is van kleur). Later bleek dat deze rode kleur het gevolg is van een zogenaamd ladings-overdracht complex (charge-transfer complex) tussen het flavine en een gedeprotoneerde SH groep (een thiolaat ion: S^-). Dit charge-transfer complex bestaat alleen als er licht op valt, m. a. w. het is een aangeslagen toestand. In het donker is er weliswaar een soort basale interactie tussen het thiolaat en het flavine, doch er vindt geen ladingsoverdracht

plaats. In de EH_2 -toestand zitten de electronen dus hoofdzakelijk op de gereduceerde disulfide.

Naast de vorming van een thioaat-flavine charge-transfer complex bleek ook de vorming van een gereduceerd flavine- NAD^+ complex op te treden. Dit uit zich door een groen tot grijs/blauwe kleur van het enzym. De verschillende kleur veranderingen (spectrale vormen) van het enzym in de verschillende toestanden heeft het mogelijk gemaakt in de pre-steady state fase een aantal reactie-tussenstappen te identificeren.

Nauwkeurige analyse van kinetische studies en de spectrale vormen had ertoe geleid dat er een base werd voorgesteld in het actieve centrum van het enzym. De functie van die base is het abstraheren van een proton van het substraat $\text{lip}(\text{SH})_2$ met als gevolg dat het gevormde thiolate gemakkelijker op de disulfide-brug van het enzym kan aanvallen. Deze base bleek een histidine te zijn. Dit is een aminozuur met een zijketen die een proton kan opnemen of afstaan bij een ongeveer neutrale pH. De pH waarde waarbij 50 % van de verbinding een proton heeft afgestaan noemt men per definitie de pK_a . De pK_a waarde van de histidine is niet onveranderlijk maar is afhankelijk van de omgeving waarin de histidine zich bevindt. Zo zal de aanwezigheid van een negatieve lading ervoor zorgen dat de pK_a omhoog gaat, dus zal de histidine minder makkelijk een proton afstaan. Omdat deze histidine zich in het actieve centrum bevindt, dicht bij de disulfide-brug kan er een proton worden opgenomen dat eigenlijk bij één van de door-reductie-onstane thiolen hoort. Dat dit gebeurt, blijkt onder andere door de charge-transfer absorptie die de rode kleur tot gevolg heeft. Veranderingen in het enzym die de pK_a van deze histidine veranderen zullen dus ook een effect hebben op de rode kleur. Daarnaast zullen deze veranderingen effect hebben op de katalytische activiteit van het enzym daar de histidine hierbij betrokken is.

Onlangs is de 3-dimensionale structuur van het lipoamide dehydrogenase uit *Azotobacter vinelandii* opgehelderd. Uit deze structuur blijkt dat het enzym uit twee identieke subeenheden bestaat. Per enzym molecuul zijn twee actieve centra aanwezig. Ieder actief centrum blijkt opgebouwd uit aminozuren die deel uitmaken van beide subeenheden. Zo behoort de redoxactieve disulfide-brug bij de ene subeenheid en de histidine bij de andere subeenheid. Het flavine zit als het ware tussen beide subeenheden in, naast de disulfide-brug en de histidine. Vlak bij de histidine blijkt nog een glutamaat te zitten. Dit aminozuur is negatief geladen en kan dus van invloed zijn op de eigenschappen van de histidine. Omdat het actieve centrum tussen beide subeenheden gelegen is, mag verwacht worden dat de stabiliteit van de subeenheid-interactie van belang is voor de katalyse.

Met de hierboven geschetste structurele en de biochemische kennis gewapend werd besloten na te gaan wat er gebeurt met het enzym als de histidine vervangen

zou worden door een aminozuur met andere eigenschappen. Daarnaast werd er ook gekeken naar het effect van vervanging van de glutamaat naast de histidine. De achterliggende gedachte hierbij is om meer inzicht te krijgen in het reactiemechanisme van lipoamide dehydrogenase. De vervanging van de aminozuren is heel eenvoudig te bewerkstelligen door de DNA-code voor het enzym iets te veranderen. De resultaten en ideeën, die bestudering van deze veranderde enzymen heeft opgeleverd, worden beschreven in hoofdstuk 2 en 3 van dit proefschrift.

In hoofdstuk 2 worden de spectrale eigenschappen van de veranderde enzymen beschreven. De nadruk is daarbij gelegd op de bestudering van de spectrale eigenschappen van de katalytisch belangrijke EH_2 toestand (zie reactie vergelijkingen boven) met name de rode kleur die een maat is voor de graad van protonering van de thiolaat die het dichtst bij het flavine zit (de charge-transfer thiolaat). De pH-afhankelijkheid van de rode kleur van de veranderde enzymen bleek niet te beschrijven met een model, gebaseerd op twee pK_a -waarden: de histidine en de charge-transfer thiol, zoals voorgesteld voor andere lipoamide dehydrogenases. Daarom werd een nieuw model voorgesteld dat uitgaat van drie pK_a -waarden. Nieuw aan dit model is niet alleen de toevoeging van een extra pK_a -waarde maar bovendien laat dit model deprotonering van de andere thiol (de 'interchange-thiol') toe en gaat er zelfs van uit dat deze thiol als eerste deprotoneert. Dit laatste is gebaseerd op resultaten verkregen met enzymen waarin de histidine is vervangen door serine, tyrosine of phenylalanine. De enzymen waarin de glutamaat vervangen werd door glutamine of aspartaat, gaven een beeld te zien dat sterk afweek van het normale enzym. De resultaten zijn evenwel nog steeds verklaarbaar met het model, doch met het verschil dat de drie pK_a -waarden zo dicht bij elkaar liggen dat ze in feite als één pK_a gemeten worden. Deze resultaten geven duidelijk aan dat de pK_a van de histidine door de glutamaat bepaald wordt.

In hoofdstuk 3 wordt het effect van de veranderingen in de enzymen op de katalyse beschreven. Alle veranderde enzymen geven verlaagde activiteit te zien. Dit is het sterkst bij de enzymen waarbij de histidine vervangen is. Hierbij is zowel de eerste als de tweede deelreactie sterk vertraagd. De oorzaak van de trage eerste deelreactie ligt in het feit dat de histidine niet meer aanwezig is en zodoende geen proton meer van het substraat kan afpakken. De omgekeerde reactie blijkt ook heel sterk vertraagd. De voornaamste oorzaak hiervan is dezelfde als die in de voorwaartse richting: de overgang van de elektronen en een proton van de gereduceerde disulfide-brug naar het flavine of omgekeerd is zeer sterk vertraagd.

De enzymen waarin de glutamaat werd vervangen werden zeer sterk geremd door het product NADH. Dit is zeer waarschijnlijk toe te schrijven aan de vorming van de inactieve EH_4 vorm. Met een aangepast substraat, i. p. v. NAD^+ , bleek wel activiteit te

meten maar deze was sterk verminderd in vergelijking met het normale enzym. Analyse van de deelreacties leerde dat niet zo zeer de eerste deelreactie hiervoor verantwoordelijk is maar ook weer de overgang van de electronen en een proton van de gereduceerde disulfide naar het flavine.

De trage overgang van de electronen en een proton hebben het mogelijk gemaakt twee reactie-intermediären te identificeren. Een reactie-intermediair dat in de literatuur was voorgesteld en dat in principe geïdentificeerd had kunnen moeten worden, werd niet waargenomen. Dit duidt erop dat het in de literatuur voorgestelde intermediair mogelijk niet voorkomt.

In hoofdstuk 4 is een onderzoek naar het effect van de subeenheid interactie op de katalyse beschreven. Hierbij is met name gekeken naar de invloed van de verwijdering van enkele aminozuren aan de staart (C-terminus) van het enzym. Deze aminozuren waren in de structuur niet te zien en leken ogenschijnlijk overbodig. Ook werd er een aminozuur veranderd van de ene subeenheid dat mogelijk een interactie met de staart van de andere subeenheid heeft. De resultaten geven zeer duidelijk aan dat de staart van de subeenheid en de wederzijdse subeenheid-interactie een sterk effect hebben op de katalyse; in het bijzonder bepalend zijn voor de mate waarin het enzym geremd wordt door het product NADH.

In hoofdstuk 5 wordt de opheldering van de DNA code van het gen voor lipoamide dehydrogenase van *Pseudomonas fluorescens* beschreven. De aminozuren van dit enzym blijken voor 84 % identiek aan dat van *Azotobacter vinelandii*. Op grond hiervan zou men geneigd zijn dat deze enzymen veel overeenkomst zouden moeten vertonen.

In hoofdstuk 6 zijn experimenten beschreven waaruit blijkt dat dit niet zo hoeft te zijn. Er is een aanzienlijk verschil tussen deze enzymen wat betreft de neiging tot de vorming van de inactieve EH_4 vorm. Het enzym uit *P. fluorescens* blijkt veel sterker bestand tegen de door-reductie naar deze EH_4 vorm. Er zijn aanwijzingen dat dit mogelijk verband houdt met de stabiliteit van het enzym: de subeenheid interactie.

Curriculum vitae

Jacques Alex Erwin Benen werd geboren op 6 november 1959 te Nuth. In 1978 behaalde hij het diploma Atheneum B aan het St. Janscollege te Hoensbroek. In datzelfde jaar werd begonnen met de studie biologie aan de Katholieke Universiteit te Nijmegen. Het kandidaatsexamen werd in 1981 behaald. De doctoraalfase werd in september 1985 afgesloten en omvatte de hoofdvakken moleculaire biologie (Prof. Dr. J. G. G. Schoenmakers) en microbiologie (Prof. Dr. G. D. Vogels) en het bijvak dierfysiologie (Prof. Dr. S. E. Wendelaar-Bonga). In 1981 werd het diploma stralingsdeskundige op het C-niveau behaald.

Van 1 augustus 1986 tot 31 maart 1991 was hij als promovendus verbonden aan de afdeling Biochemie van de Landbouwniversiteit te Wageningen. Tot oktober 1987 is hij werkzaam geweest met de klonering van het gen coderend voor para-hydroxybenzoaat hydroxylase van *Pseudomonas fluorescens*. Vanaf november 1987 tot maart 1991 werden de werkzaamheden verricht die hebben geresulteerd in dit proefschrift. Resultaten uit hoofdstuk 2, 3 en 4 werden gepresenteerd op het 'Tenth International Symposium on Flavins and Flavoproteins' gehouden van 15 tot 20 juli 1990 te Como, Italië. In januari 1991 werd gedurende drie weken een werkbezoek gebracht aan de afdeling Biological Chemistry van de University of Michigan, Ann Arbor, Michigan, USA bij Prof. Dr. C. H. Williams Jr.

List of publications

- 1) Benen, J.A.E., van Berkel, W.J.H., van Dongen, W.M.A.M., Müller, F. and de Kok, A. (1989). "Molecular cloning and sequence determination of the *lpd*-gene encoding lipoamide dehydrogenase from *Pseudomonas fluorescens*." *J. Gen. Microbiol.* 135, 1787-1797.
- 2) Westphal, A.H., Eschrich, K., van Dongen, W.M.A.M., Benen, J.A.E., de Kok, A. and van Berkel, W.J.H. (1990). "Site-directed mutagenesis of *para*-hydroxy benzoate hydroxylase from *Pseudomonas fluorescens*." in *Flavins and Flavoproteins 1990* (Curti, B., Ronchi, S. and Zanetti, G. eds.) W. de Gruyter and Co. Berlin-New York, pp. 231-234.
- 3) Benen, J.A.E., van Berkel, W.J.H. and de Kok, A. (1990). "Site-directed mutagenesis studies on lipoamide dehydrogenase from *Azotobacter vinelandii*." in *Flavins and Flavoproteins 1990* (Curti, B., Ronchi, S. and Zanetti, G. eds.) W. de Gruyter and Co. Berlin-New York, pp. 557-564.

- 4) Benen, J.A.E., Dieteren, N.A.H.M., van Berkel, W.J.H. and de Kok, A. (1990). "Lipoamide dehydrogenase from *Azotobacter vinelandii* - kinetic studies on wild type and mutated enzymes." in *Flavins and Flavoproteins 1990* (Curti, B., Ronchi, S. and Zanetti, G. eds.) W. de Gruyter and Co. Berlin-New York, pp. 565-568.
- 5) Schulze, E., Benen, J.A.E., Westphal, A.H., van Berkel, W.J.H. and de Kok, A. (1990). "Binding studies of the dihydrolipoamide dehydrogenase component (E3) in the pyruvate dehydrogenase complex from *Azotobacter vinelandii*." in *Flavins and Flavoproteins 1990* (Curti, B., Ronchi, S. and Zanetti, G. eds.) W. de Gruyter and Co. Berlin-New York, pp. 569-572.
- 6) van Berkel, W.J.H., Benen, J.A.E. and Snoek, M.C. (1991). "On the FAD induced dimerization of apo-lipoamide dehydrogenase from *Azotobacter vinelandii* and *Pseudomonas fluorescens* - Kinetics of reconstitution." *Eur. J. Biochem.* 197, 769-779.
- 7) Schulze, E., Benen, J.A.E., Westphal, A.H. and de Kok, A. (1991). "Interaction of lipoamide dehydrogenase with the dihydrolipoyl transacetylase component of the pyruvate dehydrogenase complex from *Azotobacter vinelandii*." *Eur. J. Biochem.* 200, 29-34.
- 8) Snoep, J.L., Westphal, A.H., Benen, J.A.E., Teixeira de Mattos, M.J., Neyssel, O.M. and de Kok, A. (1991). "Isolation and characterisation of the pyruvate dehydrogenase complex of anaerobically grown *Enterococcus faecalis* NCTC 775." *Eur. J. Biochem.*, in the press
- 9) Benen, J., van Berkel, W., Zak, Z., Visser, T., Veeger, C. and de Kok, A. (1991). "Lipoamide dehydrogenase from *Azotobacter vinelandii*: site-directed mutagenesis of the His450-Glu455 diad. Spectral properties of wild-type and mutated enzymes." *Eur. J. Biochem.* 202, 863-872.
- 10) Benen, J., van Berkel, W., Dieteren, N., Arscott, D., Williams Jr, C., Veeger, C. and de Kok, A. (1992) "Lipoamide dehydrogenase from *Azotobacter vinelandii*: site-directed mutagenesis of the His450-Glu455 diad. Kinetics of wild-type and mutated enzymes." *Eur. J. Biochem.*, submitted
- 11) Benen, J., van Berkel, W., Veeger, C. and de Kok, A. (1992) "Lipoamide dehydrogenase from *Azotobacter vinelandii*: Role of the C-terminus in catalysis and dimer stabilization." *Eur. J. Biochem.*, submitted
- 12) Bastiaens, P. I. H., van Hoek, A., Benen, J. A. E., Brochon, J. C. and Visser, A. J. W. G. (1992) "Conformational dynamics and intersubunit energy transfer in wild type and mutant lipoamide dehydrogenase from *Azotobacter vinelandii*. A multidimensional time-resolved polarized fluorescence study." *Biophys. J.*, submitted.